

**READY, STEADY, AND GO**

**A Transcranial Magnetic Stimulation Study of Set-Related  
Inhibitory Activity in the Human Dorsal Precentral Region**

**SARA PARMIGIANI**

**CIMEC – Centre for Mind and Brain Sciences**

**University of Trento**

**REVIEWED COPY**

**NOVEMBER 2016**

**FIRST SUPERVISOR: LUIGI CATTANEO**

**SECOND SUPERVISOR: LUCA TURELLA**

## **ACKNOWLEDGEMENTS**

I would like to express my special appreciation and thanks to my advisor Professor Luigi Cattaneo, for encouraging my research and for allowing me to grow as a research scientist. I would also like to thank my second supervisor, Professor Luca Turella, my oversight-committee members, Professor Oliver Collignon, Professor Clayton Hickey, and my reviewers, Professor Alessio Avenanti and Professor Stefano Rozzi, for their brilliant comments and suggestions, thanks to you all. I would also like to thank Professor Stephen Geyer, Pietro Avanzini, Marzio Gerbella, for their contribution and indications. I would especially like to thank Professor Francesco Pavani, as head of the Doctoral School as well as my tutor, for his invaluable support and guidance, I believe all of this made the difference, thank you. Special thanks also to Dr. Guido Barchiesi and Benedetta Zattera, since they have been there to facilitate (and cheer me up) when I discussed and implemented the experiments and the lab settings, recruited subjects and collected data for my PhD Thesis.



# TABLE OF CONTENTS

---

<b>LIST OF FIGURES</b>	<b>6</b>
<b>LIST OF TABLES</b>	<b>10</b>
<b>LIST OF PRICIPAL ABBREVIATIONS</b>	<b>11</b>
<b>INTRODUCTION</b>	<b>14</b>
<b>CHAPTER 1: THE HUMAN DORSAL PRECENTRAL REGION. ANATOMY AND FUNCTIONAL PROPERTIES</b>	<b>17</b>
<b>1.1 THE DORSAL PRECENTRAL REGION IN NON-HUMAN PRIMATES</b>	<b>18</b>
1.1.1 ANATOMY AND CONNECTIONS	18
1.1.2 FUNCTIONAL ORGANIZATION	23
<b>1.2 THE DORSAL PRECENTRAL REGION IN HUMANS</b>	<b>32</b>
1.2.1 ANATOMY AND CONNECTIONS	32
1.2.2 FUNCTIONAL ORGANIZATION	37
<b>CHAPTER 2: GENERAL METHODS</b>	<b>43</b>
<b>2.1 A VARIATION ON THE DUAL-COIL TMS APPROACH</b>	<b>44</b>
2.1.1 INTRODUCTION	44
2.1.2 INTER-HEMISPHERIC DUAL-COIL TMS APPROACHES	48
2.1.3 INTRA-HEMISPHERIC DUAL-COIL TMS APPROACHES	52
2.1.4 FROM HAND TO MOUTH: A NOVEL DUAL-COIL TMS APPROACH	55
<b>2.2 EXPERIMENTAL PROCEDURES</b>	<b>60</b>
2.2.1 NEURONAVIGATION	60
2.2.2 EMG RECORDINGS	62
2.2.3 TMS SETTING	64
2.2.4 RESPONSE ACQUISITION	65
<b>CHAPTER 3: THE HUMAN DORSAL PREMOTOR CORTEX EXERTS A POWERFUL AND SPECIFIC INHIBITORY EFFECT ON THE IPSILATERAL CORTICO-FACIAL SYSTEM</b>	<b>67</b>
<b>3.1 ABSTRACT</b>	<b>67</b>
<b>3.2 INTRODUCTION</b>	<b>68</b>
<b>3.3 METHODS</b>	<b>68</b>
3.3.2 LOCALIZATION OF TMS TARGETS	69
3.3.3 NEURONAVIGATION	70
3.3.4 INTER-STIMULUS INTERVALS (ISIs) BETWEEN COND TMS AND TEST TMS	71
3.3.5 TMS	72
3.3.6 MEP DATA PRE-PROCESSING	72
3.3.7 NORMALIZATION OF DUAL-PULSE MEPS	72
3.3.8 STATISTICAL ANALYSIS OF NORMALIZED MEPS	73
3.3.9 CONTROL ANALYSES	74
<b>3.4 RESULTS</b>	<b>74</b>
3.4.1 CONTROL ANALYSES	79
<b>3.5 DISCUSSION</b>	<b>79</b>
3.5.1 TEMPORAL SPECIFICITY	79

3.5.2 SPATIAL SPECIFICITY	80
3.5.3 CONCLUSION	81

**CHAPTER 4: HUMAN DORSAL PREMOTOR CORTEX REVISED? SET RELATED INHIBITORY INFLUENCE ON IPSILATERAL MOTOR CORTEX** **82**

<b>4.1 ABSTRACT</b>	<b>82</b>
<b>4.2 INTRODUCTION</b>	<b>83</b>
<b>4.3 METHODS</b>	<b>84</b>
4.3.1 PARTICIPANTS	85
4.3.2 LOCALIZATION OF TMS TARGETS	85
4.3.3 TMS	88
4.3.4 EMG RECORDINGS AND PRE-PROCESSING	89
4.3.5 EXPERIMENT 1 - PROTOCOL	90
4.3.6 EXPERIMENT 1 – MEP NORMALIZATION	91
4.3.7 EXPERIMENT 1 – STATISTICAL ANALYSIS	92
4.3.8 EXPERIMENT 2 - PROTOCOL	92
4.3.9 EXPERIMENT 2 - LIP RESPONSE COLLECTION	93
4.3.10 EXPERIMENT 2 – TMS	94
4.3.11 EXPERIMENT 2 - MEP NORMALIZATION AND STATISTICAL ANALYSIS	94
4.3.12 EXPERIMENT 3– PROTOCOL AND SIGNAL PROCESSING.	96
4.3.13 EXPERIMENT 3 – STATISTICAL ANALYSIS.	98
<b>4.4 RESULTS</b>	<b>98</b>
4.4.1 EXPERIMENT 1	98
4.4.2 EXPERIMENT 2 – PHYSIOLOGICAL DATA	99
4.4.3 EXPERIMENT 3	101
<b>4.5 DISCUSSION</b>	<b>102</b>

**CHAPTER 5: SHOULD I STOP OR SHOULD I GO? A DIFFERENTIAL ROLE OF PMD AND SMA IN ACTION INHIBITION** **107**

<b>5.1 ABSTRACT</b>	<b>107</b>
<b>5.2 INTRODUCTION</b>	<b>108</b>
<b>5.3 METHODS AND GENERAL PROTOCOL</b>	<b>110</b>
5.3.1 PARTICIPANTS	110
5.3.2 LOCALIZATION OF TMS TARGETS	110
5.3.3 EMG RECORDING	112
5.3.4 TMS	112
5.3.5 STOP-SIGNAL PARADIGM	113
<b>5.4 RESULTS</b>	<b>116</b>
5.4.1 EXPERIMENT 1: PMD STIMULATION	116
5.4.2 EXPERIMENT 2: SMA STIMULATION	117
<b>5.5 DISCUSSION</b>	<b>118</b>

**CHAPTER 6: CONCLUDING REMARKS AND LIMITATIONS OF THE STUDY** **124**

<b>6.1 FUTURE RESEARCH</b>	<b>125</b>
----------------------------	------------

**REFERENCES** **129**

## LIST OF FIGURES

**Figure 1.1** Microstructural maps of the primary motor, mesial, and dorsolateral premotor cortex of the macaque monkey over the last century.

**Figure 1.2.** Behavioral task and recording sites from Hoshi and Tanji, 2002.

**Figure 1.3** Recording sites and countermanding task from Mirabella et al., 2011.

**Figure 1.4** Changes of activity driven by the stop-signal onset in PMD neurons modulated during motor planning from Mirabella et al., 2011.

**Figure 1.5** Mesial and lateral view of the macaque brain and unfolded view of the intraparietal sulcus. Lateral view of the human brain with a map of the agranular frontal cortex and the somatotopic representations of the body according to the Vogts (1919) and Foerster (1936) and the suggested homologies with the macaque cortex.

**Figure 1.6** The analysis of the border between PMD and PMV indicated in Tomassini et al., 2007.

**Figure 1.7** Connectivity fingerprints of PMD and PMV in Tomassini et al., 2007.

**Figure 1.8** Cytoarchitectonic tripartite map of PMD according to Sigl et al., 2016

**Figure 2.1** Temporal and spatial resolution of the main investigation techniques in cognitive neurosciences.

**Figure 2.2** An example of a twin or dual-coil setting.

**Figure 2.3** Schematic summary of the dual-coil procedure.

**Figure 2.4** The premotor hand region, the saccadic eye movement region and the hand-M1 in the human and monkey frontal cortex. Schematic representation of the sulcal patterns in the dorsal premotor region of the human brain.

**Figure 2.5** A dual-coil experimental set-up illustrating the position of two 70 figure of eight TMS coils on subject's head from Baumer et al., 2006.

**Figure 2.6** Schematic illustration of task and the coil positions on the head that were used in Koch et al. (2006) experiment. From Rothwell, 2011.

**Figure 2.7** Experimental set-up and time course of a single trial from O'Shea et al., 2007.

**Figure 2.8** The scalp locations at which the cortical stimuli were delivered in Civardi et al., 2001.

**Figure 2.9** View of the two mini-coils aligned to each other and schematic drawing of the central coil windings used in Groppa et al., 2012.

**Figure 2.10** Coil placement in Beck et al., 2009.

**Figure 2.11** The somatotopic organization of M1 in humans.

**Figure 2.12** A cartoon depicting our dual-coil experimental approach.

**Figure 2.13** Schematic picture of the stimulation sites along the sFS in the dorsal portion of BA6 (our condTMS target) in one of the subjects of our first experiment.

**Figure 2.14** 2D Reconstruction of the brain and 3D reconstruction of the scalp.

**Figure 2.15** 3D rendering of the surface of the grey-white matter border, used for neuronavigation.

**Figure 2.16** Our ultrasound tracking system.

**Figure 2.17** Electrodes montage for the three effectors.

**Figure 2.18** Coils positioning over PMD and SMA.

**Figure 2.19** A schematic drawing of our response acquisition device.

**Figure 3.1** Lateral view of the precentral sulcal complex in all the 16 subjects.

**Figure 3.2** A schematic representation of the SP trials interleaved with DP trials.

**Figure 3.3** Representative EMG recordings from the orbicularis oris muscle of one subject.

**Figure 3.4** Representation of the experimental results.

**Figure 3.5** Individual values of the logarithm of the normalized MEP areas.

**Figure 4.1** The target points are shown for participants of all experiments (n = 28).

**Figure 4.2** Demonstration of linear covariance between background EMG activity and MEP amplitudes.

**Figure 4.3** Experiment 2 trials procedure.

**Figure 4.4** Experiment 3 trials procedure.

**Figure 4.5** An example of a single subject RTs distribution.

**Figure 4.6** Results of Experiment 1.

**Figure 4.7** Results of MEPs modulation of Experiment 2.

**Figure 4.8** Results of MEPs modulation in the three blocks of Experiment 3.

**Figure 5.1** The reconstruction of one subject's brain in AC-PC native space in which the pre-SMA and SMA regions are identifiable.

**Figure 5.2** Functional organization of human pre-SMA and SMA proper identified with PET studies from Picard and Strick, 1996.

**Figure 5.3** NO-STOP trials procedure.

**Figure 5.4** STOP trials procedure.

**Figure 5.5** Results of Experiment 1.

**Figure 5.6** Data from of Experiment 2.

## LIST OF TABLES

**Table 3.1** Talairach coordinates of condTMS in each participant.

**Table 4.1** Talairach coordinates of condTMS in each participant of Experiments 1 and 2.

**Table 4.2** Talairach coordinates of condTMS in each participant of Experiment 3.

**Table 4.3** Values of the mean log-transformed MEP ratio in the Experiments 2 and 3.

## **LIST OF PRICIPAL ABBREVIATIONS**

1DI First Dorsal Interosseus

AC-PC Anterior Commissure-Posterior Commissure

AS Arcuate Sulcus

BA 4 Brodmann Area 4

BA 6 Brodmann Area 6

condTMS conditioning pulse (TMS)

CS Central Sulcus

DLPC Dorsolateral Prefrontal Cortex

DP Dual Pulse (TMS)

EEG Electroencephalography

FEF Frontal Eye Field

fMRI functional Magnetic Resonance Imaging

GABA-A  $\gamma$ -aminobutyric acid

handM1 hand-related human primary motor cortex

IFG Inferior Frontal Girus

legM1 leg-related human primary motor cortex

M1 human primary motor cortex

MEP Motor Evoked Potential

mouthM1 mouth (orofacial)-related human primary motor cortex

MRI Magnetic Resonance Imaging

OOr Orbicularis Oris

PET Positron Emission Tomography

PMD Dorsal Premotor cortex

PMV Ventral Premotor Cortex

pre-SMA human homologous of area F6

rCBF Regional Cerebral Blood Flow

RT Reaction Times

rTMS repetitive Transcranial Magnetic Stimulation

SF Superior Frontal Sulcus

SFG Superior Frontal Gyrus

SMA Supplementary Motor Area. SMA proper is the human homologous of area F3

SMAc Supplementary Motor Area caudal portion

SMAr Supplementary Motor Area rostral portion

SP Single Pulse (TMS)

Sp Spur of AS

SP Superior Precentral Sulcus

SPS Superior Precentral Sulcus

SSRT Stop Signal Reaction Time

testTMS test pulse (TMS)

TMS Transcranial Magnetic Stimulation

VCS Anterior Commissure

VPA Posterior Commissure

## INTRODUCTION

Successfully acting largely depends on moving at the right time. Consider a member of an orchestra just few instants before starting to play her piece. She should be ready not only to launch the planned movements when appropriate, but also to stop them if required. Action initiation and control are characteristic features of many of our daily life actions.

There is a large amount of evidence in monkeys and humans suggesting that the dorsal premotor cortex (PMD) and the supplementary motor areas (SMA) might be critically involved in these features. However, the distinctive role of these areas is still matter of controversy.

The aim of the present thesis is to provide some preliminary steps toward a comprehension of whether and how the human dorsal precentral areas may selectively contribute to action initiation and control. In doing this we shall introduce and discuss a series of transcranial magnetic stimulation (TMS) experiments carried out with two different paradigms, namely dual-coil TMS and single pulse TMS paradigm. These experiments were primarily devoted to explore the structural and functional properties of PMD. They also allowed us to assess whether PMD and SMA may be differentially and selectively involved in action control.

In more detail, we first investigated the structural connectivity between PMD and the ipsilateral orofacial M1, introducing a novel dual-coil TMS approach.

Results displayed the existence of short-latency influences of the left PMD on the ipsilateral orofacial M1, measured by recording motor evoked potentials (MEPs) in the orofacial muscles.

Then, taking advantage of this novel approach, we started to explore the functional PMD-M1 connectivity. We tested the short-latency effects of TMS, as measured by changes in orofacial MEPs, during a delayed motor task. The results showed an inhibitory activity in the PMD-M1 module during the SET-period. We also manipulated the duration of the SET-period, to establish whether the effects were time-locked to the start of the delay period or rather time-locked to the predicted GO-signal.

Hence, the investigation of the PMD-M1 connectivity paved us the way to explore, first, the role of PMD in initiating action and, then, the differential role of PMD and SMA in controlling and inhibiting action. Indeed, we run a further study, in which we carried out two single pulse TMS experiments. We first stimulated PMD during a stop-signal task, then we contrasted the PMD stimulation with SMA stimulation when participants underwent the same stop-signal task.

There are five chapters to come. In Chapter 1 we shall review some key studies exploring anatomical and functional properties of PMD and SMA in both monkeys and humans, with particular emphasis on their putative role in action initiation and control. In Chapter 2 we shall focus on the methodological aspects of our experimental studies. In particular, we shall introduce the so-called twin- or dual-coil TMS paradigm, discuss its main approaches present in the literature and propose a variant of them.

In Chapter 3 we shall present and discuss our first dual-coil TMS study exploring, for the first time, the ipsilateral PMD-corticofacial system connectivity. In

Chapter 4 we shall examine three dual-coil TMS studies investigating the functional connectivity between PMD and ipsilateral M1 during a motor delayed task. Finally, in Chapter 5 we shall scrutinize two single pulse TMS studies capitalizing on a stop-signal task in order to assess the role of PMD and SMA in action control. Results and future lines of research will be sketched in the Concluding remarks.

## **CHAPTER 1: THE HUMAN DORSAL PRECENTRAL REGION. ANATOMY AND FUNCTIONAL PROPERTIES**

Our overall question concerns the putative role of the human dorsal precentral region in initiating and controlling action. In this first chapter, we shall introduce and briefly discuss some anatomical and functional properties of the main areas forming this cortical region, which turn out to be particularly relevant for our question. More specifically, in the Section 1.1 we shall briefly sketched the anatomical structure of the monkey dorsal precentral region, by emphasizing its parcellation in a mosaic of hodologically and functionally distinct areas. We shall also review some key functional studies, based on different paradigms, which explored the distinctive role of the different dorsal precentral areas in action planning and controlling. In Section 1.2. we shall describe anatomy and connections in the human dorsal precentral region. This shall allow us to shed some lights on the functional organization of this region, with particular emphasis on the role of PMD and SMA in action initiation and control.

## 1.1 THE DORSAL PRECENTRAL REGION IN NON-HUMAN PRIMATES

### 1.1.1 Anatomy and connections

Since Brodmann's work (1909), there is a large consensus that the agranular frontal cortex of primates is formed by two cytoarchitectonally distinguishable areas: area 4 (primary motor cortex) and area 6 (premotor cortex) (see [Figure 1.1A](#)). If many researchers agreed for a long time that area 4 of the macaque monkey is largely homogeneous<sup>1</sup>, this was not the case for area 6. Indeed, although Brodmann (1909) considered area 6 as a single cytoarchitectonic entity, a large number of subsequent studies demonstrated that area 6 can be subdivided into three main sectors or group of areas: SMA on the mesial cortical surface, PMD on the dorsolateral convexity, and ventral part of the premotor cortex (PMV) on the ventrolateral convexity<sup>2</sup>.

Vogt and Vogt (1919) firstly subdivided the mesial and superior area 6 into area 6α and area 6β, with the border set at the level just rostral of the arcuate sulcus ([Figure 1.1B](#))<sup>3</sup>. Thirty years later, von Bonin and Bailey (1947) described most of mesial and superior area 6 as area FB, whose rostral border was more anterior than that of Vogts' area 6α. Area FB was separated from the granular frontal cortex by area FC ([Figure 1.1C](#)). Subsequently, Barbas and Pandya (1987) identified area 6DC, a cortical strip just rostral to area 4. Rostral to 6DC, they described area 6DR and area MII, on the dorsolateral and on the mesial surfaces,

---

<sup>1</sup> See, for instance, Schieber, (1999). But see also Geyer et al., (1996), who subdivided area 4 into two anatomically and functional different sub-areas 4 anterior (4a) and 4 posterior (4p). For more recent data see also Geyer et al. (2012).

<sup>2</sup> In this section we will focus on the mesial and dorsolateral premotor cortex. For a more general picture of the parcellation of various motor areas, including those belonging to the ventral premotor cortex of the macaque monkey, see Rizzolatti and Luppino (2001) and, more recently, Geyer et al. (2012).

<sup>3</sup> For an instructive overview of the main differences between Brodmann's and Vogts' maps as well as of the relevance of these (and subsequent) classic maps for the current structural and functional studies see Zilles & Amunts, (2010) and Amunts and Zilles 2015.

respectively (Figure 1.1D). Finally, by combining cytoarchitectonic and histochemical data, Matelli and colleagues (Matelli & Luppino 1997; Matelli, Luppino, & Rizzolatti, 1991; Matelli, Luppino, & Rizzolatti, 1985; Rizzolatti, Luppino, & Matelli, 1998) parcellated, for the first time, the dorsolateral and mesial area 6 in its entire rostro-caudal extent. Rostral to the equivalent of area 4 (i.e. area F1), area F2 (caudal PMD) was described on the dorsolateral and area F3 (proper-SMA) on mesial surface. The rostral part of area 6 was subdivided into area F7 (rostral PMD) dorsolaterally and area F6 (Pre-SMA) mesially (Figure 1.1E).

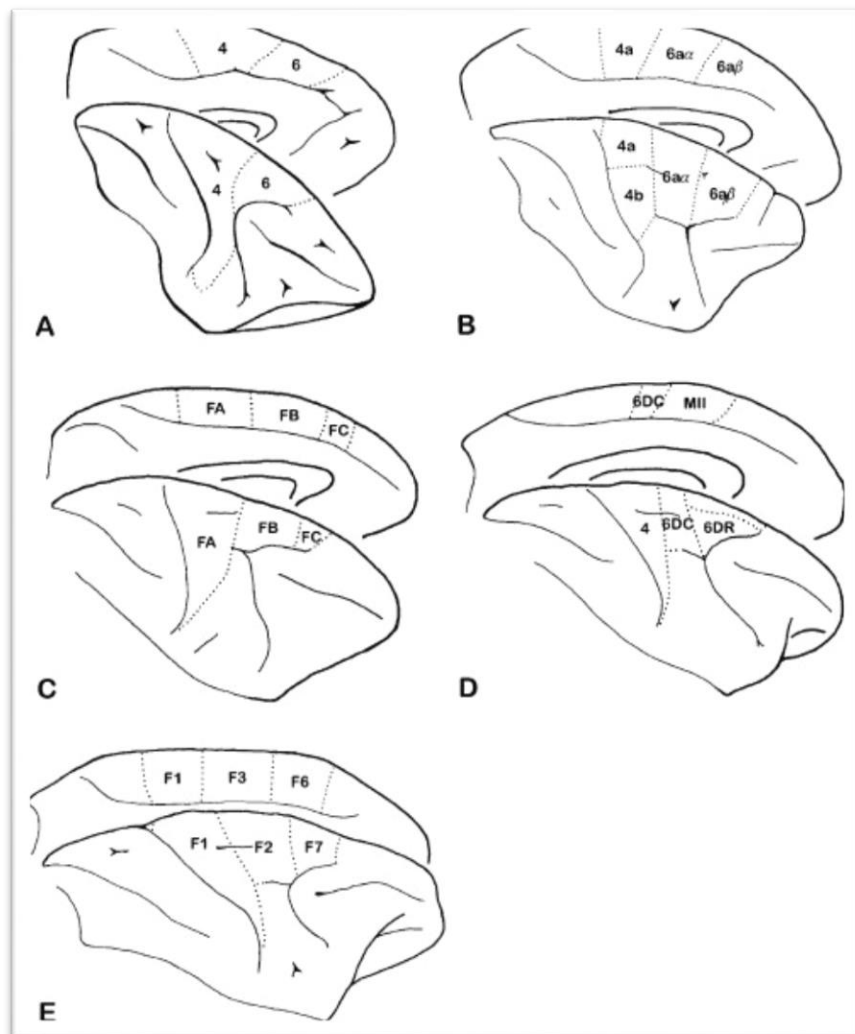


**Figure 1.1** Microstructural maps of the primary motor, mesial, and dorsolateral premotor cortex of the macaque monkey over the last century. (A) Brodmann (1909). (B) Vogt and Vogt (1919). (C) von Bonin and Bailey (1947). (D) Barbas and Pandya 1987. (E) Matelli et al. (1991). Rostral is to the right, caudal to the left.

#### 1.1.1.1 Area F2 and area F7

We have just seen that the portion of cortex lying rostral to the primary motor cortex (area F1) is commonly referred to as premotor cortex (Fulton 1935; Vogt and Vogt 1919). Its microscopic features are intermediate between the agranular pattern found in area F1 and the granular pattern found in the prefrontal cortex. The premotor cortex of primates is part of the cortical motor system (Rizzolatti et al. 1998). It can therefore generate motor outputs directly by means of corticospinal or corticobulbar projections (R P Dum & Strick, 1991; He, Dum, & Strick, 1995; Morecraft, Louie, Herrick, & Stilwell-Morecraft, 2001) or indirectly by means of a rich pattern of connections to the primary motor cortex. In this section, we shall focus on the dorsal part of premotor cortex, which has been subdivided into two rostral (area F7) and a caudal (area F2) areas.

Area F2 is somatotopically organized (Goldschalk et al., 1995; Dum & Strick, 1991; Kurata, 1989) and it has been subdivided into two hodologically and functionally independent areas, the rostroventral (F2vr) and dorsal F2 (F2d) ones (Caminiti et al. 1996; Luppino & Rizzolatti, 2000; Rizzolatti et al., 1998). F2d neurons seem to be involved in planning and controlling leg and arm movements based on somatosensory information, while F2vr neurons possibly capitalize on somatosensory and visual information for arm reaching movements (Kiyoshi Kurata, 1994; Rizzolatti et al., 1998; Wise, Boussaoud, Johnson, & Caminiti, 1997). This difference seems to be also reflected in their descending projections

(Keizer & Kupizers, 1989) as well as in their cortical connections. Indeed, while F2d is mostly targeted from a somatosensory area of the superior parietal lobule (area F2vr is the target of (I) visual or somatosensory and visual areas of the superior parietal lobule (MIP and V6A) (Luppino, Calzavara, Rozzi, & Matelli, 2001), (II) a minor but consistent projections from the dorsal section of the DLPF and (III) a relative strong input from the cingulate gyrus (areas 24a and 24b) and area 24d (Giuseppe Luppino, Rozzi, Calzavara, & Matelli, 2003).

Area F2 is related to action production not only directly, in virtue of its corticospinal projections, but also indirectly, via F1. There is a large evidence that area F2 is intensively connected with area F1 in a somatotopic manner, with massively connections with the arm- and especially to the hand-related motor areas (handF1) (see Richard P Dum & Strick, 2005; Muakkassa & Strick, 1979; Tokuno & Tanji, 1993). Interestingly, indirect anatomical data suggest that mouth movements might be also be controlled by F2-F1 circuits (Morecraft et al., 2001).

Differently from area F2, area F7 is neither directly connected to area F1 nor giving origin to the corticospinal tract, projecting rather to the brainstem. Its dorsorostral part contains the supplementary eye field (SEF) and it is richly connected to the frontal eye field (FEF) as well as to both the dorsal and ventral DLPFC, while the remaining part of F7 is the target of strong afferents from the dorsal DLPFC only (Luppino et al., 2003). Some F7 neurons have visual responses even when the stimulus is not action-related. Other F7 neurons have been reported to respond to visual stimuli when their location matches the target of an arm movement (Luppino & Rizzolatti, 2000).

### 1.1.1.2 Area F3 and area F6

As far as SMA is concerned, we already noted that mesial area 6 is composed of two distinct areas: area F3 (proper SMA) and area F6 (pre-SMA). Hodological studies showed that area F3 is the source of dense, topographically organized corticospinal projection. Connections with other motor areas, such as F1 and F2, are also topographically organized. Area F3 is also target of strong cingulate and parietal afferents from area 24d and from area PEcg, respectively. Intracortical microstimulations demonstrated that area F3 is electrically excitable with low-intensity currents, being endowed with a complete body movement representation. Movements of the hind limb are evoked from caudal sites, whereas forelimb and orofacial movements are evoked from more rostral sites, closer to the border with F6 (Luppino, Matelli, Camarda, Gallese, & Rizzolatti, 1991; Matsuzaka, Aizawa, & Tanji, 1992). Finally, single cell recordings from area F3 found frequent somatosensory responses (Luppino & Rizzolatti, 2000).

In contrast to area F3, area F6 is the source of a modest corticospinal projection and has no direct connection with area F1. Parietal afferents to area F6 are few and originate from visual areas (PFG and PG) of the inferior parietal lobule (IPL). On the contrary, area F6 is a target of strong afferents originating from DLPF and is the only motor area target of rich afferents from the cingulate area 24c and from the cingulate gyrus (Luppino, Matelli, Camarda, & Rizzolatti, 1993). Finally, area F6 is weakly excitable with intracortical microstimulations. Movement can be evoked from area F6 just with rather high current intensities, and they typically consist of slow and complex arm movement. Single cell recording from area F6 often revealed visual responses, whereas the somatosensory ones are very rare (Luppino & Rizzolatti, 2000).

Taken together, these data clearly indicate a marked difference between the posterior (area F2 and area F3) and the anterior (area F7 – area F6) premotor and mesial areas. The former is directly connected with F1, while the latter do not project into area F1. A similar subdivision can be found at the level both of the descending projections (area F2 and area F3 give rise to the corticospinal tract, whereas area F7 and area F6 project out to other sectors of the brainstem) and also of cortical organization (area F2 and area F3 get strong sensory inputs from the parietal lobe, whereas area F7 and area F6 receive their main cortical connections from the prefrontal cortex). This is not without functional implications, or so we shall argue in the next section.

### **1.1.2 Functional organization**

#### **1.1.2.1 Area F2 and area F7**

In the previous section, we briefly mentioned evidence showing that PMD (area F2) is generally involved in planning and controlling leg and arm movements, being its rostroventral sector (F2vr) especially related to reaching arm movements. In this section, we shall review some less and more recent studies, which used different experimental setting in order to shed some light on the distinctive role (or roles) of PMD in action planning and control.<sup>4</sup>

Functional properties of PMD (F2) neurons were mostly studied by employing visually instructed delay motor tasks. In these task a motor responses (e.g. an arm movement) is performed with a delay after the appearance of a visual cue instructing the monkey on to requested movements. The neuronal activity

---

<sup>4</sup> Given our purposes, we shall focus on studies concerning the relations between PMD and F1 in preparing and controlling arm movements, which are mainly (but not exclusively) represented in area F2.

occurring in the cerebral cortex of primates during the delay period when the animal is waiting for the go-signal is typically called *set-related activity*<sup>5</sup>.

Single cell recordings in many early studies reported prominent set-related activity in PMD as well as in PMV, demonstrating that it reflects *motor planning*, rather than visuo-spatial instructions or motor command per se (di Pellegrino & Wise, 1993; Godschalk, Lemon, Kuypers, & Van Der Steen, 1985; K. Kurata, 1989; K. Kurata & Wise, 1988; Weinrich & Wise, 1982; Weinrich, Wise, & Mauritz, 1984; Wise, 1985). Interestingly, it has been also reported set-related activity in PMD after the presentation of auditory instructions (Kurata, 1993; Weise et al. 1996). More recently, Hoshi and Tanji (2002) designed a target-reaching task, in which two monkeys were asked to select one of four possible movements (using both arms) in accordance with two sets of instruction cues, followed by a delay period and a subsequent set-related period, in which the monkeys were required to get ready for a movement-trigger signal to start the action promptly (see [Figure 1.2](#)). By comparing set-related neuronal activity in PMD and PMV, the author showed that arm selection as well as target location were reflected in the set-related activity of PMD neurons, whereas PMV neurons were selective for target location, thus contributing to target acquisition.

Further studies demonstrated that set-related PMD activity can be referred also to motor planning driven by memorized cues (Cisek & Kalaska, 2005; Ohbayashi, Hernandez et al., 2010; Picard, & Strick, 2016).

---

<sup>5</sup> More specifically, set-related activity is the absolute value of the difference between activity during the delay period and that during the inter-trial interval (see Weinrich and Wise, 1982). In Kurata and Wise (1988), neuronal activity was defined as set-related if it showed a statistically significant sustained increase or decrease in discharge rate during the instructed delay period (in that case, from 500ms to 1500ms after the onset of an instruction stimulus).

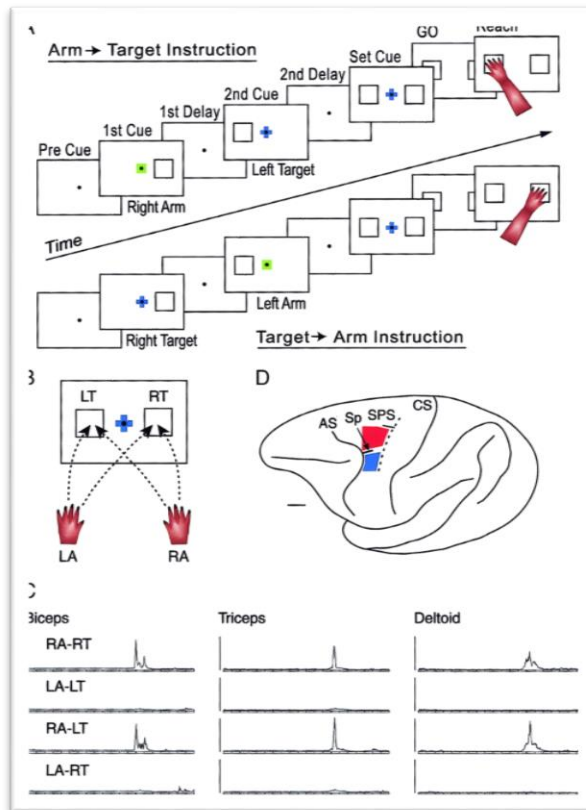


**Figure 1.2.** Behavioral task and recording sites. (A) Temporal sequence of the behavioral events. The top row shows a trial in which the 2 instructions were given in the order “arm” then “target.” The bottom row shows a trial in which the 2 instructions were given in the order “target” then “arm.” (B) the 4 movements performed by the monkeys. During the set-cue period, they prepared to perform the 4 movements indicated by dotted lines. RA, right arm; LA, left arm; RT, right target; LT, left target. (C) 3 examples of electromyographic (EMG) activity. This report refers to the activity of neurons found in the 2 cortical motor areas: the dorsal (red) and ventral (blue) premotor areas (PMD and PMVV, respectively). AS, arcuate sulcus; CS, central sulcus; SPS, superior precentral sulcus; Sp, spur of AS. (from Hoshi & Tanji, 2002)

Two other paradigms have been often used in order to assess the distinctive role, if any, of PMD (area F2) in action planning and control. The first paradigm is the so-called GO/NOGO paradigm. In a seminal paper, Kalaska and Crammond (1995) recorded neuronal activity in monkeys when performing reaching movements in two opposite directions in a symmetrically rewarded

GO/NOGO task with an instructed-delay period. While the initial response of most PMD cells to the appearance of the instructional cues in GO and NOGO trials was similar, by the end of the delay period, the responses of most PMD cells were statistically different between the two trial types, and the population signals were much less directional in the NOGO trials than in the GO trials. Similar results have been also found in Ledberg et al. (2007) who recorded local field potentials from up to 15 cerebral cortical regions of monkeys that performed a conditional GO/NOGO task. The results showed that cortical activity in PMD allowed to predict the monkey's choice after 150 ms.

The second paradigm is the so-called stop-signal (or countermanding) paradigm. This paradigm probes individual's ability to withhold a planned movement triggered by a go-signal when a stop-signal is presented after a variable delay. It is worth noting that, differently from the GO/NOGO paradigm, in the stop-signal paradigm is an ongoing motor response, rather than a mere potential movement, that has to be halted. However, it is reasonable to assume that these different kinds of action restraining may have a cortical overlap (Battaglia-Mayer et al., 2014). Indeed, it has been recently showed that PMD reaching-related neurons modulated their activity before the stop-signal reaction time, that is the behavioral estimate of the time it takes to stop an ongoing movement. Mirabella et al. (2011) recorded from PMD neurons of two monkeys performing both no-stop and stop trials in a countermanding task. In the No-Stop trials, the monkeys should execute a speeded reaching movement at the appearance of a suitable target. In the Stop trials, after a variable delay, a stop signal appeared, instructing the monkeys to inhibit the movement initiation (see [Figure 1.3](#)).

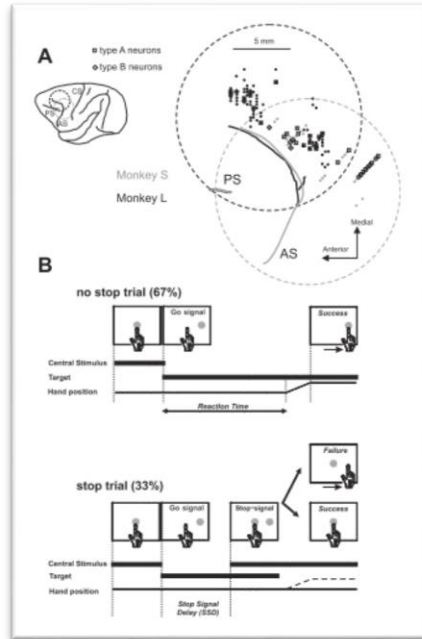


**Figure 1.3** Recording sites and countermanding task. (A) location of recording sites in the 2 monkeys. The relative positions of the recording chambers (large circles) are indicated over a standard model of rhesus monkey brain. Dots indicate the entry points of electrodes. (B) temporal sequence of the visual displays for no-stop and stop trials in the countermanding reaching task. In stop trials, if the monkey countermanded the planned movement, keeping the arm on the central stimulus, the trial was scored as a stop-success trial. Otherwise, the trial was scored as a stop-failure trial (Mirabella et al. 2011).

The results showed that more than one third of recorded PMD neurons involved in motor planning exhibit a countermanding modulation. These neurons changed their pattern of discharge when a reaching movement were executed with respect to when it was inhibited, and this change preceded the end of the stop-signal reaction time (see **Figure 1.4**).

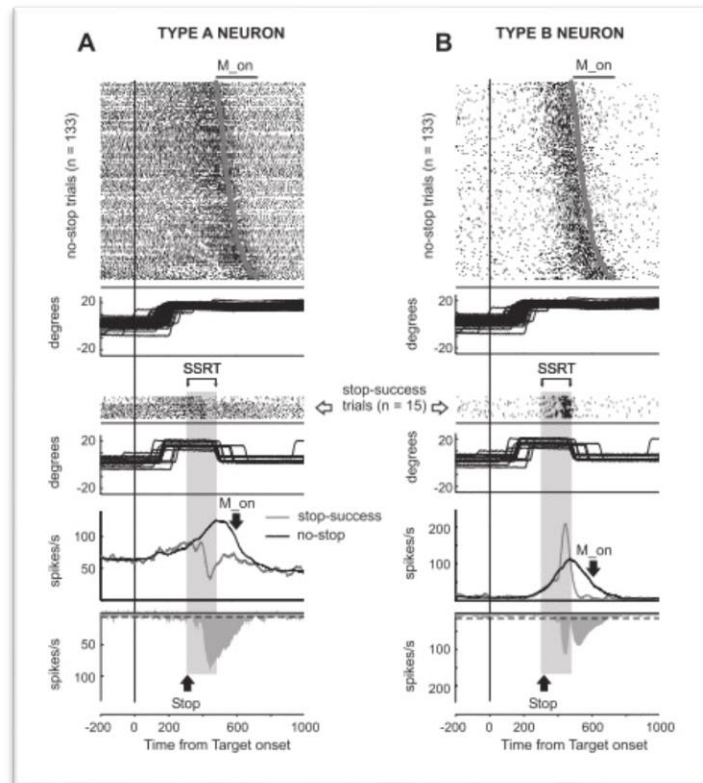


**Figure 1.4** Changes of activity driven by the stop-signal onset in PMD neurons modulated during motor planning. The activity of 2 neurons is shown for no-stop and latency-matched stop-success trials. In each panel the top graph represents the raster plots of neural activity in no-stop trials. The horizontal components of eye movements during no-stop trials are represented below. The raster plot in the 3rd row represents the neural activity in stop-success trials. Just below the eye movements for stop-success trials are displayed. The 2 lower graphs represent the spike density functions for no-stop trials (black lines) and for stop-success trials (gray lines) and the differential spike density functions (gray areas), respectively. The gray band represents the estimated duration of the SSRT in the session. (A) Neuron type A. This the most common class of recorded PMD neurons. Their activity during stop-success trials decrease before the end of the SSRT with respect to that recorded during no-stop trials: (B) Neuron type B. Movement inhibition is associated with a temporary increase of their activity with respect to the activity recorded during no-stop trials (Mirabella et al. 2011).

These findings support a distinctive planning and controlling role of PMD over movement production. This seems to be in line also with lesion data. Indeed, the injection of GABA-A antagonists within PMD reduces the ability of monkeys to

withhold movements (Sawaguchi, Yamane, & Kubota, 1996). Similarly, lesions to PMD may result in increased frequency of impulsive and uncontrolled reaching movements (Moll & Kuypers, 1977).

#### 1.1.2.1 Area F3 and area F6

A large number of studies have been devoted to investigate the functional properties of F6 and F3 neurons. We already mentioned that these areas mainly differ with respect to both corticospinal projections (rich in area F3 and sparse in area F6) and reciprocal connections with area F1 (present in area F3 and absent in area F6). A possible interpretation of these main differences is that area F3 (proper SMA) is involved in more executive planning and control functions, directly related to motor output production, whereas area F6 (pre-SMA) is mainly involved in higher-order motor planning and control functions.

These different functional properties have been mainly studied by using paradigms, in which animals were trained to perform single reaching actions or hierarchical organized sequence of actions. For instance, it has been shown, in a single action task, that a large number of F6 neurons discharge well in advance of the onset of action, whereas this is not the case of F3 neurons, that mostly discharge just before the onset of action (Alexander & Crutcher, 1990; Matsuzaka et al., 1992). In a similar vein, Rizzolatti et al. (1990) showed that F6 neurons did not directly control distal or proximal arm movement, becoming active upon presentation of objects that were target of actions. Note that this activity was not related to object size, shape or location; rather, it mainly reflected whether or not an object could be acted upon.

As far as action sequences are concerned, Tanji and Shima (1994) seminally demonstrated that SMA neurons are critically involved in sequences of multiple

movements performed in a particular order. These findings are in line with a muscimol injection study, in which the inactivation of both F6 and F3 areas impaired the monkeys to perform three actions (turn, push or pull) in the correct order. Strikingly the impairment didn't affect the performance of the three actions when individually guided with visual instructions (Shima & Tanji, 1998).

In a follow-up study, the same authors systematically scrutinized neuronal activity in F3 and F6 areas in monkeys that were trained to perform three different actions separated by waiting times, in four or six different orders (Tanji, Shima, & Matsuzaka, 2002). Three types of neuronal activity were of particular interest: (I) the sequence selective activity, which eased when the monkeys initiated the first action, (II) interval selective activity that appeared in the interval between action particular and the next, and (III) the rank order selective activity, which concerned the process of preparing the first, second, or third actions in individual trials. The results showed that both F6 and F3 neurons were involved sequencing multiple actions over time. But this with some significant differences: the interval-selective activity was more prevalent in area F3, whereas the rank-order selective activity was more frequently recorded in area F6. Furthermore, the contrast between the action-related activity recorded from F6 and F3 neurons had as result that the great majority action-related activity in area F6 showed selectivity for either the sequence or rank order, whereas F3 neurons were more selective for the specific kind of action to be performed.

Similar results have been obtained by investigating action sequence learning. For instance, Nakamura et al. (1998) trained two monkeys to perform sequential button press actions in predetermined orders that the animals had to learn by trial and error. Single neurons were recorded from area F6 and area F3 during both the

acquisition of new action sequences and the execution of well-learned sequences. The results showed that the proportion of neurons, which were more active during the performance of new action sequences than during the execution of well-learned sequences, was greater in area F6 than area F3. To illustrate, F6 neurons preferentially discharging during a given button press action when the monkeys were learning a new action sequence, did no longer discharge during the execution of the same button press action, when the monkey had mastered the action sequence.

Finally, the role of area F6 and area F3 in action planning and control has been recently investigated by Scangos and Stuphorn (2010). They recorded from F6 and F3 neurons of monkeys performing an arm countermanding task. The results showed a large action-related activity in both F6 and F3 neurons, with a significant earlier onset of action-related activity in F6 neurons. But, with the surprise of the authors themselves, this activity seemed to be not sufficient to control action initiation: almost all F6 and F3 action-related neurons appeared to fail to exhibit time-locked activity changes predictive of action initiation. Interestingly, a certain percentage of F6 and F3 neurons showed a significantly higher activity on canceled trials than on no-stop signal trials, with some F6 neurons being more active on cancelled trials before the SSRT. However, only a very small percentage of recorded neurons (2.4%) were actually involved in action inhibition (we shall come back to this study and its implication in [Chapter 5](#)).

## 1.2 THE DORSAL PRECENTRAL REGION IN HUMANS

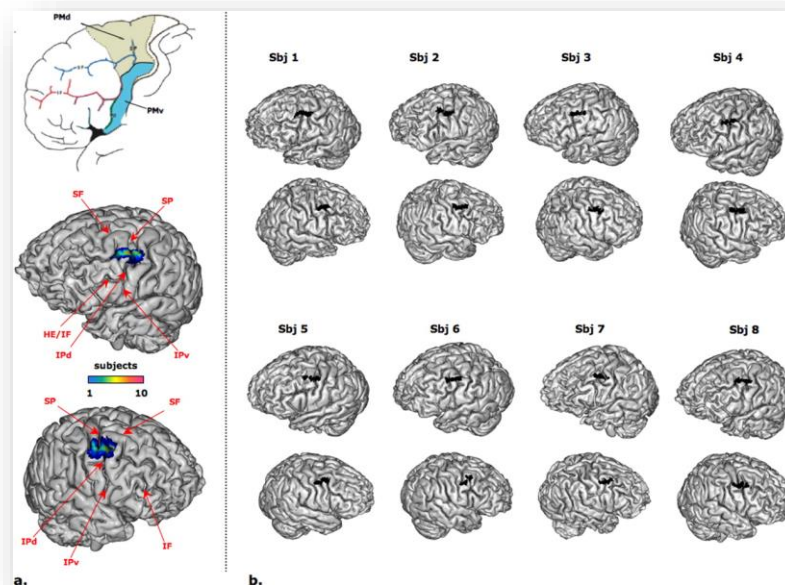
### 1.2.1 Anatomy and connections

Cytoarchitectonic features and topography of human precentral motor region are partially similar to the non-human primates. Also in humans, BA6 is characterized by large and elongated pyramidal cells in lower layer III; at the border between BA6 and BA4 they decrease in size. Giant pyramidal cells are scattered throughout the caudal sector of BA6; at the border between BA6 and BA4 they abruptly increase in size and density (Geyer, 2004; Geyer et al. 2012). Differently from the monkey, on the human cortical convexity there is not a macro-anatomical landmark (i.e. the arcuate sulcus) separating brain the agranular frontal from the granular prefrontal cortex. Nevertheless, cytoarchitectonic studies in a series of human specimens (Geyer, 2004) showed that their border can be identified in an observer-independent way by means of the histological processing of postmortem brains. Indeed, at the rostral border of BA6 with PFC the large and elongated pyramids in lower layer III decrease in size. But the most important feature of the border between BA6 and the PFC is a gradually emerging inner granular layer (layer IV).

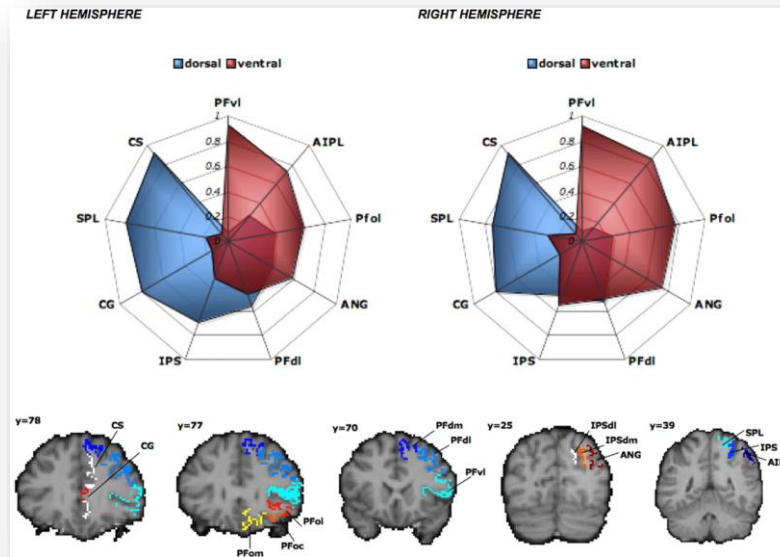
Thus, the spatial distribution of agranular cortex is similar in monkeys and humans, with the prefrontal cortex extending in the middle of the dorsolateral convexity and receding rostrally in the dorsomedial and ventrolateral parts of the convexity. It has been proposed that the superior frontal and superior precentral sulcus represent the human homologue of the monkey superior arcuate sulcus (Rizzolatti et al., 1998). Accordingly, the two areas that occupy the rostral part of the precentral gyrus and the caudal part of the superior frontal gyrus correspond to macaque areas F2 and F7, respectively (see [Figure 1.5](#)).



Figure 1.6), with a close correspondence to the location of a functional border defined using previous fMRI (Mayka, Corcos, Leurgans, & Vaillancourt, 2006). Connectivity fingerprints demonstrated that putative human PMD has a high probability of connection with the superior parietal lobule, dorsal prefrontal cortex, and cingulate cortex, whereas human PMV has a higher probability of connection with the anterior inferior parietal lobule and ventral prefrontal cortex (see Figure 1.7).



**Figure 1.6** a, Top, Hypothesized subdivision of human PM (modified from Geyer et al., 2000). Bottom, Group map of the border between PMD and PMV displayed on the three-dimensional cortical surface from one individual structural image. The color scale indicates the number of subjects sharing a given location (top, left hemisphere; bottom, right hemisphere). b, Overlay of the left and right PMD/PMV borders on the individual three-dimensional cortical surfaces. In the majority of cases, the border lies between the superior and the inferior parts of the precentral sulcus. (Tomassini et al., 2000).



**Figure 1.7** Connectivity fingerprints in the left hemisphere (top left) and the right hemisphere (top right). The values indicate the relative connection probability between PMD (blue) or PMV (red) and the prefronto-parietal targets, the masks of which are shown in the bottom row. (Tomassini et al., 2007).

Finally, a very recent study by Amunts and colleagues (Sigl et al. 2016) subdivided the human putative PMD into three cytoarchitecturally distinct areas: caudal area 6d1 on the dorsal precentral gyrus and precentral sulcus, and rostral areas 6d2, on caudal superior frontal gyrus, and 6d3, in caudal superior frontal sulcus (Figure 1.8). Area 6d1 abutted M1, ventral and mesial PM. Area 6d2 bordered mesial PM dorsally, 6d3 adjoined ventral PM. 6d2 and 6d3 bordered dysgranular BA 8 rostrally. From a functional point of view, 6d1 seems to play a role in action execution and interoception, being particularly connected to M1 and thus developing programs for it (Davare, Zénon, Desmurget, & Olivier, 2015). 6d2 is involved in action imagination and execution and is linked to prefrontal areas, turning out to a connector between higher cognition and action. Finally, 6d3

showed activity while analyzing optical motion and performing saccades and anti-saccades. It co-activated with higher visual areas, making it a candidate for the assumed second part of the human frontal eye field (Cameron et al. 2015).

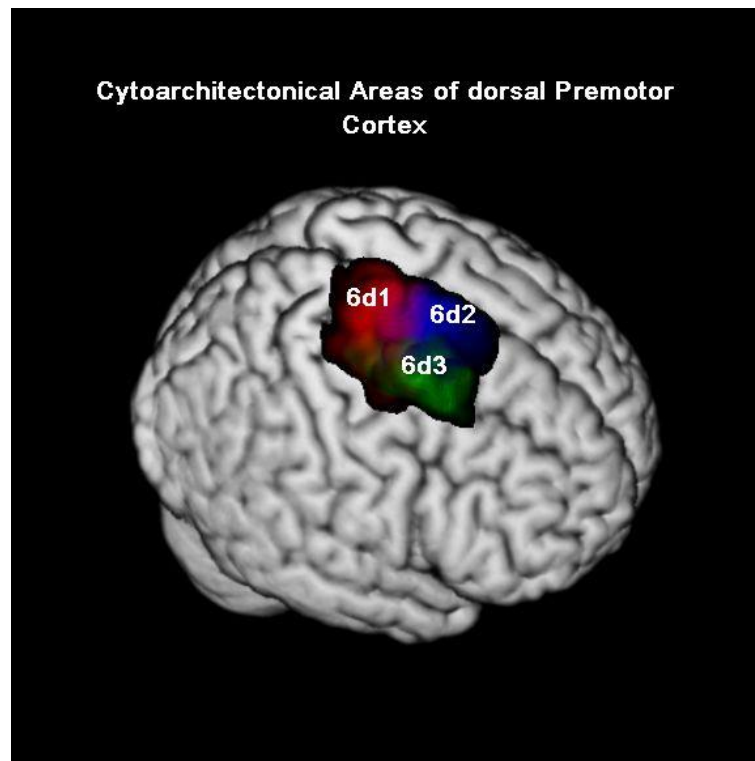


**Figure 1.8** Cytoarchitectonic tripartite map of PMD according to Sigl et al. 2016

Cytoarchitectonic similarities between humans and monkeys are also evident on the mesial cortical surface. It has been found striking architectonic similarities between macaque areas F3 (proper SMA) and F6 (pre-SMA) and the mesial parts of area  $6\alpha$  and area  $6\beta$  (according to the Vogts' nomenclature), respectively, in humans (Zilles et al. 1995, 1996). The border between M1 and area  $6\alpha$  coincides approximately the vertical through the posterior commissure (VPA), while the border between area  $6\alpha$  and area  $6\beta$  with the vertical through the anterior commissure (VCA) (see Johansen-Berg et al., 2004; Picard & Strick, 1996;

Vorobiev, 1998). It is worth noting that the proper SMA has been further subdivided into a caudal (SMAc) and rostral (SMAr) part (Vorobiev et al. 1998). Considering the cytoarchitectonic characteristics of SMAc and SMAr, it has been speculated that these two areas evolved from a common precursor, anatomically similar to area F3 in macaque, as a consequence of the differentiation of a single field into two fields (Geyer et al., 2012). Finally, connections from SMA proper were reported to the corticospinal tract, precentral gyrus, and ventrolateral thalamus, whereas connections from pre-SMA were found to the superior frontal gyrus, medial parietal cortex, inferior frontal cortex and anterior thalamus.

## **1.2.2 Functional organization**

### **1.2.2.1 PMD**

We have already seen that PMD seems to play a planning and controlling role over movement production in monkeys. There is evidence that something similar may happen also in humans, but it is worth noting that the results are somehow less robust, being sometimes inconsistent between studies, possibly because they took advantage of very different experimental paradigms involving different tasks and using different techniques<sup>6</sup>.

For instance, repetitive TMS applied over PMD have been demonstrated to determine changes in motor excitability, where these changes turned out to involve an increased or a decreased motor excitability (Gerschlagler, Siebner, & Rothwell, 2001; Münchau, Bloem, Irlbacher, Trimble, & Rothwell, 2002) – and this because the connections between PMD and M1 are both facilitatory and inhibitory (Gosh & Porter 1998; Tokuno & Nambu, 2000). By combining TMS and PET

---

<sup>6</sup> Given our current purposes, we shall mainly focus on TMS studies which provided a privileged way of exploring the contribution of PMD in controlling and initiating movements.

methods, Chouinard et al. (2003) showed that low level repetitive TMS applied both over PMD and M1 produced similar inhibitory effects on MEPs, but influenced cerebral areas differently, with PMD being embedded in larger network than M1, which encompasses frontal and parietal regions typically involved in coupling arbitrary sensory cues to actions.

Facilitatory and inhibitory effects of PMD over M1 have been also investigated by using dual-coil TMS technique (for more details on this technique see [Section 2.1](#)). For instance, Mochizuki et al (2004) found that a condTMS over the right PMD at 90% or 110% of the resting motor threshold (RMT) reduced the amplitude of MEPs in hand muscles elicited by a testTMS to the left M1. The effect was more evident when the interstimulus interval (ISI) was 8–10 ms. On the contrary, Baumer et al. (2006) found facilitation of contralateral test MEPs, when they applied left PMD conditioning stimuli of lower intensity, i.e. 80% active motor threshold (AMT) at ISI = 8 ms prior to test MEPs elicited from the right M1.

Koch et al. (2006) asked subjects to hold an isometric object in each hand and to squeeze the appropriate hand as rapidly as possible after an arbitrary auditory cue (low or high tone) was presented. The action was monitored by recording the muscle activity in the right or left 1DI muscle. Facilitatory and inhibitory left PMD – right handM1 interactions were tested at 50, 75, 100, 125, 150, 200 ms after the auditory cue presentation. They found that excitability of the left PMD–right handM1 interactions was considerably modulated. The inhibitory or excitatory interactions that could be probed at rest were no longer evident during most of the task. As pointed out by the authors (see also Rothwell, 2011, for a review), it was as if placing subjects in a situation where they were prepared to move at any time had an immediate effect on the “resting state” connectivity

observed in relaxed subjects. However, at specific intervals in the reaction period, this pattern changed. Facilitatory connections from left PMD to right handM1 became excitable 75 ms after a tone that indicated subjects should move the left hand, whereas inhibitory connections were more excitable 100 ms after a tone indicating a movement of the right hand (while the left hand remained stationary). In effect, output to the intended left hand movement was in receipt of facilitatory input early in the reaction period, whereas if the left hand had to remain stationary then inhibitory input was prominent. These connections were modulated only for muscles that might be involved in the upcoming movement; no effects were observed in non-involved muscles.

Similar results have been obtained by O'Shea et al. (2007). They tested PMD–handM1 inter-hemispheric interaction during action selection with visual rather cues. Since Mochizuki et al. 2004 showed that MEP amplitude can be altered by applying a conditioning TMS pulse to the contralateral PMD 8 ms prior to the M1 pulse, O'Shea and colleagues investigated whether the causal impact of the PMD pulse on M1, at this same interpulse interval, would change during the process of response selection. They found that PMD–M1 pulses applied 75 ms after a cue to select a manual response facilitated MEPs. MEPs were also facilitated at 50 ms in a control task of response execution, suggesting that PMD–M1 interactions at 75 ms are functionally specific to the process of response selection. Dual-pulse confined to M1 did not produce these effects, confirming the causal influence of PMD inputs. These results were combined with an analysis of the individual patterns of anatomical connectivity between PMD and handM1 as revealed with fMRI of each subject's brain. Measurement of the fractional anisotropy of the white matter linking these areas (a measure of the directional

diffusion of water molecules, which is thought to relate to the degree of organization of the connection) showed that subjects who had the greatest modulation of PMD–M1 excitability also had the greatest fractional anisotropy of the anatomical connection.

Finally, Civardi et al (2001) explored the cortical the connections between premotor areas and M1 with the dual-coil approach in the same hemisphere. They found that stimulation at two sites anterior to the motor cortex could reduce the amplitude of responses to an M1 test pulse if the interval between the pulses was around 6 ms. They speculated that these sites corresponded to PMD and supplementary motor areas (SMA) respectively.

Although inhibitory (or facilitatory) activity in the module of PMD-M1 cannot be considered *per se* as evidence for an inhibitory (or facilitatory) role of PMD on action initiation (on this point see Miniussi et al., 2008; Miniussi, Ruzzoli, & Walsh, 2010), some data seems to suggest a controlling role of PMD over M1. Patients with focal lesions, especially in the left superior portion of BA6 (putative PMD and SMA), have been demonstrated to succumb to an increased number of false alarms, thus revealing a clear deficit in inhibiting responses to a no-go stimulus (Picton et al., 2007).

### 1.2.2.1 SMA and pre-SMA

Several lines of evidence suggest that SMA and pre-SMA are involved in action planning and control also in humans, even if their precise role in these functions is still matter of controversy. For instance, brain imaging studies reported greater activity in pre-SMA when actions were internally chosen instead of being driven by some external cues (Deiber, Honda, Ibañez, Sadato, & Hallett, 1999; Jenkins, Jahanshahi, Jueptner, Passingham, & Brooks, 2000; Nachev, Rees, Parton,

Kennard, & Husain, 2005). This seems not to be true for SMA, which turned out to be activated similarly before both internally and externally generated actions (Cunnington, Windischberger, Deecke, & Moser, 2002). Interestingly, SMA has been shown to be also active when people merely view graspable objects, without any intention to act upon them (Grèzes & Decety, 2002). Such an activity has been interpreted in terms of an automatic inhibitory process concerning actions, which might be afforded by the viewed object but are in fact not required to be performed (see Nachev, Kennard, & Husain, 2008). This interpretation is consistent with lesion data indicating that patients with microlesion of SMA, differently from healthy people and control patients with pre-SMA damage, are impaired in automatic suppression of evoked motor plans (Sumner et al., 2007). On the contrary, pre-SMA lesions can lead to a selective deficit in the ability to inhibit a response in the context of competition between actions (Nachev et al., 2008).

Brain imaging studies have suggested that pre-SMA activity may be related to altering motor plans, by stopping a given movement or by switching from one movement to another (Curtis, Sun, Miller, & D'Esposito, 2005; Li, Huang, Constable, & Sinha, 2006). Successful stopping is associated with pre-SMA activation, but the magnitude of activation in pre-SMA did not correlate with SSRT (Aron et al., 2007). There is evidence that right inferior frontal gyrus is also involved in stopping (Rubia, Smith, Brammer, & Taylor, 2003) and it has been hypothesized that right IFG contributes to response inhibition and not to monitoring performance or adjusting behavior (Chevrier, Noseworthy, & Schachar, 2007), whereas pre-SMA seems to be mainly involved in monitoring or resolving the conflict between the opposing task demands in the stop-signal paradigm (Nachev,

Wydell, O'Neill, Husain, & Kennard, 2007). Response inhibition is impaired in patients with lesions to right IFG but not left IFG (Aron, Fletcher, Bullmore, Sahakian, & Robbins, 2003); moreover, the magnitude of the lesion to right IFG correlated with SSRT but not with go RT. Similarly, lesions to right SMA and pre-SMA impaired stopping without influencing going very much (Floden & Stuss, 2006).

More recently, a meta-analysis (Swick et al., 2011) conducted on 21 brain imaging studies, which investigated motor inhibition by using either GO/NOGO or stop-signal tasks, pointed to the functional relevance of the pre-SMA for successful performance in response inhibition across the two different tasks. Finally, and even more interesting for our purposes, Obeso et al (2013) combined repetitive TMS (rTMS) with PET scans during a stop-signal task. The results showed that rTMS over the pre-SMA increased the efficiency of the inhibitory control over powerful ongoing responses. A significant interaction was present in the left IFG along with an increase in regional cerebral blood flow (rCBF) in the left pre-SMA, left IFG, right premotor and right inferior parietal cortex.

## CHAPTER 2: GENERAL METHODS

In the previous chapter, we have introduced and discussed some relevant anatomical and functional properties of the dorsal precentral region, with particular emphasis on its putative role in initiating and controlling action. In this chapter we shall focus on the methodological aspects of our studies, which will be described in detail the following chapters (see [Chapters 3-5](#)).

More specifically, in the [section 2.1](#) we shall introduce the so-called twin- or dual-coil TMS paradigm, discuss its main approaches present in the literature and propose a variant of the conventional paradigms. This novel approach paves the way to an innovative investigation of the contribution of human PMD to action planning and control, or so we shall argue and provide evidence for. In the [section 2.2](#) we shall outline the overall experimental procedures at the basis of our studies.

## 2.1 A VARIATION ON THE DUAL-COIL TMS APPROACH

### 2.1.1 Introduction<sup>7</sup>

Transcranial magnetic stimulation (TMS) allows the stimulation of the human brain through the intact skull without producing significant discomfort (Barker, Jalinous, & Freeston, 1985). This stimulation of the human brain is characterized by a high temporal resolution and a spatial resolution allowing for high focality also in addressing cortical areas during cognitive tasks (see [Figure 2.1](#))

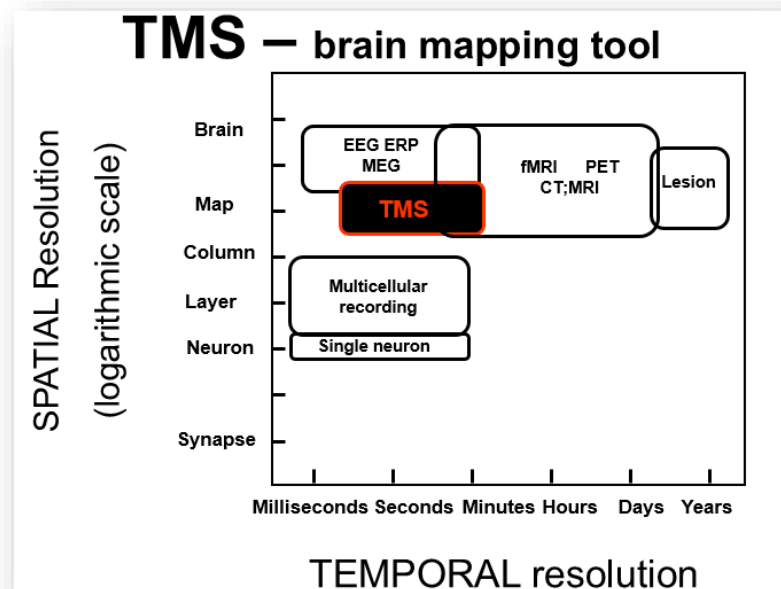


**Figure 2.1** Temporal and spatial resolution of the main investigation techniques in cognitive neurosciences.

The stimulator consists of a wire causing a large current, usually around 2000 A, to flow for 1 or 5 ms typically. This current produces a large equally

<sup>7</sup> A survey of all the different TMS paradigms used in the motor and cognitive domains is out of the scope of this introductory section. We will focus here on the foundations of TMS dual-coil approach only.

transient magnetic field which penetrates the scalp and skull easily, and because it changes so rapidly (from zero to a very large value, then back again to zero in 1 ms) it induces electrical currents in the brain under the coil. The induced current pulse lasts about 200  $\mu$ s. The intensity of the magnetic field declines quickly with distance from the coil. So, provided that the stimulus intensity is not very high, neural activation is limited to elements in the cortex or subcortical white matter, or so it is usually assumed (see Rothwell, 2011 for a review).

Most of the experimental work on the effects of TMS has been performed on the human motor cortex. Stimulation here produces a visible muscle twitch that is readily measured using EMG electrodes and which provides considerable insight into the action of TMS within the brain. The main features of the response to a single TMS pulse recorded in a voluntarily pre-activated muscle are a short latency excitatory EMG potential (motor-evoked potential, MEP) followed by a much longer lasting period of silence in the ongoing EMG.

TMS has been used in the motor domain in two main ways:

- (I) by recording the variations of cortical output (the MEP) in different experimental situations
- (II) by interfering with a given aspect of motor behavior after focal stimulation of specific nodes in the motor system.

The first study presented and discussed in the current thesis took advantage of the first application of TMS (see [Chapter 3](#)), while the second and third study mainly capitalized on the second application (see [Chapters 4 and 5](#)).

As Rothwell (2011) pointed out, the simplest example of TMS connectivity is the MEP in response to stimulation of M1. This is the consequence of a nervous impulse transmitted through at least two synaptic connections from the

corticospinal tract to the spinal motoneuron at the spinal cord and from peripheral motor axon to muscle in the periphery. The consequence of TMS-induced activity in the corticospinal tract is easy to be measured. However, TMS stimulation of motor areas generally have many other outputs that are much more difficult to detect.

In order to probe connectivity between structures, a number of paradigms allow now for detecting the motor cortical outputs of a TMS pulse in a variety of cortical, subcortical and brainstem site. The most employed paradigms combined TMS with :

- (I) EEG: TMS at one point on the scalp evokes EEG activity at other scalp sites; or with
- (II) fMRI: TMS pulses given in an fMRI scanner lead to changes in BOLD activity distant from the site of stimulation.

Technical considerations mean that TMS–EEG is perhaps simpler to combine than TMS–fMRI as well as having a higher temporal resolution, although fMRI has the advantage of being able to monitor activity in projections to deep structures such as thalamus, basal ganglia, and cerebellum, which are not identifiable in EEG (Bestmann et al., 2008).

A further paradigm often employed is the so-called twin- or dual-coils TMS paradigm. This paradigm involves the use of two magnetic stimulators connected to two distinct coils, both of which are used simultaneously on the participant's scalp. One coil (testTMS) is placed over the primary motor cortex and delivers supra-threshold stimuli, ultimately generating motor evoked potentials (MEPs). Prior to the testTMS stimulus, a conditioning stimulus (condTMS) is delivered by a second coil (see [Figures 2.2](#) and [2.3](#)). The second coil is placed over a cortical

area that is hypothetically connected to M1. If the prior delivery of condTMS were to change the amplitude of MEPs generated by testTMS, this would indicate that there is an influence of the cortical area on M1 (Rothwell 2011).



**Figure 2.2** An example of a twin or dual-coil setting.

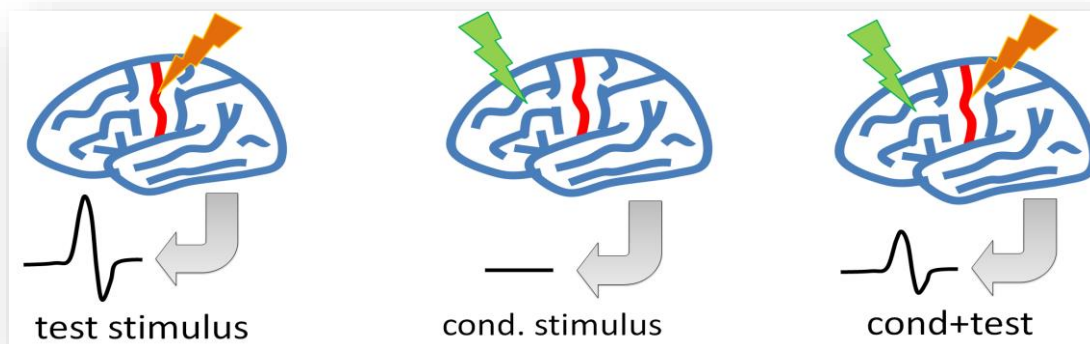


**Figure 2.3** Schematic summary of the dual-coil procedure.

There are two main characteristic properties of this paradigm that made it particularly appealing for our purposes. First, it allows for detecting inputs from various cortical areas onto M1. Second, it is particularly appropriate for investigating both the structural connectivity and the functional interference during action planning and control (Rothwell 2011).

A large number of dual-coil TMS studies have been carried out over the last twenty years. They mainly differ from one another because of the targeted areas as well as of the TMS setting. Indeed, some studies have investigated the transcallosal connectivity between M1 in the 2 hemispheres (Chen et al., 2003; Daskalakis, Christensen, Fitzgerald, Roshan, & Chen, 2002; Di Lazzaro et al., 1999; Ferbert et al., 1992; Hanajima et al., 2001), while others have probed structural and functional connectivity between supplementary motor or premotor areas and the ipsilateral or contralateral M1. Given the aim of the current thesis, in the following sections we will focus mainly on the dual-coil TMS studies testing structural and functional connectivity between PMD and M1.

### **2.1.2 Inter-hemispheric dual-coil TMS approaches<sup>8</sup>**

As already mentioned in the previous chapter, there is robust evidence that PMD is somatotopically organized, with hand and arm movements highly represented. Is it therefore not surprising that TMS dual-coils studies mostly targeted PMD and the hand-related M1 (from now on hand-M1). However, this was not without limitations and difficulties.

The main technical difficulty involved in applying the dual-coil paradigm arises from the close proximity between the PMD and hand-M1 (Heidi Johansen-

---

<sup>8</sup> In this and in the following sections we will consider the reviewed studies from a methodological and procedural point of view. For a description of their results see [Chapters 1, Section 1.2.2.1](#).

Berg et al., 2002; Schluter, Rushworth, Passingham, & Mills, 1998). To illustrate, consider the ventral premotor cortex (PMV) or the mesial supplementary motor areas (SMA): the distance between these areas and the hand-M1 does not represent a technical obstacle: two commercially available coils (65/70 mm) can be easily used to selectively stimulated the targeted areas. On the contrary, in the case of the PMD, the actual distance from the hot-spot of the hand-M1 seems to be too short both for placing two commercially available coils in a way to ensure the selective stimulation of the two targeted cortical sites. Indeed, functional imaging studies indicate that the focus of PMD activity is around 1.5-2 cm from the ipsilateral handM1 (Amiez et al. 2006; Fink et al. 1997; Schluter et al. 1998). This can be inspected from **Figure 2.4** (see in particular subfigures (a) and (d)).

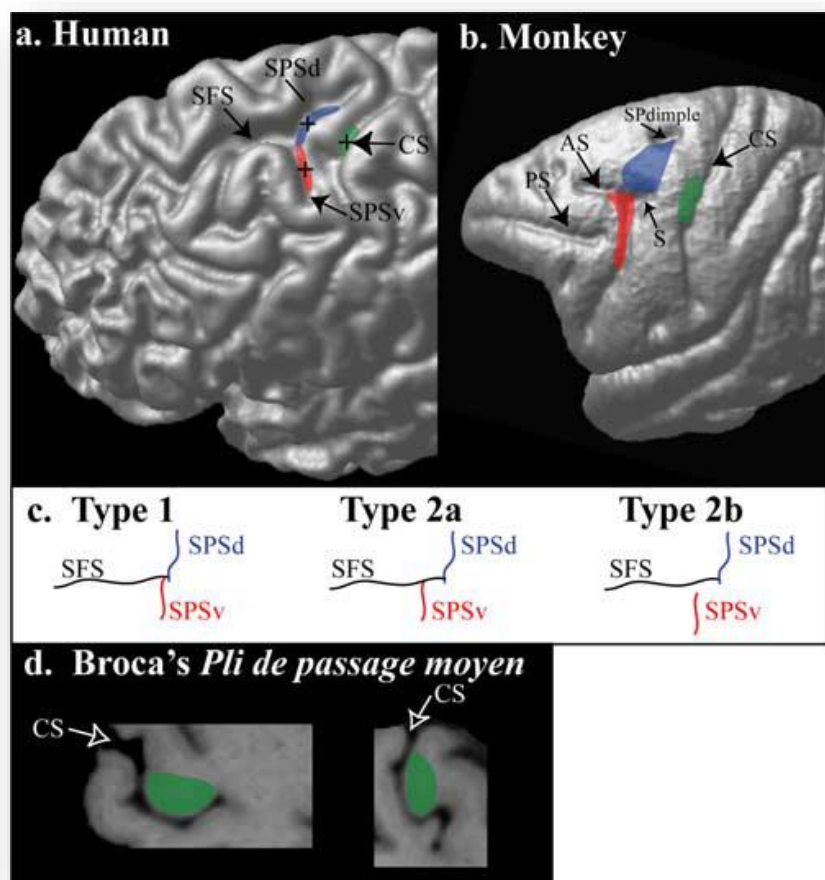


**Figure 2.4** The premotor hand region (blue) the saccadic eye movement region (red), and the hand-M1 (green) in the human (a) and monkey (b) frontal cortex. (c) Schematic representation of the sulcal patterns in the dorsal premotor region of the human brain. (d) the hand-M1 (area 4) in the human brain lies within the central sulcus at the level indicated in green in a. Within the central sulcus, the hand representation occupies a distinct morphological feature, a fold known as the precentral knob. A horizontal (left) and a sagittal (right) section through this part of the central sulcus illustrate this distinct morphological feature. CS, Central sulcus; AS, arcuate sulcus; PS, principalis sulcus; S, spur; SPdimple, superior precentral dimple. From Amiez et al., 2006.

Many researchers have tackled the proximity problem by targeting the contralateral cortices.

To our knowledge, the first TMS study directly investigating the inter-hemispheric PMD-M1 structural connectivity was carried out by Mochizuki, Huang, and Rothwell (2004). They delivered the condTMS pulse over the right PMD and measured the amplitude of MEPs in hand muscles elicited by a testTMS coil applied over the left M1. Similarly, Baumer et al. (2006), applied a conditioning stimuli to the left PMD in order to record MEPs in the left first dorsal interosseus muscle (1DI) elicited from the test stimulation of the right hand M1 (see **Figure 2.5**).

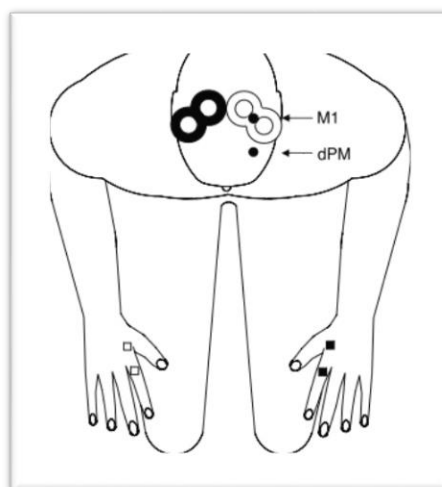


**Figure 2.5** A dual-coil experimental set-up illustrating the position of two 70 figure of eight TMS coils on subject's head. TMS test pulses were applied over right hand-M1 (filled coil), while TMS conditioning pulses were given over M1 and PMd (open coil). MEPs were recorded from the left first dorsal interosseus muscle (1DI).

The dual-coil TMS approach was further used to characterize the variations of PMd-M1 connectivity in different aspects of motor behaviour. For instance, Koch et al. (2006) asked participants to squeeze with their hands an isometric object as soon as they heard a cue sound. In the interval between the auditory cue and the movement onset, PMD–handM1 interactions were probed by recording participants' muscle activity from the right (or left) 1DI muscle following the deliverance of the condTMS pulse onto the left PMd and the test-TMS pulse onto the right hand-M1 (see **Figure 2.6**).

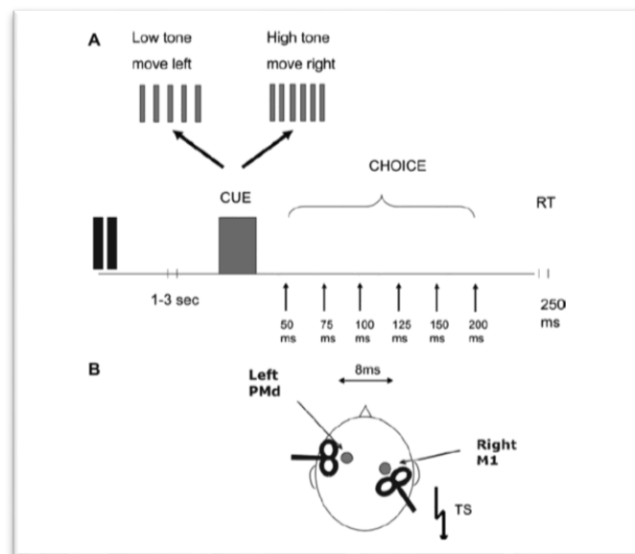


**Figure 2.6** (A) Participants hear a high or a low tone that signals that they should move the right or the left hand as quickly as possible. In the interval between the tone and the movement, PMD–handM1 interactions are probed with the dual-coil TMS approach. (B) Schematic illustration of the coil positions on the head that were used in this experiment (TS, testTMS) (Koch et al., 2006; Rothwell, 2011).

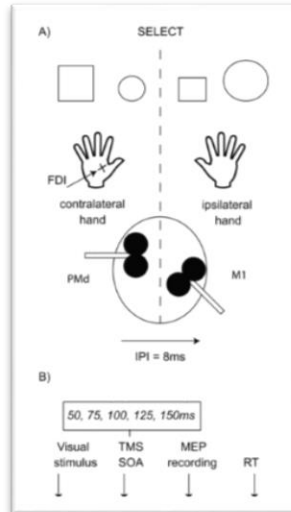


**Figure 2.7** (A) Experimental set-up. During the Select task, a single shape stimulus was presented on each trial, and subjects made an index finger button-press response with the right or left hand according to a learned rule. The condTMS coil was placed over the PMD while the testTMS coil was applied over the contralateral handM1. MEPs were recorded from 1DI muscle contralateral to the stimulated hand-M1. (B) Time course of a single trial. A visual shape stimulus was presented until the button press response. Following stimulus presentation, TMS was delivered according to the trial type. TMS onset occurred at one of five SOAs: 50, 75, 100, 125 or 150 ms after the onset of the visual stimulus (O’Shea, 2007).

A similar approach can be also found in O’Shea et al., (2007). They tested PMD–handM1 inter-hemispheric interaction during action selection with visual rather than acoustic cues (see Figure 2.7).

### 2.1.3 Intra-hemispheric dual-coil TMS approaches

In the previous section we have reported some dual-coil TMS studies investigating the PMD-handM1 connectivity from both a structural and a functional point of view. All these studies delivered the condTMS and testTMS pulses over PMD and the contralateral M1, so that the measured effect (MEPs modulation) was mainly mediated by a transcallosal pathway between the two hemispheres. This pathway

was compatible with the existence of direct commissural fibers from PMD to contralateral M1 in monkeys (Marconi, Genovesio, Giannetti, Molinari, & Caminiti, 2003).

While the inter-hemispheric PMD-M1 connectivity has been extensively explored, much less research has been devoted to investigate the intra-hemispheric PMD-M1 connectivity. A seminal study has been carried out by Civardi et al. (2001). They used two very small TMS stimulating coils (eight coil with 4 cm diameter internal loop) applied over M1 and two ipsilateral sites which speculatively corresponded to PMD and supplementary motor areas (SMA), respectively (see Figure 2.8). In this pioneering study however, the putative sites of condTMS were re-evaluated a posteriori and are probably represented by more cranial structures.

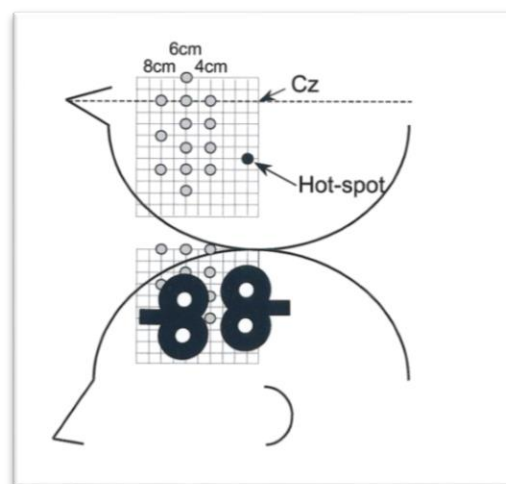


**Figure 2.8:** The scalp locations at which the cortical stimuli were delivered. The hot spot for activating the right FDI is shown by the filled black circle. The 13 points at which conditioning stimuli were applied are shown in gray (Civardi et al., 2001).

More recently, Groppa et al. (2012) applied dual-coil TMS over the left PMD and the ipsilateral hand-M1 by using two special noncommercial minicoils (see [Figure 2.9](#)).

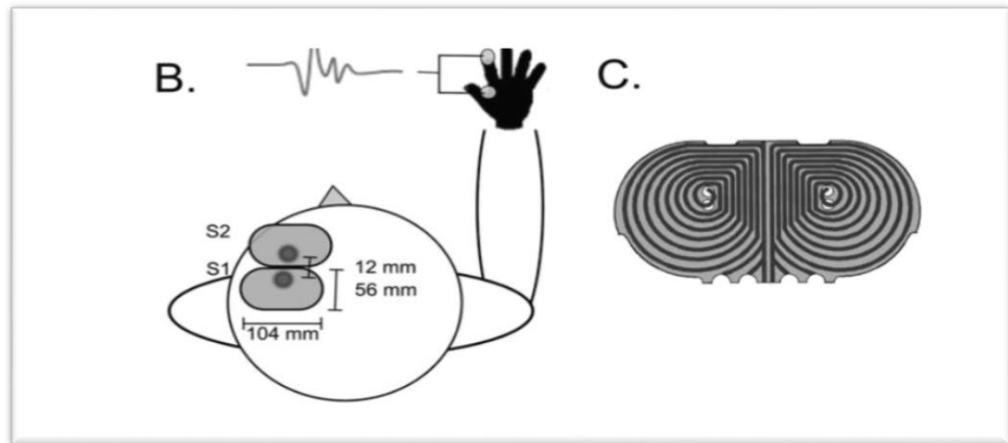


**Figure 2.9:** (B) View of the two mini-coils aligned to each other. The stimulation current was switched in one coil and achieve same current direction in both coils. (C) Schematic drawing of the decentral coil windings. (Groppa et al., 2012).

Finally, a dual-coil setting in the same hemisphere was also attempted in a study with patients. Beck and colleagues (2009) aimed to assess the role of left PMD in patients with focal hand dystonia (FHD). They used a dual-coil TMS paradigm, with a sub-threshold condTMS pulse over the left PMD followed by a supra- threshold testTMS pulse over the ipsilateral hand-M1. The targeted PMD portion was the same as in Civardi et al., (2001). Its coordinates were 8% of the individual distance between nasion and inion (i.e., approx. 3cm) anterior and 1cm medial to the “motor hotspot” for 1DI. The condTMS coil was placed in antero-posterior direction with the handle pointing forward, while the testTMS coil was positioned perpendicular to the central sulcus. So, “due to spatial interference of the two coils, the conditioning coil was placed directly on the skull, while the test

pulse coil over M1 was slightly elevated” (see [Figure 2.10](#); an analogous dual-coil TMS paradigm has been developed by Pirio Richardson et al. 2014 ).



**Figure 2.10** Coil placement. When both coils were used together, the test coil over M1 was slightly elevated, if needed, and stimulation intensity was adjusted to evoke a test MEP of 1mV in all subjects. A tightly fitting cap was used to mark and control coil placement throughout the experiment (Beck et al., 2009).

#### **2.1.4 From hand to mouth: a novel dual-coil TMS approach**

The dual-coil TMS studies reviewed in the two previous sections provided two different ways of meeting what we may call the *coil placement* and *selective stimulation* requirements. The distance between PMD and the hot-spot of the ipsilateral hand-M1 seems to be too short for placing commercially available coils in a way to ensure the selective stimulation of the two targeted cortical sites.

As we have seen above ([Section 2.1.2](#)), the most intuitive and influential strategy was to place the condTMS coil over the PMD and the testTMS coil over the contralateral hand-M1. This strategy suitably meets both the coil placement

and the selective stimulation requirements. But it prevented from raising any question about the intra-hemispheric cortico-cortical connections between PMD and M1 as well as their functional properties, of course.

On the contrary, the dual-coil TMS studies examined in the [Section 2.1.3](#) aimed to directly face these questions, exploring the intra-hemispheric structural and functional connectivity between PMD hand-M1. They also met the coil placement requirement by either reducing the coil sizes or overlapping them. However, both these solutions did not fully ensure the selectivity of the stimulation, even when very small custom-made coils were employed. Indeed, coil size reduction did rule out the possibility that the pulse of one coil spread over targeted site of the other coil, and vice-versa: the condTMS pulse delivered over PMD could also affect portions of hand-M1 which should be reached by the testTMS pulse only, and *vice-versa*. In our own data we acquired clear evidence in favor of this possibility: stimulating the caudal portion of PMD produced MEPs in the distal upper limb in more than one third of the tested subjects. It is highly plausible that the MEPs were due to spreading of current to the adjacent M1 (for more details on this point see [Section 3.4](#)).

All of this indicates that, on the one side, the inter-hemispheric approaches suitably meet both the coil placement and selective stimulation requirements, but the inter-hemispheric PMD-M1 connectivity was left completely uninvestigated. On the other side, the intra-hemispheric approaches aimed to explored such connectivity, but they did not fully meet the selective stimulation requirement, and this might undermine, at least partly, their results. We proposed a variant of the intra-hemispheric dual-coil TMS paradigm that combines both the requirements. In a nutshell, this way consists in putting more distance between the two coils, by

applying the condTMS coil over PMD and shifting more ventrally the test-TMS coil over the ipsilateral M1, where orofacial movements, rather than hand movements, were represented (mouth-related M1, from now on mouthM1), and recording the MEPs from the *orbicularis oris* muscle (OOr). To make it vivid, consider the **Figure 2.11** clearly illustrating that the more lateral is the representation of a muscle or an effector in M1, the more distant from the ipsilateral PMD, and the **Figure 2.12** depicting the proposed approach.

At first glance, this dual-coil TMS approach seems to provide more problems than solutions. As reported in Chapter 1, there is a robust evidence in both non-human primates and humans that PMD is primarily concerned with planning and controlling limb movements, while there are no studies on non-human primates reporting the presence of a mouth representation in PMD. How to deal with it?

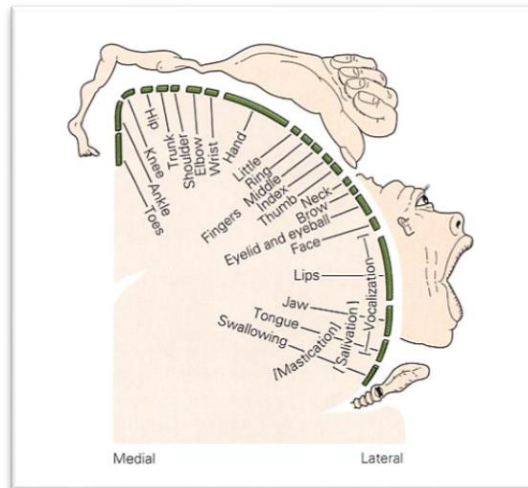


**Figure 2.11** The somatotopic organization of M1 in humans. The more lateral is the representation of a muscle or an effector, the more distant from the ipsilateral PMD.

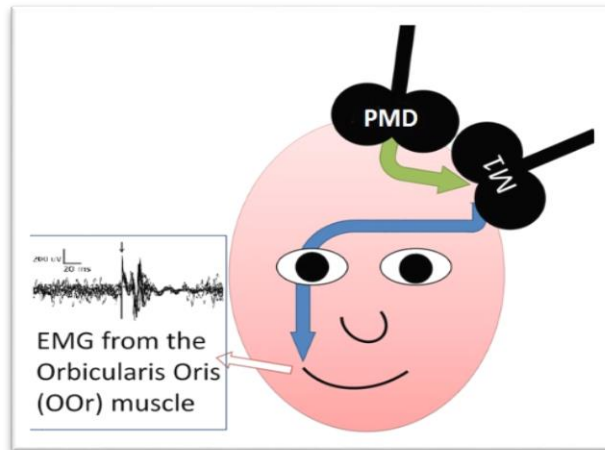


**Figure 2.12** A cartoon depicting our dual-coil experimental approach

A working hypothesis could be that in humans the lower face evolved a much larger motor representation in M1 and that the PMD developed a lip/mouth representation. This would be also in line with the evidence of the emergence of direct cortico-motorneuronal connections (Kuypers, 1958).

The main aim of our first study was to test this hypothesis. In doing this we couldn't make any a priori assumption on the PMD topography, of course. For this reason we decided to stimulate 3 different standard spots along the superior frontal sulcus (sFS) identified on individual anatomical MRI scans by means of frameless stereotaxic neuronavigation. As illustrated by Figure 2.13, the position of these spots was planned to cover in a caudo-cranial direction the whole span of dorsal BA6 (Brodmann, 1909; Geyer, 2004). The scalp projection of the mouthM1 was functionally localized as the spot where highest amplitude MEPs were elicited with the minimal intensity in the muscle of interest.

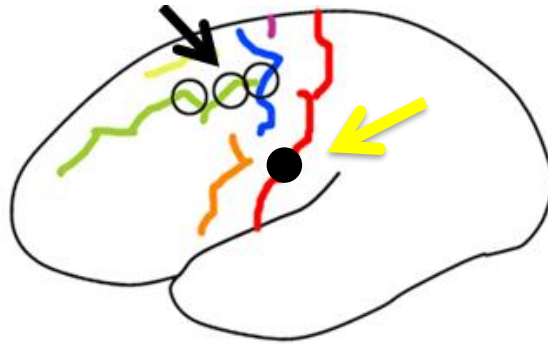


**Figure 2.13** Schematic picture of the stimulation sites along the sFS in the dorsal portion of BA6 (our condTMS target) in one of the subjects of our first experiment. The three circles represent the three different points of stimulation; the black arrow indicates the effective spot (condTMS); the yellow arrow the mouth M1 target of stimulation (testTMS). For more details, see [Chapter 3](#).

What we found was that there was a spot in PMD that, when suitably stimulated by a condTMS pulse, consistently affected the MEPs resulting from delivering the test-TMS pulse on the ipsilateral mouth-M1. The spot was located 1.5 cm rostral to correspond to the junction between the superior precentral sulcus (sPreCS) and the sFS. This allowed us to demonstrate, for the first time, not only the existence of a mouth representation in the PMD, but also the possibility of an intra-hemispheric dual-TMS coil approach overcoming both the coil placement and selective stimulation problems. Both these findings will be extensively presented and discussed in the next chapter ([Chapter 3](#)).

## 2.2 EXPERIMENTAL PROCEDURES

In this section, we shall outline the overall experimental procedures which are common to all the experimental studies introduced and discussed in the following chapters. More in detail, we shall describe how the ultrasound tracking system we employed to neuronavigate the participants' brain (Section 2.2.1), how we recorded the EMG signal (Section 2.2.2), the stimulator setting and the coils we used (Section 2.2.3), and finally the devices of the response acquisition (Section 2.2.4).

### 2.2.1 Neuronavigation

In each of our studies the positioning of the coils in non-primary motor areas (i.e. PMD and SMA) was achieved by means of frameless stereotaxic neuronavigation investigating macro-anatomical anatomical landmarks. Therefore, before the TMS experimental sessions, each subject underwent a scan of the brain in order to acquire the structural magnetic resonance images (MRI), which allowed a detailed investigation of the relevant anatomy of each subject and the MRI-neuronavigated positioning of the coils. A high-resolution T1-weighted magnetization prepared rapid gradient echo sequence (176 axial slices, in-plane resolution 256 x 224, 1-mm isotropic voxels, generalized autocalibrating partially parallel acquisition with acceleration factor = 2, time repetition = 2700 msec, time echo = 4.180 msec, time to inversion = 1020 msec, flip angle = 7°) scan of the brain of each subject was obtained using a MedSpec 4-T head scanner (Bruker BioSpin GmbH, Rheinstetten, Germany) with an 8-channel array head coil. Starting from this scan, a 3D reconstruction of the scalp and the grey matter surfaces (see Figures 2.14

and 2.15) was produced using MesH morphing tool included in the Brainvoyager software (Brain Innovation BV, The Netherlands).

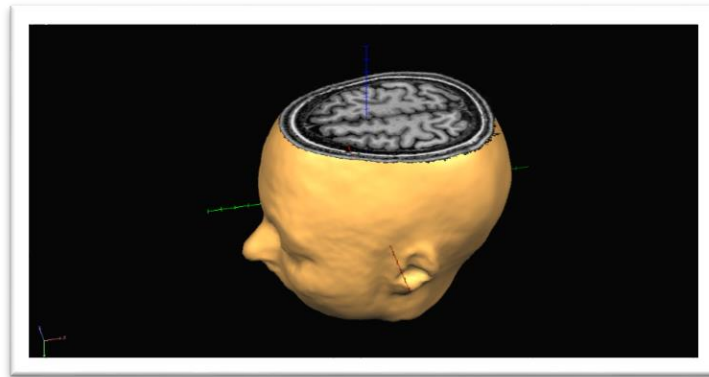


**Figure 2.14** 2D Reconstruction of the brain and 3D reconstruction of the scalp.

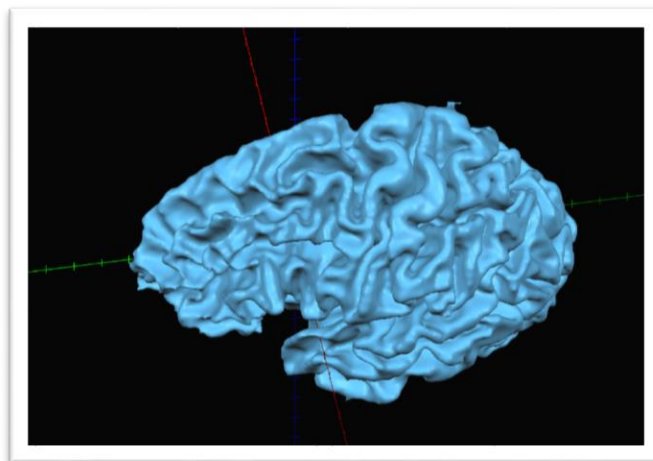


**Figure 2.15** 3D rendering of the surface of the grey-white matter border, used for neuronavigation.

We investigated the anatomy in the brain MRIs of all participants in the AC-PC (Anterior Commissure-Posterior Commissure) native space. Afterward, the BrainVoyager neuronavigation software combined with an ultrasound tracking system, CMS205S (Zebris Medical GmbH, Isny, Germany), was used to coregister

the 3D scalp reconstruction with the actual participant's head, thus marking the target points for TMS on the real head.



**Figure 2.16** Our ultrasound tracking system.

### **2.2.2 EMG recordings**

The right side of the OOr and the right 1DI were recorded with surface electrodes in the first two studies (see **Chapters 3 and 4**). TestTMS coil for the first two studies was therefore applied to M1 at the point where largest MEPs could be elicited from the OOr muscle. In the third study, also the right *tibialis* anterior muscle (TA) was recorder.

On the OOr the two electrodes were placed parallel to the muscle fibers on the lower lip. The montage of all the muscles is depicted in **Figure 2.17**. The analog signal was amplified 1000x and band-pass filtered between 5 Hz and 2 kHz and by means of a 1902 two-channel amplifier (Cambridge Electronic Design, Cambridge, UK).

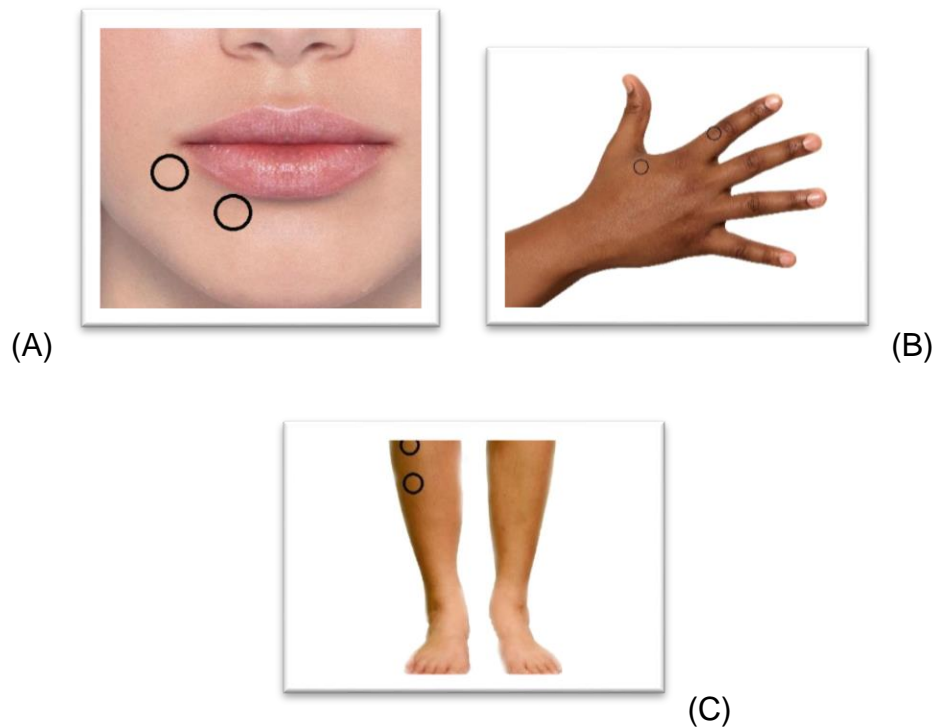


**Figure 2.17** Electrodes montage for the three effectors. (A) OOr, (B) 1DI, (C), TA

In all the studies, participants were given a stick to be held in their mouth with their lips only and in the first two studies (Chapters 3 and 4) they were asked to generate muscular tension matching a peak-peak amplitude of the EMG signal of around 200  $\mu$ V. MEPs in the facial region may be difficult to obtain at rest because of high threshold of the orofacial motor cortex to TMS (Cattaneo & Pavesi 2013). It is therefore common practice to record facial MEPs during active contraction of the target muscle. The operator assisted them in finding the desired amount of contraction and monitored it during the whole experimental session. Furthermore, they could see the EMG signal on the screen of the computer and had to remain with their contraction into the boundaries of the two cursors indicating the required level of contraction (e.g. -0.1 mV and 0.1 mV). The analog EMG signal was then digitalized (with a sampling frequency of 4 kHz) by means of

a 1401 micro Mk-II unit (Cambridge Electronic Design). Recordings and triggers were dealt with via the Signal software (Cambridge Electronic Design).

### **2.2.3 TMS setting**

During the proper experimental sessions, participants wore earplugs and were sitting comfortably with their head on a chin rest and with an additional lateral head-constraint, which was adjusted individually to allow for a comfortable posture as well as to assure head stability and minimal movement. Coils were held by an articulated mechanical arm (Manfrotto 244, VitecGroup, Italy).

To achieve the dual-coil stimulation, two magnetic stimulators were used. The one delivering the testTMS to M1 was a MagPro stimulator (Medtronic, Denmark), connected to a figure-of-eight coil with 55 mm windings (Dantec B55, Skovlunde, Denmark), oriented perpendicularly to the midline with the handle pointing medially. The one delivering the condTMS over the PMD was a MagPro Compact (MagVenture, Skovlunde, Denmark), connected to an MC-B35 figure-of-eight coil with windings of 35 mm diameter (MagVenture, Skovlunde, Denmark); the condTMS coil was positioned tangentially to the scalp in varied orientations according to the mechanical interaction between the two coils (see [Figure 2.18A](#)). For the single-pulse paradigm (Chapter 5), the MagPro stimulator was connected to a MCFB65 coil with 65 mm windings (MagVenture, Skovlunde, Denmark) applied over PMD and SMA, respectively ([Figure 2.18B](#)). Sham stimulation was achieved with a MCF-P-B65 placebo figure-of-eight coil MagVenture, Skovlunde, Denmark).

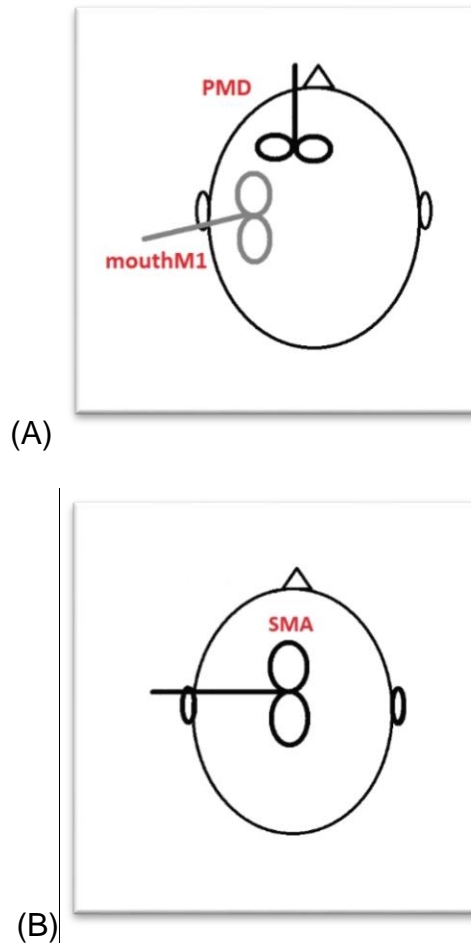


**Figure 2.18** Coils positioning. (A) In black the figure-of-eight coil (35 mm) for the condTMS over the PMD; in gray the figure-of-eight coil (55 mm) for the testTMS over the mouthM1. (B) The figure-of-eight coil (65 mm) for single-pulse stimulation over SMA.

### 2.2.4 Response acquisition

The stick held by the participant's lips weighted 15 g, and was connected to a circuit delivering a trigger signal through the USB port to the stimulus presentation PC. The trigger was delivered whenever the stick was lifted above a given height by means of the active movement of the lips during the voluntary response (see **Figure 2.19**). The timing of the response was logged by the E-Prime 2.0 software and displayed to give on-line feedback. At the same time, a 3-axes analog accelerometer embedded in the stick tip allowed a very accurate acquisition of the

onset and the evolution of the orofacial movements. The signal from the accelerometer was recorded by the 1401 micro Mk-II unit and stored by the Signal Software on a dedicated channel for offline analysis. The response times indicated by E-prime were used uniquely for the display of single-trial feedback. The reaction times (RT) to be used for the statistical analysis were collected on the accelerometer's recording, as the onset point of the deflection related to the voluntary response.

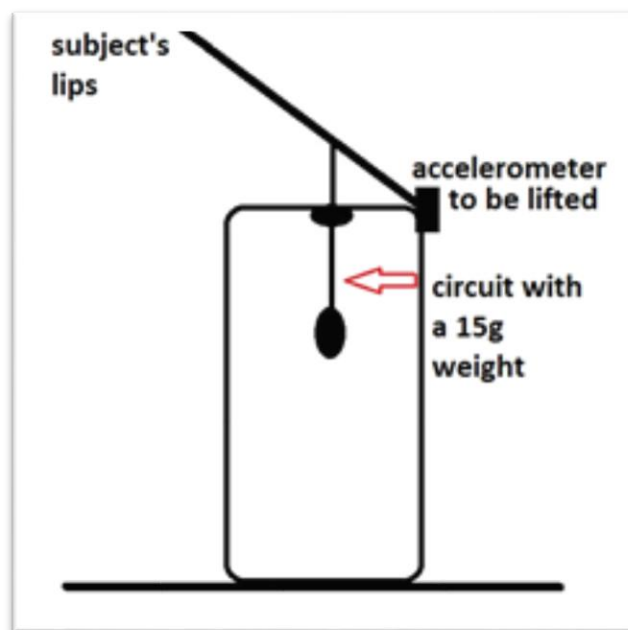


**Figure 2.19** A schematic drawing of our response acquisition device.

## **CHAPTER 3: THE HUMAN DORSAL PREMOTOR CORTEX EXERTS A POWERFUL AND SPECIFIC INHIBITORY EFFECT ON THE IPSILATERAL CORTICO-FACIAL SYSTEM**

### **3.1 ABSTRACT**

A rich pattern of connectivity is present in nonhuman primates between the dorsal premotor cortex (PMD) and the motor cortex (M1). By analogy, similar connections are hypothesized in humans between the PMD and the ipsilateral hand-related M1. However the technical difficulty of applying a dual-coil TMS paradigm to two cortical regions in such close spatial proximity renders their in-vivo demonstration difficult. The present study aims at assessing in humans the existence of short-latency influences of the left PMD on the ipsilateral corticofacial system by means of TMS. A dual-coil TMS paradigm was used with 16 participants. Test TMS pulses were applied to the left orofacial M1 and conditioning TMS pulses were applied to 3 distinct points of the ipsilateral PMD along the caudal part of sFS. The inter-stimulus interval (ISI) between condTMS and testTMS varied in 2 ms steps between 2 ms and 8 ms. MEPs in the active OOr muscle were recorded. CondTMS exerted a robust effect on the corticofacial system only when applied to one specific portion of the PMD and only at one specific ISI (6 ms). The effect consisted in a systematic suppression of facial MEPs compared to those obtained by testTMS alone. No other effect was found. We provide evidence for a specific short-latency inhibitory effect of the PMD on the ipsilateral M1, likely witnessing direct cortico-cortical connectivity in humans. We also describe a novel paradigm to test ipsilateral PMD-M1 in humans.

## **3.2 INTRODUCTION**

In this chapter, we present and discuss a dual-coil TMS study exploring, for the first time, the ipsilateral PMD-cortico facial system connectivity.

In Chapter 2 (see Section 2.1.2) we emphasized that most of the previous dual-coil TMS studies investigated the inter-hemispheric PMD-M1 connectivity (Baumer et al. 2009; Koch et al. 2006; Mochizuki et al. 2004; O'Shea et al. 2007). This because the spatial proximity between the PMD and the ipsilateral handM1 made prevented from a selective stimulation of either target on the same hemisphere.

In this study we adopted a different strategy: instead of the handM1, we stimulated mouthM1, which is located ventrally. Test TMS pulses were applied to the left mouthM1 and conditioning TMS pulses were applied to 3 distinct sites of the ipsilateral PMD along the caudal part of sFS. The inter-stimulus interval (ISI) between condTMS and testTMS varied in 2 ms steps between 2 ms and 8 ms. MEPs were recorded from the active OOr muscle.

This novel paradigm allowed us to solve the problem of the selective stimulation of the targeted areas, providing direct evidence for a specific short-latency inhibitory effect of the PMD on the ipsilateral M1, likely witnessing direct cortico-cortical connectivity in humans.

## **3.3 METHODS**

### **3.3.1 Participants and general protocol**

Sixteen healthy volunteers (11 women, mean age 25.13, range 19-32, SD 3.76) took part in this study. All gave written informed consent to the experiment and none had contraindications to TMS (Rossi & Hallett, 2009). This study was

approved by the University of Trento Ethical Committee (protocol 2031-032) and conducted in compliance with the revised Helsinki declaration (Association, 2009).

The present work aimed at assessing the short-latency influences of the left PMD on the ipsilateral corticofacial system with the dual-coil technique. CondTMS was applied to the PMD and testTMS was applied to the orofacial motor cortex (mouthM1). The scalp projection of the mouthM1 was functionally localized as the spot where highest amplitude MEPs were elicited with the minimal intensity. On the contrary, there was no clear a priori hypothesis on the PMD topography and therefore three different points were tested in the standard positions of the Brodmann area 6 along the superior frontal sulcus (sFS). The three points were identified on individual anatomical MRI scans by means of frameless stereotaxic neuronavigation (see [Section 2.2.1](#)). Participants were tested during active contraction of the lips but with no other active task.

### **3.3.2 Localization of TMS targets**

In each participant, three different stimulation points over the putative dorsal premotor region were identified. The 3 spots will be referred to as P1-P3 and were identified on the basis of macro-anatomical landmarks. P1 was located to correspond to the junction between the superior precentral sulcus (sPreCS) and the sFS. The two other spots were located along the sFS. P2 was located 1.5 cm rostral to P1 and P3 was located 3 cm rostral to P1. Variability in the morphology of the precentral sulcal pattern of this region is subject to considerable inter-individual variations (Germann, Robbins, Halsband, & Petrides, 2005) and therefore needed accurate participant-by-participant investigation. In certain participants, the sPreCS consisted in one continuous sulcus, whereas in others it is composed of two separate folds. In each participant, the pattern was correctly

identified and 3/16 had a discontinuous sulcus. The sFS was separated from the sPreCS in 8/16 of cases. The minor sulci, namely the medial precentral (MeP) and the caudal paramidline (PaM) sulci were identified so that no confusion with the sFS proper could be made. The anatomy of all participants' is shown in **Figure 3.1**.

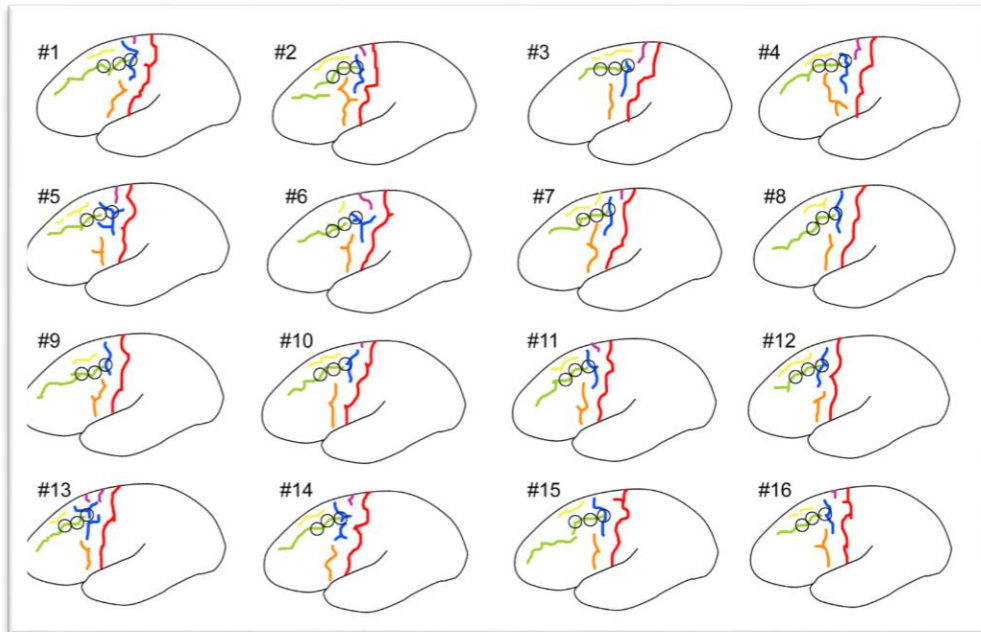


**Figure 3.1** Lateral view of the precentral sulcal complex in all the 16 subjects. Red: Central Sulcus; blue: Superior Precentral Sulcus; orange: Inferior Precentral Sulcus; green: Superior Frontal Sulcus; purple: Medial Precentral Sulcus; yellow: Paramidline Sulcus. The individual localization of the 3 stimulation points, P1-3, is indicated with hollow circles.

The position of the 3 spots was planned to cover in a caudo-cranial direction the whole span of dorsal BA6 (Brodmann, 1909; Geyer, 2004) (see discussion). TestTMS was applied to the motor cortex at the point where largest MEPs could be elicited from the OOr muscle.

### 3.3.3 Neuronavigation

The position of the condTMS coil was determined by frameless stereotaxic neuronavigation (see [Section 2.2.1](#)).

### 3.3.4 Inter-stimulus intervals (ISIs) between condTMS and testTMS

In each trial TMS could be delivered either as a single testTMS pulse (single-pulse trials) or as the combination of condTMS+testTMS (dual-pulse trials). Five different ISIs were used: 8 ms, 6 ms, 4 ms, 2 ms and -1 ms (the negative sign indicates that condTMS was delivered after testTMS in this single ISI). Single-pulse trials were interleaved with dual-pulse trials, as shown in [Figure 3.2](#).

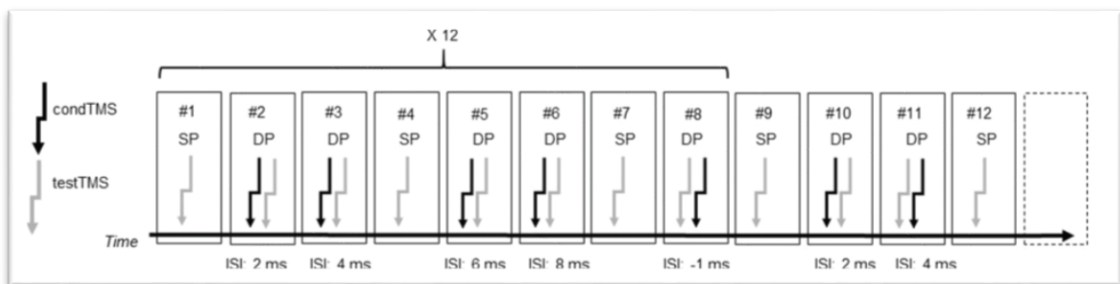


**Figure 3.2** A schematic representation of the SP trials interleaved with DP trials. Each ISI were repeated 12 times for each of the 3 points of stimulation, for a total of 96 trial with each stimulation point (36 single-pulse trials and 60 dual-pulse trials). Normalization procedure: trials #2 and #3 were divided by the average of trials #1 and #4, trials #5 and #6 by the average of trials #4 and #7, trial #8 by the average of trials #7 and #9 and so on. SP: single-pulse; DP: dual-pulse; ISI: inter stimulus interval.

Dual-pulse trials of a given ISI were repeated 12 times for each of the 3 points of stimulation. Ultimately, a total of 96 trials was associated with each stimulation point: 36 single-pulse trials and 60 dual-pulse trials.

### **3.3.5 TMS**

The intensity of the condTMS as well as the testTMS stimuli was around 120% of the active motor threshold (AMT) of the OOr and set on a subject-by-subject basis. AMT was defined as the minimum stimulus intensity required to produce a MEP in the recorded muscle of approximately 200 $\mu$ V in 5 out of 10 consecutive trials during a mild voluntary contraction.

### **3.3.6 MEP data pre-processing**

The EMG signal was pre-processed according to the following steps: 1) The signal was high-pass filtered at 20 Hz. 2) The EMG was rectified. 3) The area under the curve in the time window between 10 and 30 ms after the testTMS stimulus was extracted. The particular time window was chosen to cover the duration of MEPs in the orofacial region (Cattaneo & Pavesi, 2014). 4) The baseline EMG activity was defined as the area under the rectified EMG signal in the 200 ms prior to condTMS and was extracted for each trial. 5) Given that MEP amplitudes covariate strictly with the background EMG activity, we performed a baseline correction by dividing the MEPs areas by the baseline in individual trials. The procedure of baseline correction is already known in the literature to deal with the variability of MEP amplitudes from cranial muscles during active contraction (Sato, Buccino, Gentilucci, & Cattaneo, 2010; K. E. Watkins, Strafella, & Paus, 2003; K. Watkins & Paus, 2004).

### **3.3.7 Normalization of dual-pulse MEPs**

Dual-pulse MEPs were normalized to single-pulse MEPs. To do so, a procedure of normalizing single trials of dual-pulse MEPs to the average of single-pulse MEPs in a sliding window that followed the dual-pulse trials was adopted (Cattaneo &

Barchiesi, 2011; Maule, Barchiesi, Brochier, & Cattaneo, 2015). The two single pulse trials immediately adjacent to the dual-pulse trial were used as the sliding window. Their value was averaged and was used as a denominator in a ratio in which the numerator was the value of the dual-pulse MEP in between the 2 single pulses, thus obtaining a normalized index. The normalization procedure is schematized in [Figure 3.2](#). The resulting data are a ratio, and therefore are distributed between 0 and  $+\infty$ . This distribution is by definition not normal. In order to achieve normality of the data we applied a further manipulation, i.e. a base 10 logarithmic transformation, to each value (Tukey, 1977). In this way, data were symmetrically distributed around 0, between  $-\infty$  and  $+\infty$ . Individual pools of data were then successfully tested for normality by means of Shapiro-Wilk's test. In this novel distribution of data, negative values indicated amplitude of dual-pulse MEPs smaller than the instantaneous value of MEPs from single-pulse alone, whereas positive values indicated amplitude of dual-pulse MEPs larger than the instantaneous value of MEPs from single-pulse alone. In conclusion, the final result of the procedure was a series of 60 normalized dual-pulse MEPs for each stimulation point.

### **3.3.8 Statistical analysis of normalized MEPs**

The normalized MEPs were used as dependent variable in an ANOVA for repeated measures with 2 within-subjects factors. The TARGET factor indicated which point had been stimulated with condTMS and had 3 levels: P1, P2 or P3. The ISI factor had 5 levels corresponding to each of the 5 different ISI between condTMS and testTMS. Post-hoc analyses were conducted with Newmann-Keuls' test.

### **3.3.9 Control analyses**

All MEP amplitudes were corrected by the baseline EMG activity prior to TMS, as described above. However, to rule out the possibility that baseline EMG could be non-randomly distributed between the different experimental conditions, thus producing a bias, we analyzed the pre-stimulus EMG area of the 200 ms prior to TMS in a TARGET \* ISI ANOVA.

The analysis of the dual-pulse condition by normalizing with the sliding window is relatively novel (Cattaneo & Barchiesi, 2011). Hence, we decided post-hoc to perform, alongside to the main analysis, a conventional analysis based on averaging all MEPs within conditions and computing the ratio between the grand averages of the dual-pulse trials and that of the single-pulse trials as is generally done in dual-coil TMS experiments (Davare et al. 2009; Koch et al. 2006; O'Shea et al. 2007b). For each subject we thus obtained 15 values (3 TARGETS x 5 ISIs) values of the single-pulse/dual-pulse MEPs ratio. This ratio was higher than 1 if facilitation had occurred or lower than 1 if inhibition had occurred. We therefore used t-tests for single samples to test the hypothesis that the mean values of the ratio were different from 1.

## **3.4 RESULTS**

None of the subjects reported undesired effects of TMS. In all participants, a repeatable and consistent MEP was obtained from the activated OOr muscle. The mean active motor threshold for the OOr muscle was 60.3% (SD=3.8%) of the stimulator's output. The mean stimulation intensity was therefore 72.5% (SD=4.5%), ranging between a minimum of 65% to a maximum of 80%.

Figure 3.3 displays a representative recording from the OOr of one subject. A MEP in the 1DI was observed in 6 subjects, and limitedly to dual-pulse trials with the condTMS coil over P1. Since the 1DI MEPs were limited to the dual-pulse trials (no MEPs in the 1DI were obtained by stimulating mouth-M in the single-pulse trials, even in the P1 trials) it is highly plausible that they are due to the condTMS over the P1, considered the close proximity of this portion of area 6 with the handM1.

This is in line with the drawback of dual-pulse technique applied over the PMD and the ipsilateral handM1, which does not guarantee a selective stimulation, and corroborate our initial purpose to stimulate the mouthM1 (on this point see also Section 2.1.4). It could be speculated that 72% of stimulator output is too high an intensity to guarantee focality of stimulation. Indeed other authors have found cortico-cortical connectivity to M1 from the supplementary motor area (Arai et al. 2012), which is not far from the dorsal premotor region over which we applied the condTMS. However, the coils that we used for condTMS were considerably smaller (35 mm of outer diameter) than conventional coils, therefore assuring focality of stimulation (Deng, Lisanby, & Peterchev, 2013).

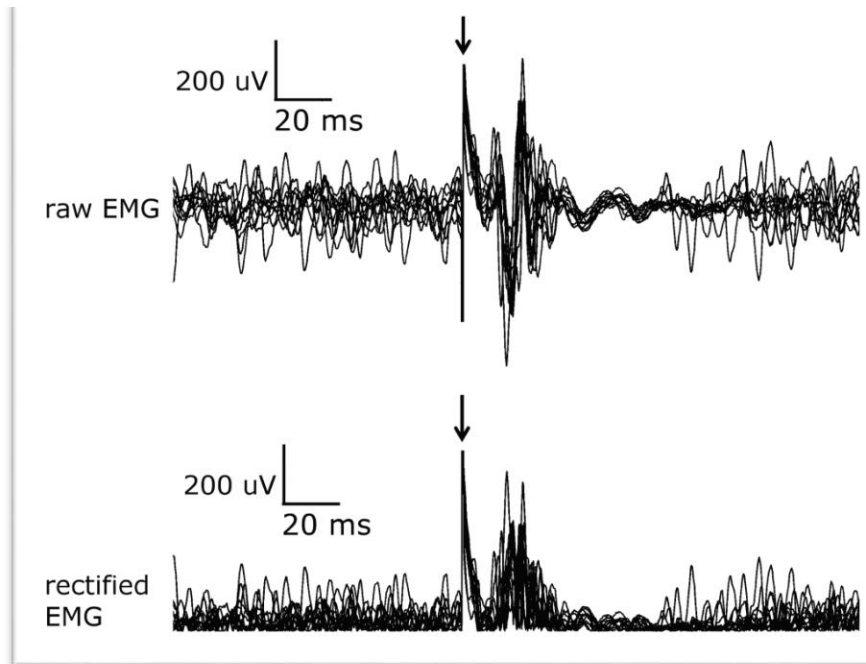


**Figure 3.3** Representative EMG recordings from the orbicularis oris muscle of one subject. 10 consecutive recordings from single-pulse trials are shown. The upper panel shows the raw EMG data and the lower panel the data after rectification of the signal, prior to extraction of the MEP area. The arrows indicate the time of TMS over the mouth motor cortex.

The results of the ANOVA showed a significant interaction of TARGET \* ISI ( $F(8, 120)=2.1492, p=0.036$ ). **Figure 3.4** illustrates the interaction. This was further explored by three different univariate ANOVAs, one for each TARGET level, with ISI as sole within-subject factor. The results showed that only the ANOVA with the data from P2 was significant ( $F(4, 60)=4.49, p=0.003$ ). The other ps were all  $> 0.47$ . Post-hoc comparisons showed that the data at ISI=6 ms were significantly different from all the other ISIs, while none of the other ISIs showed any reciprocal difference. The final analysis was to test whether any data from single ISIs were significantly different from a distribution with mean value=0, therefore indicating a significant effect of condTMS over testTMS. This comparison was carried out with t-tests for single sample. The significance threshold was set to 0.003 in order to

correct for the 15 multiple comparisons. The results showed that exclusively in P2, at ISI of 6 ms, the data were significantly different from 0 ( $t(15)=-6.4$ ;  $p=0.00001$ ). All other ps were  $>0.15$ . **Figure 3.5** shows the individual values of the normalized MEP areas.

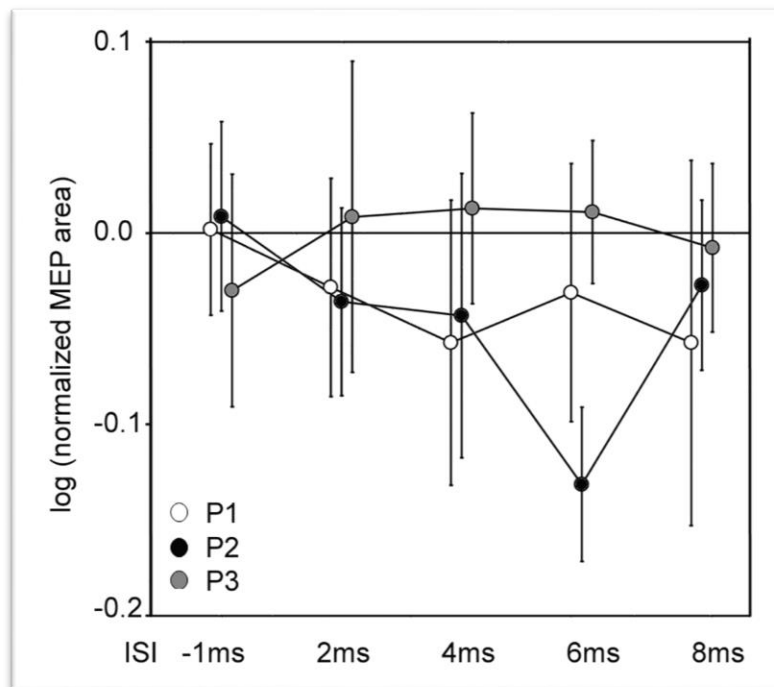


**Figure 3.4** Representation of the experimental results. The average values ( $n=16$ ) of the logarithm of the normalized MEP areas subjects are shown for each of the ISI and each of the target points. Error bars indicate 95% confidence intervals.

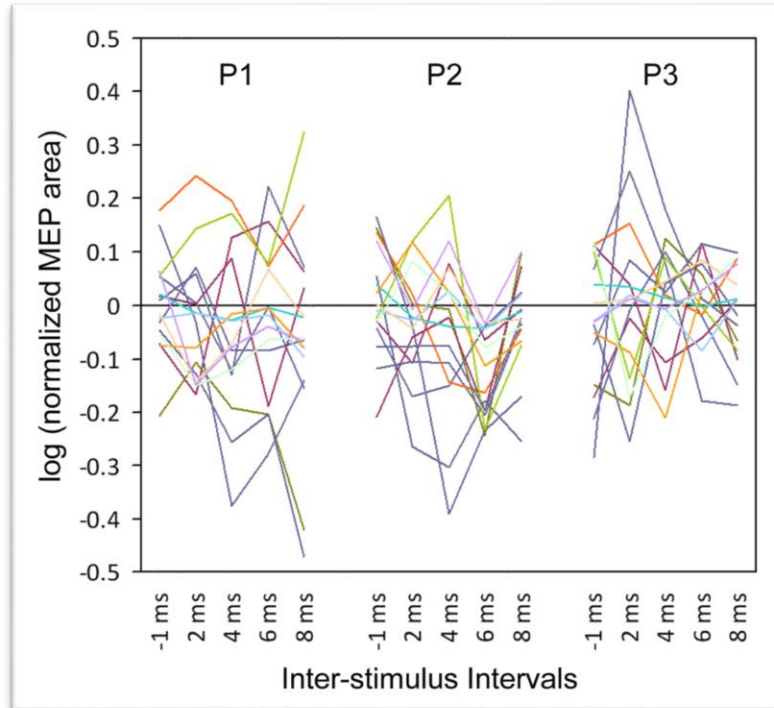


**Figure 3.5** Individual values of the logarithm of the normalized MEP areas. Note the robust inhibitory effect with conditioning TMS applied to P2 at an ISI of 6 ms.

Finally, given the spatial specificity of the results, which were significant only in the P2 point, we described its position in a second modality, different from the anatomical one used to localize it in the first place. We transformed the brain MRIs of all participants into the Talairach space by means of the BrainVoyager software. We collected the P2 Talairach coordinates from all participants. The resulting coordinates are listed in [Table 3.1](#).

<i>Participant</i>	<i>X</i>	<i>y</i>	<i>Z</i>
#1	-22	- 1	64
#2	-25	0	62
#3	-25	-3	66
#4	-20	0	63
#5	-25	-3	61
#6	-22	-1	63
#7	-21	-4	65
#8	-33	6	51
#9	-21	6	61

#10	-24	3	60
#11	-25	6	60
#12	-17	3	63
#13	-23	0	62
#14	-24	-2	67
#15	-21	1	66
#16	-23	0	63
Average:	-23	1	62

**Table 3.1:** Talairach coordinates of P2 in each participant

### 3.4.1 Control analyses

The baseline EMG (namely, the rectified EMG signal in the 200 ms prior to condTMS) was also analyzable according to the TARGET \* ISI design. None of the interactions are significant for the single-pulse and baseline EMG data (min  $p = 0.16$ ). The conventional analysis performed post-hoc confirmed the main finding. Only the data from TARGET P2 and at ISI of 6 ms showed a distribution significantly different from 1 ( $p=0.04$ ). All other  $p$ 's were  $>0.16$ .

## 3.5 DISCUSSION

### 3.5.1 Temporal specificity

The present results indicate that condTMS over the PMD exerts a powerful inhibitory effect on the cortico-facial system. This effect is inhibitory and shows consistent spatial and temporal resolution. It was present exclusively for stimulation at ISI = 6 ms and limitedly to stimulation of P2. The temporal specificity is consistent with cortico-cortical connections. In fact, other studies exploring cortico-cortical connections between areas the distances between which are similar to that between the PMD and the mouthM1 have found interactions at ISIs around 6 ms. (Baumer et al., 2009; Cattaneo & Barchiesi, 2011; Davare, Lemon, &

Olivier, 2008; Davare, Montague, Olivier, Rothwell, & Lemon, 2009; Davare, Rothwell, & Lemon, 2010). It should be noted that the physical distance between the dorsal premotor cortex and the mouthM1 is of around 6 cm, entirely compatible with a direct cortico-cortical connection.

However, the present data cannot exclude the possibility that the interaction between the PMC and the mouthM1 occurs at the brainstem level rather than in a cortico-cortical pathway, particularly given that the PMD is known to send direct descending axons to the facial nucleus. The hypothesis that cortico-cortical interactions occur is nevertheless more likely for two reasons. First because the effect at 6 ms ISI would imply that cortico-bulbar axons from the PMD are much slower than those from the mouthM1. The MEP onset latency in the perioral region is ~10 ms (Cattaneo & Pavesi, 2014) and the supposed latency of the cortico-spinal volley from the PMD would therefore be ~16 ms. The second argument against a direct cortico-bulbar effect of the PMD is the specifically inhibitory effect of the stimulation: pyramidal neurons are supposed to be excitatory neurons.

### **3.5.2 Spatial specificity**

The spatial specificity of the effect is intriguing. Where exactly is P2 on conventional brain maps? We already mentioned the cytoarchitectonic study on BA6 carried out by Geyer (2004) showing that PFC and PMD grade into each other (see [Section 1.2.1](#)). Taking into account the results of this study, the assumptions made about the extension of BA6 necessary for the present study were supported. Accordingly, all 3 points P1-3 are within the PMD, with P3 at its rostral border with PFC. Finally, it is worth noting that the spatially and temporally specific inhibitory effect described here are extremely robust, as can be observed

in **Figure 3.5**. All 16 participants were consistent in showing inhibition of the mouthM1 output.

### **3.5.3 Conclusion**

In the this first study, we strongly corroborate our initial working hypothesis. By moving the target of testTMS from the handM1 to the mouthM1 it is possible and easily feasible to assess ipsilateral PMD-M1 circuitry by means of the dual-coil technique. This allowed us to define a specific region in the PMD that gives origin to premotor-motor connections. The technique described offers novel possibilities for using neurostimulation as a tool to assess the physiological properties of the PMD.

## **CHAPTER 4: HUMAN DORSAL PREMOTOR CORTEX REVISED? SET RELATED INHIBITORY INFLUENCE ON IPSILATERAL MOTOR CORTEX**

### **4.1 ABSTRACT**

Previous evidence in non-human primates indicates that PMD might be involved in action planning and control. However, the role of PMD in action initiation and control is still largely debated in humans. To tackle this issue, we took advantage of a dual-coil transcranial TMS paradigm, testing the short-latency effects of condTMS delivered over the left PMD on the output of testTMS delivered over the ipsilateral orofacial M1. Participants performed a delayed motor task, lifting a stick with their lips in response to a GO-signal presented after a predictable SET-period. The results showed an inhibitory activity in the PMD-M1 module during the SET-period. This inhibitory activity was slightly modulated by the preceding sensory information on the onset of the SET-period, being more influenced by its predicted duration. This could suggest that in humans PMD might be critical not only in action selection and initiation, but also in action control and inhibition.

## 4.2 INTRODUCTION

In the first Chapter we have reviewed evidence demonstrating that PMD and F1 are densely interconnected to each other (Hatanaka, Nambu, Yamashita, Takada, & Tokuno, 2001; Kiefer, Marzinzik, Weisbrod, Scherg, & Spitzer, 1998; Muakkassa & Strick, 1979; Tokuno & Tanji, 1993). Furthermore, single cell recordings showed set-related activity in premotor cortices (di Pellegrino & Wise, 1993; Godschalk et al., 1985; K. Kurata & Wise, 1988; K Kurata & Wise, 1988; Weinrich et al., 1984; Wise, 1985), with a clear involvement of PMD neurons in preparing and realizing cue-related movements (Hoshi et al., 2014).

We also mentioned evidence suggesting that PMD exerts a control over M1 also in humans. In particular, several dual-coil TMS studies investigated the functional connectivity between PMD and the contralateral M1 during hand movement preparation and execution. The results showed facilitatory as well as inhibitory effects between the PMD and the contralateral handM1, both in the left and right hemispheres (Mochizuki et al. 2004; Bäumer et al. 2006; Koch et al. 2006; O'Shea, et al. 2007; Baumer et al. 2009; Rothwell 2011; for a more detailed discussion of these studies see [Section 1.2.2.1](#)).

However, the functional connectivity between PMD and ipsilateral M1 in humans is still largely hypothetical. As we have already seen ([Section 2.1.3](#)), a strategy could be to place the coil over PMD directly on the skull, with the coil over M1 being either elevated or overlapped (Beck, Houdayer, Richardson, & Hallett, 2009; see also Pirio Richardson, Beck, Bliem, & Hallett, 2014). But this is not without consequences for the selectivity of the stimulation of both targets. An alternative strategy could be to probe the ipsilateral PMD-M1 functional connectivity by changing the target of testTMS, putting more distance between the

two coils. In the experiment described in Chapter 3 and now published as Parmigiani et al. (2015), we delivered testTMS pulses over the left mouthM1, rather than over the left handM1. The results showed that PMD may exert a robust short-latency effect on ipsilateral mouthM1 (for more details on this point see [Section 3.4](#)).

The aim of the current study was to take advantage of this novel paradigm to investigate the ipsilateral PMD-M1 functional connectivity during a delayed motor task. Participants were required to prepare and perform a specific mouth movement after a variable, but highly predictable, SET-period. We tested the short-latency effects of condTMS delivered over the left PMD on the output of testTMS pulse delivered over the ipsilateral mouthM1, as measured by changes in orofacial MEPs.

### **4.3 METHODS**

Three experiments, employing the dual-coil technique, were carried out in the current study in order to investigate the functional properties of the PMD-M1 module. Experiment 1 was performed to confirm the short-latency connectivity between the intermediate portion of the dorso-lateral BA6 identified in Parmigiani et al. (2015) and the mouthM1 at rest (see also Chapter 3). In Experiment 2 we tested the PMD-M1 module during the delay period of a delayed simple motor task. The delay period was constant in all trials (900 ms). Given the results of Experiment 2, showing a specific effect of condTMS between 300 and 600 ms from onset of the delay period, we performed Experiment 3 to assess whether the effects of condTMS were time-locked to the start of the delay period or rather time-locked to the predicted GO-signal. In Experiment 3 we applied dual-coil TMS

during the delay period of the same task as in Experiment 2 but we applied different, albeit always predictable, delay intervals, ranging from 900 to 2100 ms.

#### **4.3.1 Participants**

Sixteen healthy individuals (11 women, mean age 25.8, ranging 18-38 years, SD 4.8) took part in Experiment 1 and Experiment 2. Twelve healthy individuals (7 women, mean age 25.4 years, ranging 18-41 years, SD 6.54) participated in Experiment 3. They all provided informed consent. All were screened for any contraindication to TMS (Rossi & Hallett 2009). The study was approved by the local ethical committee (protocol 2031-032) and was conducted in compliance with the revised Helsinki declaration (Association, 2009).

#### **4.3.2 Localization of TMS targets**

The targets for testTMS and condTMS were the same in the three experiments. TestTMS was delivered to the mouthM1, which was localized functionally, without the aid of the neuronavigation system, as the spot on the scalp where the larger MEP from the OOr muscle could be obtained with the lowest intensity. CondTMS was delivered over the mouth-related PMD as defined in Parmigiani et al. (Parmigiani, Barchiesi, & Cattaneo, 2015), which was localized by means of neuronavigation on individual anatomies (see also [Section 2.1.4](#)). It was found 1.5 cm rostral to the junction between the superior precentral sulcus (sPreCS) and the superior frontal sulcus (sFS). Mean distance from CZ are -3.55 lateral, 2.45 anterior (SD 0.63, 0.68).

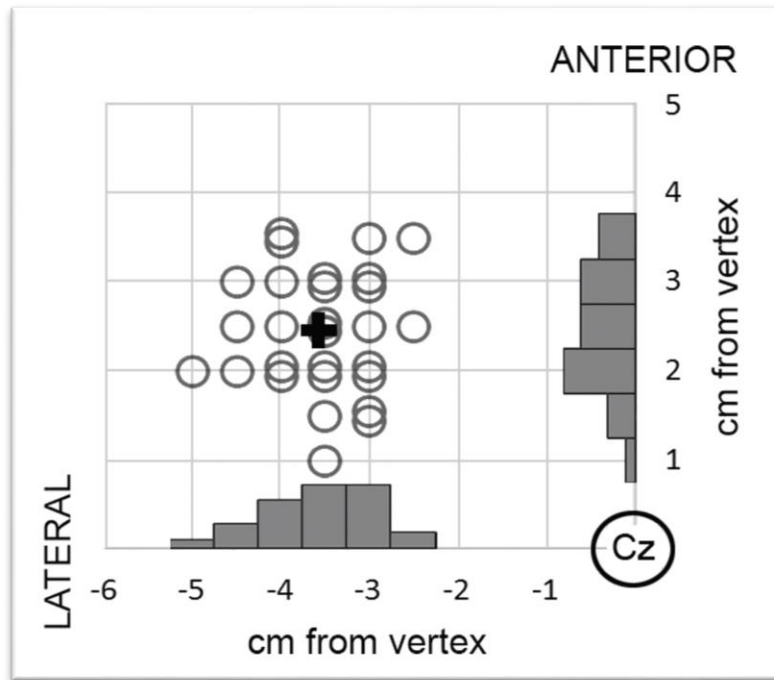


**Figure 4.1** The target points are shown for participants of all experiments (n = 28). Circles indicate data from single participants. For the sake of illustration clarity, a slight offset has been applied to overlapping spots so that they can be identified as multiple subjects. Histograms indicate the frequency of spots on the corresponding coordinates. Coordinates are given in 0.5 cm steps.

**Figure 4.1** shows the target points in all participants. After their use for neuronavigation, the brain images of all participants were transformed in Talairach space to identify the coordinates of the PMD target (see **tables 4.1 and 4.2**).

<i>Participant</i>	X	Y	Z
#1	-25	-3	61
#2	-24	-2	62
#3	-21	-4	65
#4	-17	3	63
#5	-16	-12	62
#6	-20	4	50
#7	-17	-8	50
#8	-25	-3	53
#9	-24	2	48

#10	-22	-6	58
#11	-18	8	54
#12	-21	1	54
#13	-24	4	46
#14	-22	2	49
#15	-26	3	49
#16	-26	-3	53
<b>Average:</b>	-22	-1	55

**Table 4.1** Talairach coordinates of condTMS in each participant of Experiments 1 and 2.

<i>Participant</i>	<i>X</i>	<i>Y</i>	<i>Z</i>
#1	-18	8	54
#2	-17	-8	50
#3	-24	-3	46
#4	-17	3	63
#5	-24	-2	62
#6	-26	-1	49
#7	-21	-4	65
#8	-21	-1	51
#9	-21	-2	50
#10	-17	3	63
#11	-26	-3	53
#12	-25	-3	61
<b>Average:</b>	-21	-1	56

**Table 4.2** Talairach coordinates of condTMS in each participant of Experiment 3.

The average coordinates were of  $x=-22$ ,  $y=-1$  and  $z=55$ . These coordinates were strikingly similar to those extracted from a separate population of subjects in our previous study (Parmigiani et al. 2015), that is  $x=-23$ ,  $y= 1$  and  $z= 62$ . Furthermore, our coordinates for PMD compare favorably with the spot where PMD is localized by meta-analyses of fMRI studies (Hardwick et al. 2013, 2015).

### 4.3.3 TMS

We already describe the general features of our TMS setting in [Section 2.2.3](#). As far as the specific features of the TMS setting used in the present experiments are concerned, the intensity of the condTMS as well as the testTMS stimuli was around 120% of the active motor threshold (AMT) of the OOr muscle. AMT was defined as the minimum stimulus intensity required to produce a MEP in the recorded muscle of 200 $\mu$ V of average amplitude over 10 consecutive trials during a mild voluntary contraction. Since it is common practice to record facial MEPs during active contraction of the target muscle, due the high threshold of the orofacial motor cortex to TMS (Cattaneo & Pavesi, 2014), participants were tested during active contraction of the lips. To achieve a stable contraction they were asked to hold a stick in their mouth with their lips only and to generate muscular tension matching an amplitude of the EMG signal of around 200  $\mu$ V. The operator inspected the EMG trace online and provided feedback to the participant whenever she deviated from the desired contraction level.

In each trial TMS could be delivered either as a single testTMS pulse (single-pulse trials) or as the combination of condTMS + testTMS (dual-pulse trials). The relative timing of condTMS and testTMS required a sub-millisecond temporal resolution and was therefore controlled by an input-output board, the1401 micro Mk-II unit (Cambridge Electronic Design). TMS single or dual-pulses were time-locked to the visual stimuli in Experiments 2 and 3 by means of the E-Prime 2.0 software (Psychology Software Tools Inc.).

#### 4.3.4 EMG Recordings and pre-processing

We already accounted EMG acquisition in [Section 2.2.2](#). Once acquired, the EMG signal was rectified. In the OOr channel, the area under the rectified EMG in the time window between 10 and 30 ms after testTMS was considered as representative of the MEP and the area of the 200 ms prior to condTMS was considered as baseline EMG activity. In the 1DI channel the area between 20 and 40 ms from testTMS was considered representative of the MEPs. Participants were keeping a stable voluntary contraction of the OOr muscle. However, MEP amplitudes are known to covariate strictly with the background EMG activity in the upper limb, and likely also in the cranial district. The facilitatory effect of voluntary contraction introduces a great deal of variance in MEP amplitudes that is not related to the experimental manipulation but rather to spontaneous variations in the voluntary drive. To correct for this source of noise we performed a baseline correction of MEP amplitudes from the OOr muscle, by dividing the MEP area by the relative baseline area in individual trials. (See also Chapter 3; Watkins et al., 2003; Watkins & Paus, 2004; Sato et al., 2010; Parmigiani et al., 2015). At this point of EMG pre-processing, each trial was associated with a single value of the baseline-corrected MEP areas. Finally, as post-hoc confirmation of the relation between voluntary contraction and MEP amplitude in the orofacial cortico-bulbar system, we performed a simple regression analysis between non-corrected MEP areas and the relative background activity. The results showed a robust linear co-variation of MEPs with the amount of voluntary activity (see [Figure 4.2](#)). The further step in the processing of MEPs was that to relate the dual-pulse MEPs to the single-pulse MEPs. This process was performed differently in the three Experiments and is described in detail below.

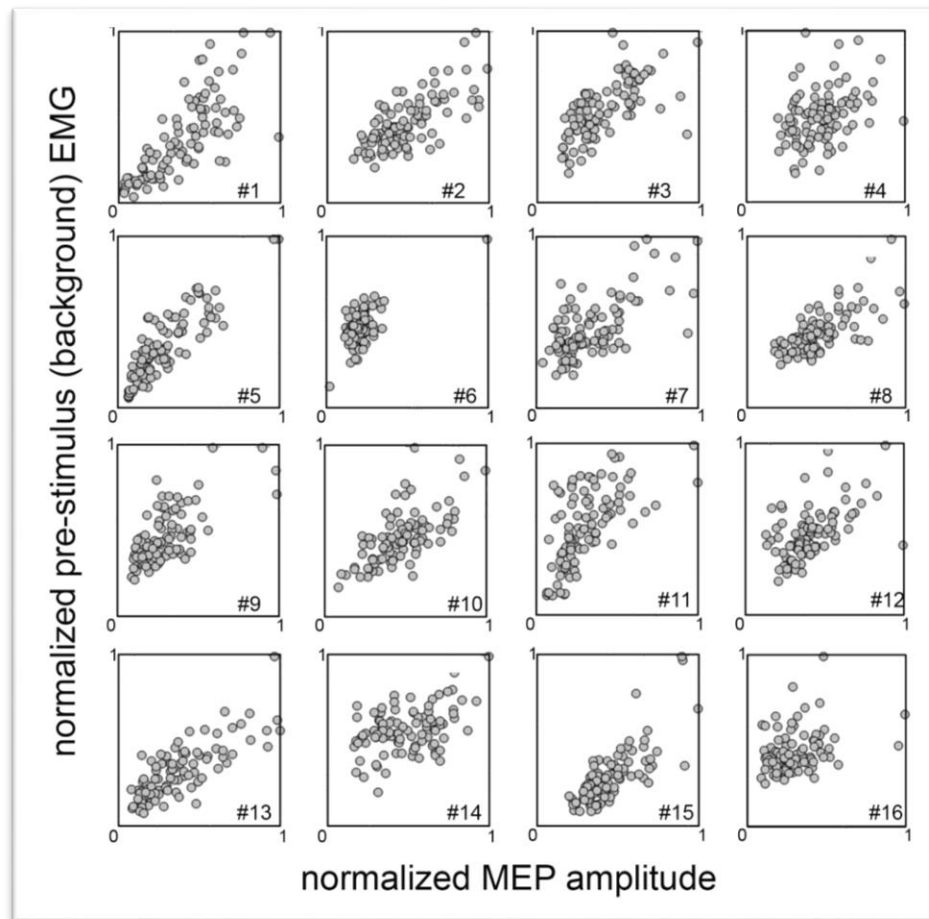


**Figure 4.2** Demonstration of linear covariance between background EMG activity and MEP amplitudes. The data from each of the 96 trials of each single subject are shown. For the sake of comparison between-subjects, both the background EMG and the facial MEP amplitudes were normalized within each subject to the maximum value in the distribution. The normalized values were therefore comprised between 0 and 1. Single regression analysis between EMG and MEP values showed a high degree of covariance. Individual  $R^2$  values ranged between 0,18 and 0.72. The grand average of individual  $R^2$  values was of 0.47. This indicated that around half of the variance of MEP amplitudes was fully accounted for by variations in voluntary EMG contraction preceding TMS. This source of variability was eliminated from the main analysis of MEP by the procedure of baseline correction described in the methods.

#### 4.3.5 Experiment 1 - Protocol

Participants were sitting comfortably, the head on a chin rest and eyes freely open, wearing earplugs. They were asked to stay completely at rest aside from the

controlled voluntary contraction of the OOr muscle. Five different inter stimulus intervals (ISIs) were used in dual-pulse trials: -1 ms, +2 ms, +4 ms, +6 ms and +8 ms (condTMS was delivered after testTMS in the -1ms ISI). Dual-pulse trials of each ISI were alternated with single-pulse trials in a fixed sequence that contained 5 dual-pulse trials (one for of the 5 ISIs) and 3 single-pulse trials. The sequence was: single-pulse; dual-pulse; dual-pulse; single-pulse; dual-pulse; dual-pulse; single-pulse; single pulse. The elementary sequence was repeated 12 times. The whole experimental session was therefore made of a total of 96 trials (36 single-pulse trials and 60 dual-pulse trial).

#### **4.3.6 Experiment 1 – MEP normalization**

Dual-pulse MEPs were normalized to single-pulse MEPs. To do so, a procedure of normalizing single trials of dual-pulse MEPs to the average of single-pulse MEPs in a sliding window that followed the dual-pulse trials was adopted (Cattaneo & Barchiesi, 2011; Maule et al., 2015; Parmigiani et al., 2015). Their value was averaged and was used as a denominator in a ratio in which the numerator was the value of the dual-pulse MEP in between the 2 single pulses, thus obtaining a normalized index. The resulting data are a ratio, distributed between 0 and  $+\infty$ , and in order to achieve normality of the data we applied a further manipulation, i.e. a base 10 logarithmic transformation, to each value (Tukey, 1977). In this way, data were symmetrically distributed around 0, between  $-\infty$  and  $+\infty$  (tested for normality by means of Shapiro-Wilk's test). Negative values indicated amplitude of dual-pulse MEPs smaller than the instantaneous value of MEPs from single-pulse alone, whereas positive values indicated amplitude of dual-pulse MEPs larger than the instantaneous value of MEPs from single-pulse alone. At this step, the result of

the procedure was a series of 60 MEP ratios (5 ISIs \* 12 repetitions) for each participant.

#### **4.3.7 Experiment 1 – Statistical analysis**

We first excluded trials with MEPs that exceeded 2 standard deviations (SD) from the individual average values. The aim of statistical analysis was to assess whether in any of the 5 ISIs, the MEP ratio was significantly deviating from the value of zero, ultimately indicating whether dual-pulse MEPs were significantly different from single-pulse MEPs. To do so we performed a series of 5 t-tests, assessing the null hypothesis that the mean of the MEP ratios was not different from zero. The p-value was Bonferroni-corrected for the 5 multiple comparisons, and adjusted to  $p=0.01$ .

#### **4.3.8 Experiment 2 - Protocol**

In Experiment 2, participants performed a delayed simple motor task and TMS was delivered in an event-related timing, during the delay period. Participants had an additional lateral head-constraint on the chin rest, which assured head stability and minimal movement during the execution of the orofacial action. They wore earplugs and, as in Experiment 1, they were asked to keep the contraction of the muscles constant, in a way in which they were able to hold a stick between their lips firmly also while they were waiting for the cues, assisted by the operator behind them. Stimuli were presented with the E-Prime 2.0 software, on a 75 Hz (1680 x 1050 resolution) 20" monitor, at 45 cm of distance from the participant eyes. The experiment was organized in four similar blocks, each consisting of 96 trials. The inter trial interval was randomly jittered between 2500 and 3500 ms. Trials started with a green fixation cross, indicating the delay period (SET-period),

during which participants had to stay still and wait for the GO-signal (a circle in the middle of the screen), occurring 900 ms later. After the response (lifting a stick with their lips as fast as possible) was given, the corresponding reaction time was displayed on the screen, serving as feedback of individual performance. Any anticipation of the response prior to the GO-signal was considered as error. It should be noted that, given the fixed duration of the SET-period, the onset of the GO-signal was entirely predictable throughout the experiment (see [Figure 4.3](#)).

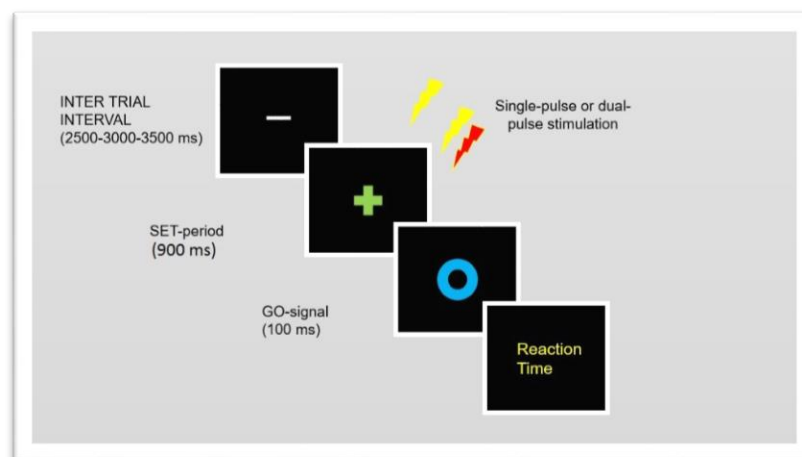


**Figure 4.3** Experiment 1 trials procedure.

#### **4.3.9 Experiment 2 - Lip response collection**

The stick held by the participant's lips weighted 15 g, and was connected to a circuit delivering a trigger signal through the USB port to the stimulus presentation PC. The trigger was delivered whenever the stick was lifted above a given height by means of the active movement of the lips during the voluntary response. The timing of the response was logged by the E-Prime 2.0 software and displayed to give on-line feedback. At the same time, a 3-axes analog accelerometer embedded in the stick tip allowed a very accurate acquisition of the onset and the

evolution of the orofacial movements. The signal from the accelerometer was recorded by the 1401 micro Mk-II unit and stored by the Signal Software on a dedicated channel for offline analysis. The response times indicated by E-prime were used uniquely for the display of single-trial feedback. The onset point of the deflection related to the voluntary response were collected with the accelerometer's recording.

#### **4.3.10 Experiment 2 – TMS**

The configuration and placement of the two TMS coils was the same as in Experiment 1. TMS was delivered as single-pulses or dual-pulses. The ISI for dual-pulse TMS was set to 6 ms as this had been proven to be the optimal interval to test cortico-cortical connectivity between PMD and M1 (see Parmigiani et al. 2015, and Experiment 1 in this chapter). In each trial only one single- or dual-pulse TMS was delivered, specifically during the SET-period. However, the timing of TMS was varied between trials in order to cover the whole duration of the SET-period (900 ms). Four different timings were used corresponding to 0 ms, 300 ms, 600 ms and 900 ms after the onset of the SET-period. Dual-pulse trials were interleaved with single-pulse trials in a fixed order. The timing of TMS on the contrary was randomized across trials. Overall, trials were classified according to a STIMULATION (2 levels: single- or dual-pulse) \* TIME (4 levels: 0, 300, 600 and 900 ms) factorial design, in which each trial type was repeated 48 times, for a total of 384 trials per participant.

#### **4.3.11 Experiment 2 - MEP normalization and statistical analysis**

Before proceeding with the normalization of the MEPs, we excluded trials with MEPs that exceeded 2 SD from the individual average values and trials with

anticipation of the response. Trials with anticipation of responses were defined as all the trials that lie before the 2 SD from the individual mean of reaction times. Similarly, we excluded all the trials exceeding the 2 SD in the right side of the individual mean of reaction times. Therefore, the sampling interval of individual reaction times was  $\pm 2$  SD of the individual mean, clearly excluding trials in which the subjects responded before the delivering of the TMS, see [Figure 4.4](#). Since adjacent trials could be randomly attributed to different TMS timing, we were not able to perform a “sliding window” normalization of dual-pulse MEPs over single-pulse MEPs. We adopted therefore the canonical approach of performing a grand-average of MEPs within each of the 8 cells of the experimental design and then dividing, within each subject and within each TMS timing, the average area of dual-pulse trials by the average area of single-pulse trials. The result was that each subject was characterized by 4 values of MEP area ratios, one for each of the TMS timings. The final step was to log-transform the MEP ratios to obtain a normal distribution of the values (tested for normality by means of Shapiro-Wilk’s test). Statistical analysis was performed by means of one-way ANOVA with the within-subjects factor TIME (4 levels: 0, 300, 600 and 900 ms). Given that the inter trial interval was unpredictable (jittered between 2500 and 3500 ms), when TMS was delivered at 0 ms from the onset of the SET-period, the participant’s brain had no information on the proximity of the trial and therefore this timing was considered as a sort of “baseline” measurement. For this reason, we planned to explore the ANOVA results by comparing the data from TMS at 0 ms to that of each of the 3 other TMS timings. Significance threshold was corrected for multiple comparisons to  $p=0.016$ .

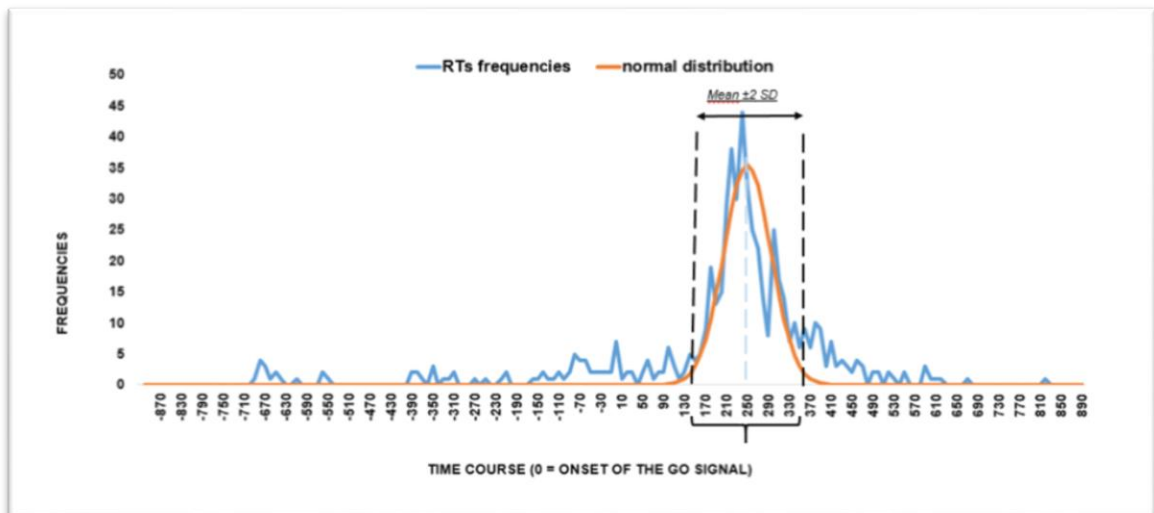


**Figure 4.5** An example of a single subject RTs distribution (mean 250 ms, SD 45). The sampling interval is  $\pm 2$  SD of each subject mean.

#### 4.3.12 Experiment 3– Protocol and signal processing.

Experiment 3 was structured similarly to Experiment 2, but explored different durations of the SET-period. Instead of a single block with a 900 ms SET-period (as in Experiment 2), we used 3 different SET-periods, 1500 ms, 1800 ms and 2100 ms, each in one of 3 different within-subjects blocks (see Figure 4.5). The 3 blocks were presented in counterbalanced order between the subjects. The duration of the SET-period did not vary within each block, allowing the predictability of the timing of GO-signal. Trial structure and behavioral tasks were the same as in Experiment 2, but with a varying number of TMS timings, in order to cover the whole of the SET periods in steps of 300 ms. Trials in the 1500 ms block had 6 different TMS timings: 0 ms, 300 ms, 600 ms, 900 ms, 1200 ms and 1500 ms. Trials in the 1800 ms block had 7 different TMS timings: 0 ms, 300 ms,

600 ms, 900 ms, 1200 ms, 1500 ms and 1800 ms. Trials in the 2100 ms block had 8 different TMS timings: 0 ms, 300 ms, 600 ms, 900 ms, 1200 ms, 1500 ms, 1800 ms and 2100 ms. Consequently, the 1500 ms block was designed according to a 2\*6 within-subjects factorial design with 2 STIMULATION types and 6 TMS TIME. The 1800 ms block was designed according to a 2\*7 within-subjects factorial design with 2 STIMULATION types and 7 TMS TIME. The 2100 ms block was designed according to a 2\*8 within-subjects factorial design with 2 STIMULATION types and 8 TMS TIME. In all blocks, the number of repetitions per experimental condition was set to 9 trials, resulting in 108 trials in the 1500 ms block, 126 trials in the 1800 ms block and 144 trials in the 2100 block. Processing and normalization of MEPs and trimming of trials were performed as in Experiment 2, but within each of the 3 blocks separately. Similarly, average values for dual-pulse trials were divided by average values of single-pulse trials and the ratio was log-transformed.

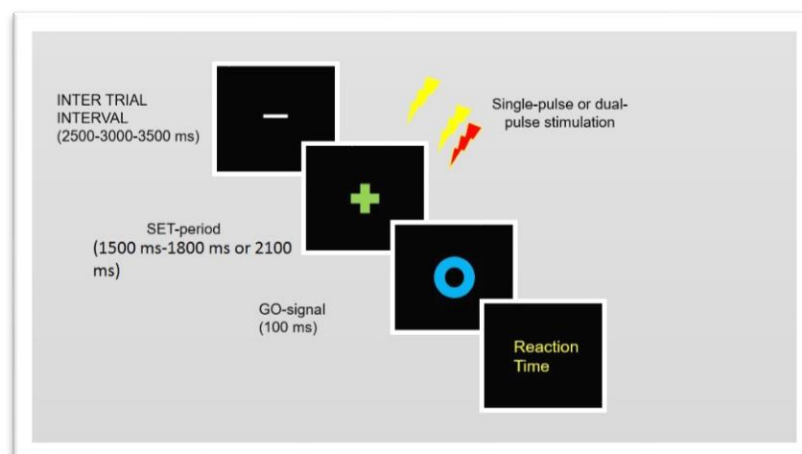


**Figure 4.5** Experiment 2 trials procedure.

### **4.3.13 Experiment 3 – Statistical analysis.**

Statistical analysis was performed separately for each block, because the variable number of TMS timings prevented a balanced within subjects analysis of the whole dataset. Three separate repeated-measures one-way ANOVAs were performed, with TIME as factor. As in Experiment 2, the ANOVA results were explored by comparing the normalized MEP ratio at 0 ms to the MEP ratio at all the other timings. Significance thresholds were corrected to  $p=0.008$  in the 1500 ms block; to  $p=0.007$  in the 1800 ms block and to  $p=0.006$  in the 2100 block.

## **4.4 RESULTS**

None of the subjects reported any significant discomfort from stimulation and no side-effects of TMS, neither immediate nor delayed, were observed in any of them. Across all 3 experiments, the mean motor threshold for the OOr muscle was 61% (SD=4.78) of the stimulator's output. Mean stimulation intensity was 70% (ranging 57%-79%) of maximal stimulator output.

### **4.4.1 Experiment 1**

All participants were able to keep the desired target activation of the OOr muscle. Frequent pauses in the experiment allowed for minimal fatiguing in an otherwise demanding task if performed continuously. The mean log-transformed MEP ratios are shown in [Table 4.3](#) and illustrated in [Figure 4.6](#). Statistical analysis by means of Bonferroni-corrected t-tests (corrected significance threshold:  $p=0.01$ ) showed significant deviation of the mean values of normalized MEP ratios from the zero value only for the 6 ms ISI ( $p=0.0033$ ), all others  $p$ -values  $> 0.2$ .

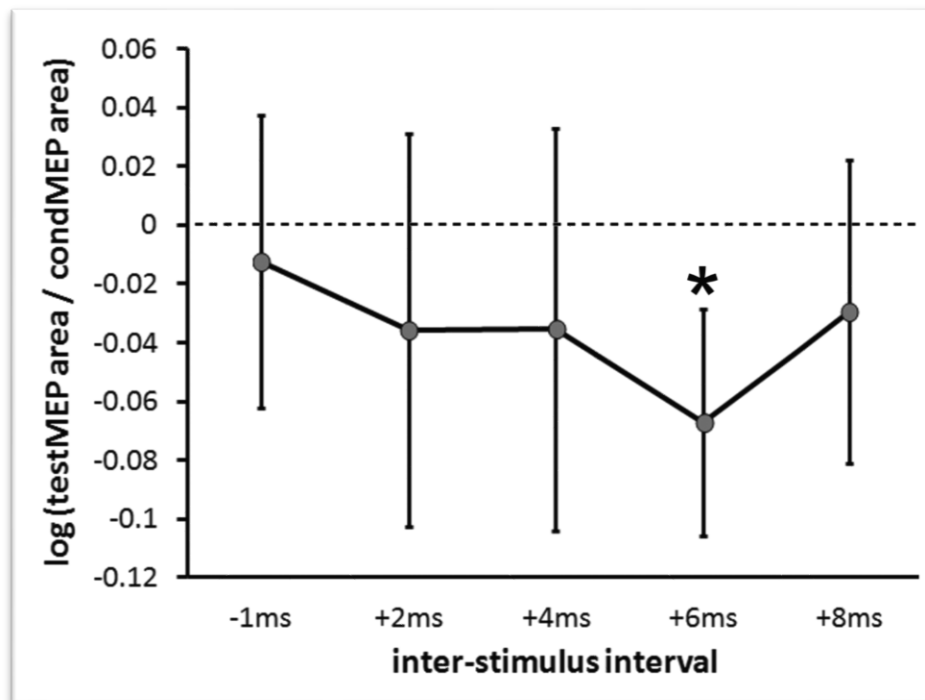


**Figure 4.6** Results of Experiment 1. The average values ( $n = 16$ ) of the logarithm of the normalized MEP areas subjects are shown for each of the ISIs. Error bars indicate 95 % confidence intervals.

#### 4.4.2 Experiment 2 – Physiological data

The mean log-transformed MEP ratios are shown in [Table 4.3](#) and illustrated in [Figure 4.7](#). The one-way ANOVA showed a significant main effect of TIME ( $F(3, 45)=3.8127, p= 0.016$ ). The distribution of the data was investigated as planned with respect to the values obtained at 0ms that were considered as baseline. The resulting 3 comparisons between the 0 ms and the 3 later TIMES yielded a significant difference only for the 600 ms TIME. Overall the results indicated that condTMS exerted an inhibitory effect of on testTMS around 600 ms after the onset of the SET period, that is, 300 ms before the onset of the predictable GO-signal. The current results did not allow disentangling whether the inhibitory effect of condTMS was time-locked either to the onset of the SET period or to the

upcoming, predictable, GO-signal. Experiment 3 was designed to address this issue.

	0 ms	300 ms	600 ms	900 ms	1200 ms	1500 ms	1800 ms	2100 ms
<b>Experiment 2</b>								
	0,0221	0,0444	-0,0333	0,0714	-	-	-	-
<b>Experiment 3 (1500ms)</b>								
	0.0367	0,0014	-0,1295	-0,0627	0,0151	0,0506	-	-
<b>Experiment 3 (1800ms)</b>								
	-0,0032	-0,0103	-0,0302	-0,0560	-0,0476	-0,0114	0,0179	-
<b>Experiment 3 (2100ms)</b>								
	0.0000	-0,0125	-0,0034	-0,0660	-0,0666	-0,0132	0,0224	0,0103

**Table 4.3** Values of the mean log-transformed MEP ratio in the Experiments 2 and 3

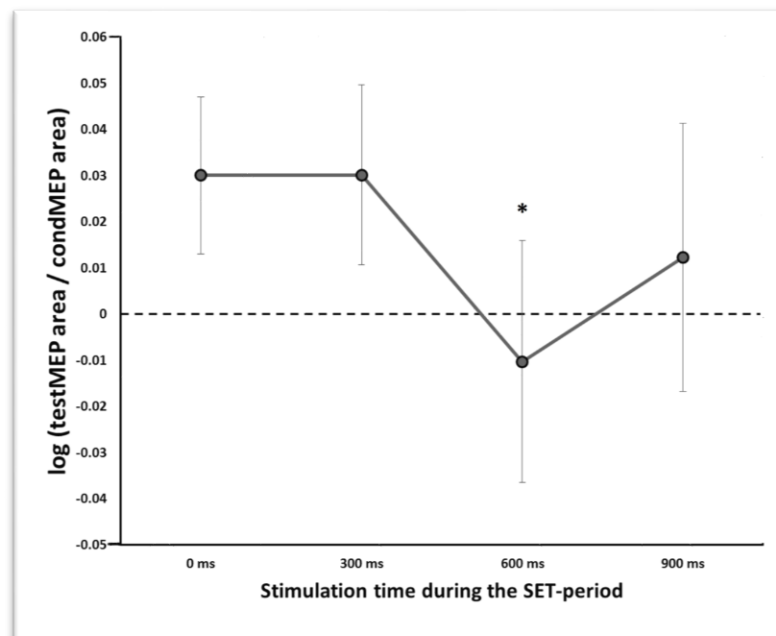


**Figure 4.7** Results of MEPs modulation of Experiment 2. The average values (n = 16) of the logarithm of the normalized MEP areas subjects are shown for each stimulation time. Error bars indicate 95 % confidence intervals.

### 4.4.3 Experiment 3

The values of the mean log-transformed MEP ratio in the different experimental conditions are reported in [Table 4.3](#) and outlined in [Figure 4.8](#). The analysis was conducted separately for each of the 3 durations of the SET-periods (1500, 1800 and 2100 ms). A main effect of TMS timing was found in the 1500ms data ( $F(5, 50)=2.41, p=0.049$ ), in the 1800 ms data ( $F(6, 60)=2.83, p=0.017$ ) but not for the 2100 ms data ( $F(7, 70)=1.04, p=0.41$ ). Comparison of data obtained at later times to the 0ms (baseline) timing showed a significant decrease of the MEP ratio when TMS was delivered at 600 ms in the 1500 ms data ( $p=0.007$ ), at 900 ms in the 1800 ms data ( $p=0.007$ ) and at 900 ms in the 2100 ms data ( $p=0.01$ ).

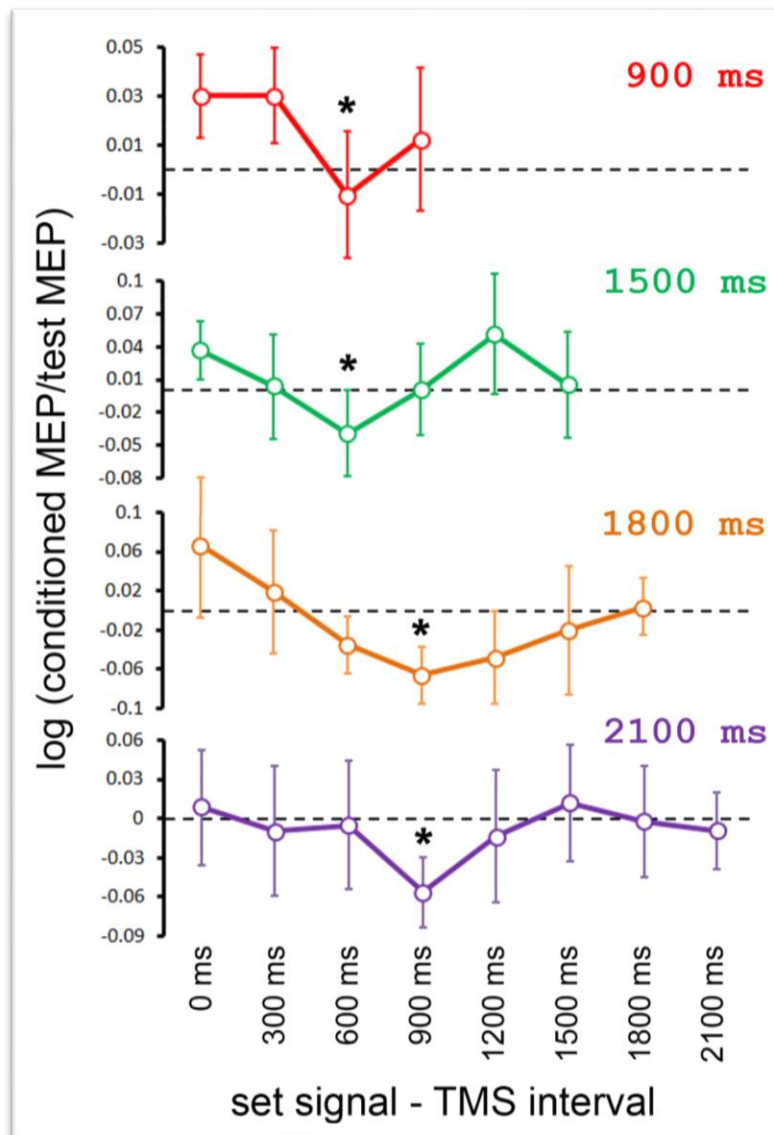


**Figure 4.8** Results of MEPs modulation in the three blocks of Experiment 3. The average values ( $n = 12$ ) of the logarithm of the normalized MEP areas subjects are shown for each stimulation time in each of the blocks. Error bars indicate 95 % confidence intervals.

## 4.5 DISCUSSION

The aim of the present study was to take advantage of a dual-coil TMS paradigm in order to investigate the functional connectivity of the PMD-M1 module.

In the study presented and discussed in Chapter 3 we demonstrated that PMD and ipsilateral M1 are directly connected in humans (Parmigiani et al., 2015).

This finding was corroborated by the Experiment 1 of the present study. Indeed, condTMS applied to PMD modified the excitability of testTMS to the orofacial M1 when the ISI was of 6 ms. There is consensus that such a short-latency effect is a signature of direct or quasi-direct cortico-cortical connectivity (see, for instance, Davare et al., 2008, 2009, 2010; Baumer et al., 2009; Cattaneo & Barchiesi, 2011).

For this reason, Experiments 2 and 3 investigated the functional properties of PMD-M1 by using a 6 ms ISI only. In both experiments the task consisted in two distinct phases: an inhibitory phase (SET-period), in which participants had to stay inactive, and a release phase (after the GO-signal), in which they had to lift a stick with their lips as fast as possible. The duration of the delay period was completely predictable and the impending action was always the same in all the trials, so participants should not be challenged in any motor choice or decision.

Overall, Experiment 2 revealed inhibitory activity in the PMD-M1 module during the SET-period. Baseline was measured by dual-coil TMS delivered at the onset of the SET-period, after an unpredictably jittered inter trial interval. Compared to the baseline, the excitability of the PMD-M1 module was significantly decreased at 600 ms from the onset of the SET-period (see [Figure 4.7](#)). Because of the fixed duration of the SET-period (900 ms), the observed inhibition corresponded also to 300 ms before the GO-signal. Thus, a natural question arises as to whether the phase-dependent inhibitory activity was time-locked either to the onset of the SET-period or to the upcoming GO-signal. Indeed, two distinct neural mechanisms may underpin these different time-locked activities. Premotor activity could be time-locked to a preceding sensory event, in this case the SET-signal. This is typically due to a bottom-up sensory-driven process (see, for

instance, Hoshi & Tanji, 2006). Otherwise, premotor activity could be time-locked to a forthcoming sensory event, namely the GO-signal. The latter case is generally ascribed to a predictive, top-down process, mostly independent from current sensory information. Experiment 3 was designed to disentangle between these two possible mechanisms. We varied the duration of the SET-period (1500, 1800, 2100 ms, respectively) in a blocked design. Thus, in spite of its variation, the SET-period was always predictable within single blocks. The results confirmed the presence of a suppression of PMD-M1 excitability. This inhibitory activity occurred at 600 ms from the onset of a 1500 ms SET-period and at 900 ms from the onset of a 1800 ms SET period. Data obtained with a 2100 ms SET-period were less strong, but also in this case an inhibitory effect could be identified around 900 ms from the onset of the SET-period (see Figure 4.7). Taken together, these results showed that the inhibition of the PMD-M1 module is not strictly time locked to the duration of the SET-period. A possible explanation is that the inhibitory activity seems to be mildly temporally linked to the preceding sensory information on the onset of the SET-period, but the difference we can see in the timing of the inhibitory activity seems to be more strongly influenced by a top-down modulation exerted by the predictive, top-down process, independent from current sensory information concerning the onset of the GO-signal.

The finding of an inhibitory activity in the PMD-M1 module might seem at odd with the reported role of PMD in action selection and initiation (O'Shea et al., 2007; Bestmann et al., 2008). We have already mentioned the dual-coil TMS study by O'Shea et al. (2007). They stimulated the left PMD and the contralateral handM1 during two different tasks, a simple motor task and an action selection task respectively. They found that dual-pulse inter-hemispheric stimulation

significantly facilitated MEPs both when applied 50 ms after the onset of the GO-signal in the simple motor task and also when occurred at 75 ms after the onset of the GO-signal in the action selection task.

There could be therefore the temptation to construe the inhibitory activity we reported in the PMD-M1 module as primarily due to an unforeseen stimulation of the neighbor supplementary motor area (SMA), which is sometimes defined as a “negative area” (see, for instance, Burle, Vidal, Tandonnet, & Hasbroucq, 2004; Nachev et al., 2008; Verbruggen & Logan, 2008; but see also Chapter 5). However, there are good reasons to resist this temptation. A first reason is the high focality of the stimulation provided by a 35 mm figure of-eight coil (on this point see also Parmigiani et al. 2015). A further reason is that previous direct connectivity studies clearly demonstrated inhibitory effects between PMD and M1 (see also Mochizuki et al., 2004).

A possible explanation of the contrast between our and previous dual-coil TMS results concerning the functional connectivity of the PMD-M1 module may appeal to differences in methodology and in task. Indeed, in the present study we stimulated the left PMD and the ipsilateral mouthM1, rather than the contralateral handM1. Furthermore, participants should perform a delayed motor task, which required to move their lips after a variable, but highly predictable, SET-period ranging from 900ms to 2100ms. A such delay-period was not present in previous dual-coil TMS studies. Finally, PMD-M1 activity has been demonstrated to vary with the varying of the task, being inhibitory rather than excitatory when action selection requires movement suppression. Indeed Koch and colleagues (Koch et al., 2006) stimulated the left PMD and the contralateral handM1 during a task in which participants should squeeze one of the two hands as rapidly as possible

after an arbitrary auditory cue was presented. The results showed not only facilitatory but also inhibitory PMD–handM1 interactions. In particular, facilitatory activities from left PMD to right M1 were found 75 ms after the onset of the auditory GO-signal requiring participants to move their left hand, whereas inhibitory activities were found 100 ms after the onset of the auditory GO-signal when the required movements concerned their right hand rather than their left hand, which should remain still. This indicates that PMD might play a role not only in facilitating movement initiation, but also in suppressing movements which should be prepared but not initiated, or so the author claimed.

Of course, the inhibitory activity in the module of PMD-M1 can not be considered per se as evidence for an inhibitory role of PMD on action (on this point see Miniussi et al. 2008, 2010). Nevertheless, our findings are consistent with previous evidence suggesting a role for premotor cortex in action inhibition. Indeed, patients with focal lesions, especially in the left superior portion of BA6, have been demonstrated to succumb to an increased number of false alarms, thus revealing a clear deficit in inhibiting responses to a no-go stimulus (Picton et al. 2007).

To sum up, the present study suggests that PMD might be more critical for action preparation and control than previously thought, being involved not only in action selection and initiation but also in action inhibition. After all, acting when required is a crucial feature of action preparation and control and our findings revealed a prominent action-related inhibitory connectivity between PMD and ipsilateral M1 that could be critically involved in action initiation and control.

## **CHAPTER 5: SHOULD I STOP OR SHOULD I GO? A DIFFERENTIAL ROLE OF PMD AND SMA IN ACTION INHIBITION**

### **5.1 ABSTRACT**

Controlling action may sometimes require to promptly stop an initiated movement. A large number of studies have focused on this aspect of action control, by exploring various cortical areas with different techniques and paradigms. Nevertheless, how those areas work is still a matter of controversy. The aim of the current study is to take advantage of a single-pulse TMS technique to assess whether and how two of the putative areas involved in action initiation and control, that is, PMD and SMA may contribute to stop a motor performance. TMS allows high focal on line modulation of selected areas in healthy subjects while they are performing the target behaviour, e.g. stopping a fast response only when required. The stop-signal paradigm is a popular tool for the study of this behaviour in an experimental setting. In the present version of this paradigm, subjects perform a go task, (i.e. moving an item with the mouth as fast as possible from a starting point to a final position). In half of the trials, the go stimulus is followed by a stop signal, which instructs the subjects to withhold the response and not complete the movement, going back to the starting point. A single-pulse TMS is delivered during different percentiles of the subjects individual reaction times (response phase) over PMD and SMA. Real stimulation error rates are compared with sham stimulation error rates. Results showed that subjects' performance was clearly affected by real stimulation at early times during the response phase in both areas. But this effect was different between the two areas. Indeed, real stimulation of PMD produced a strong and highly replicable increase in error rates in the stop-trials only, while the stimulation of SMA slightly improved participants' performance, regardless of the type of trials in which they are involved. Taken together, these results suggest a differential contribution of PMD and SMA in action inhibition, or so we shall argue.

## 5.2 INTRODUCTION

Being able to stop an ongoing action when required or just because it is no longer relevant for our purposes is an essential as well as fascinating aspect of action initiation and control. In the executive's repertoire, action inhibition is indeed critical for motor and cognitive control. As we have seen in [Sections 1.1.2](#) and [1.2.2](#), a large number of studies in both non human primates and humans have been focused on action initiation and control. Two main areas have been supposed to be mainly involved in action inhibition: PMD and SMA. However, how these areas actually contribute to action inhibition is still a matter of controversy.

The aim of the current study is to take advantage of a single-pulse TMS technique to assess whether and to what extent PMD and SMA play a distinctive role in stopping a motor performance. In our previous study (see [Chapter 4](#)), we found a prominent action-related inhibitory connectivity between PMD and ipsilateral M1, which suggested a putative role for PMD in action inhibition. This was in line with Koch et al. (2006), who stimulated the left hand-related PMD and the contralateral handM1, suggesting that PMD might play a role in suppressing movements which should be prepared but not initiated.

However, our and Koch et al. (2006) studies can not be considered per se as evidence of a inhibiting role of PMD in the executive control of action inhibition (Miniussi et al. 2008, 2010). For this reason, we decided to take a step further. In a first experiment we directly investigated the putative role of PMD in action control and inhibition by interfering with TMS with the performance of healthy volunteer in a stop-signal task. This task usually probes individual's ability to halt an ongoing motor response triggered by a go-signal when a stop-signal is presented after a

variable delay. We applied real and placebo TMS over the left mouth-related PMD, while participants had either to fully lift a stick with their lips or to suddenly stop their lifting movement. The accuracy of participant's performance was measured.

In a second experiment we tested the SMA involvement in action inhibition by using the same paradigm. In [Sections 1.1.2](#) and [1.2.2](#) we discussed the functional properties of SMA, by distinguishing between proper-SMA and pre-SMA. However, TMS stimulation does not allow us to selectively target one of the two areas only. Nevertheless, TMS stimulation provides a privileged way of exploring cortical areas contribution to on-line action control, because of its higher temporal resolution (on a ms scale).

## **5.3 METHODS AND GENERAL PROTOCOL**

In this study, we carried out two TMS experiments targeting two different cortical areas in the dorsal and mesial precentral regions in healthy humans, i.e. PMD and SMA. In Experiment 1, single-pulse TMS was delivered over the left mouth-related PMD while in Experiment 2 single-pulse TMS was delivered over the mouth-related SMA proper and pre-SMA. In both experiments, participants underwent four blocks of the same stop-signal behavioural task. We measured the error rates in the STOP-trials as a function of stimulation, real vs. placebo.

### **5.3.1 Participants**

Twenty healthy individuals (15 women, mean age 24.2, ranging 20-29 years, SD 2.8) took part in Experiment 1. Thirteen different healthy individuals took part in Experiment 2. (9 women, mean age 23.8 years, ranging 19-29 years, SD 3.2). They all provided informed consent. All were screened for any contraindication to TMS (Rossi & Hallett, 2009). The study was approved by the local ethical committee (protocol 2031-032) and was conducted in compliance with the revised Helsinki declaration (Association, 2009).

### **5.3.2 Localization of TMS targets**

Neuronavigated-TMS was used also for this study, see [Chapter 2](#), section [2.2.1](#). The targeted areas were localized by means of individual investigations of anatomical landmarks. In Experiment 1, TMS was delivered to the left mouth-related PMD as defined in our first study (see [Chapter 3](#)). In Experiment 2, TMS was delivered to the face/mouth-related left SMA proper and pre-SMA. In order to localize this areas, we took advantage of Picard and Strick (1996) review (see also

Johansen-Berg et al., 2004; Vorobiev, 1998 and [Section 1.2.1](#)), in which they summarized the results of several positron emission tomography (PET) studies that examined functional activation on the medial wall of humans aimed to providing a common frame of reference for studies of medial wall function (medial portion of BA 6). According to this map, the AC projection crosses exactly in the middle the face area of pre-SMA and SMA proper and therefore to identify this area we used an AC-PC translation of the brain MRIs from each participants and stimulated over the AC projection on the scalp (see [Figures 5.1](#) and [5.2](#)).

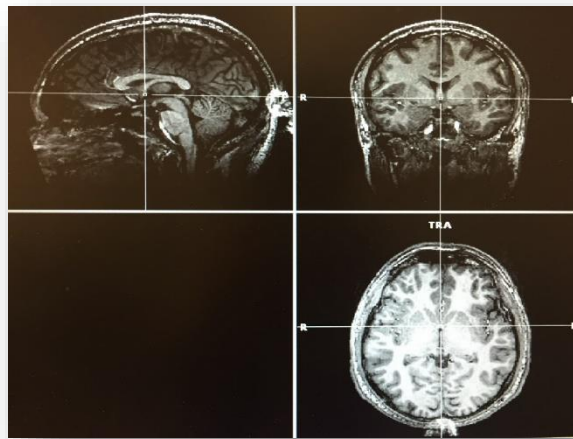


**Figure 5.1** The reconstruction of one subject's brain in AC-PC native space in which the pre-SMA and SMA regions are identifiable.

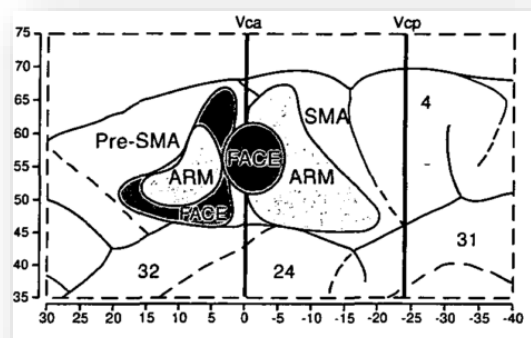


**Figure 5.2** Functional organization of human pre-SMA and SMA proper identified with PET studies. (Picard and Strick, 1996)

### 5.3.3 EMG Recording

Since no primary motor areas were stimulated in these two experiments, no MEPs were collected for further analysis. However, before the experimental session the right 1DI was localized and recorded for each subject, and was used to establish the individual RMT in the PMD experiment. In addition, the OOr was recorded in the PMD experiment in order to exclude an unwanted stimulation of the mouthM1. In the SMA experiment, the leg-related M1 (legM1) was functionally localized and recorded in the right TA in order to have first the individual RMT and second an individual scalp distance from the legM1 hot-spot to the SMA.

### 5.3.4 TMS

Single-pulse stimulation was achieved by means of a MagPro biphasic magnetic stimulator (Medtronic, Denmark) connected to a MCFB65 coil with 65 mm windings (MagVenture, Skovlunde, Denmark) for REAL stimulation. SHAM stimulation was achieved with a MCF-P-B65 coil with 65 mm windings placebo figure-of-eight coil (MagVenture, Skovlunde, Denmark). Both coils were held by an articulated mechanical arm (Manfrotto 244, VitecGroup, Italy). The PMD coil was positioned with a medio-lateral orientation of the induced current. The SMA coil was positioned tangentially to the midline with the handle positioned caudally (see [Figure 2.18B](#)). The intensity of was around 100% of the RMT of the right 1DI muscle in PMD experiment and at 100% of the RMT of the right TA muscle in SMA experiment. The stimulation was delivered during the subjects' RT period of the stop-signal task. See the following section for a more detailed description of the stimulations combined to the behavioral task.

### 5.3.5 Stop-signal paradigm

Before the experiment, participants were tested for their RTs in a simple reaction time task. After a variable foreperiod (600 ms, 1200 ms, 3000 ms, 4500 ms), signaled by a black screen with colored stars, a pink circle appeared in the center of the screen (GO signal), informing the participants to perform a lifting of the stick, always kept between their lips, from the starting point to the arriving point (see [Figure 2.19](#)). Participants were instructed to respond as quickly as possible to the GO stimulus. They underwent at least 200 trials of this task. Then, the first, the second and the third percentiles of the single subject RTs were extracted and used in order to define the timing of the TMS pulses and the onset of the STOP signal.

Proper experiment consisted in four blocks of a STOP-signal task. The STOP-signal task was composed of a combination of NO-STOP and STOP trials (see [Figures 5.3](#) and [5.4](#)).

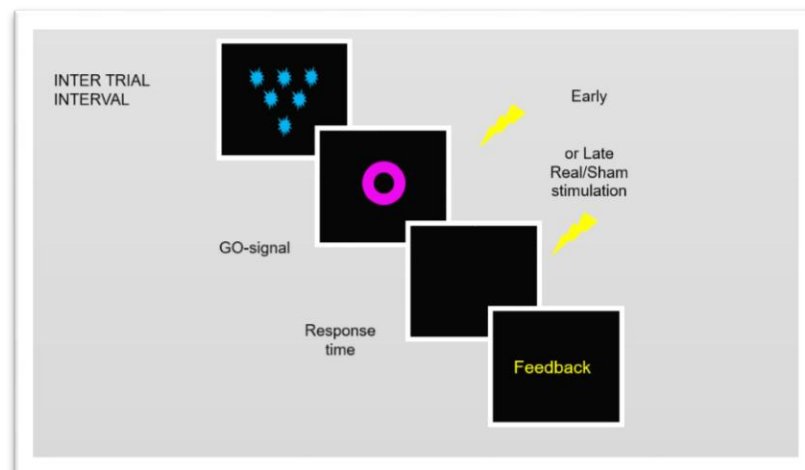


**Figure 5.3** NO-STOP trials procedure.

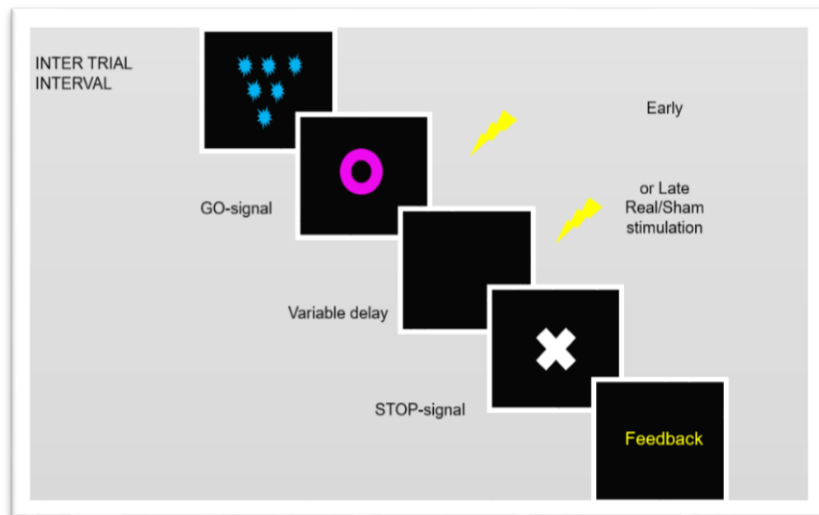


**Figure 5.4** STOP trials procedure.

In the NO-STOP trials, a go signal is presented and participants were instructed to respond as quickly as possible with the mouth movement. On STOP trials, participants were instructed to stop their response when a stop signal appeared. After a variable foreperiod (2100 ms, 3000 ms, 4500 ms), the pink circle always occurred, informing the participants they were required to move. In half of the trials, a white cross appeared after always the same delay determined by the participant RTs, informing her to inhibit the movement (STOP-signal trials only, see [Figure 5.4](#)). While participants were required to respond as quickly as possible to the GO stimulus in the NO STOP trials, they were also instructed to try to withhold their response on STOP trials, but not wait for the STOP signal to occur (Obeso et al., 2013; Verbruggen & Logan, 2008). On line feedback informed participants if they successfully accomplished the NO-STOP or STOP trials (*Good!*) or failed (*Wrong!*). In case they took more time than their mean of RTs, they were “pushed” to not get slower with an appropriate feedback (*Warning! You are too slow!*), on the contrary, in case they did not wait for the GO-signal to occur, they were warned to do not anticipate (*Don’t anticipate!*).

During the response period, single-pulse TMS was delivered over PMD (Experiment 1) or SMA (Experiment 2) after the occurring of the GO signal. Two possible timing were used: at the first percentile of the subjects' RTs (early TMS) or at the third percentile (late TMS). The STOP signal unvaried across trials, so always occurred at the second percentile of single subject's RTs. In two of the blocks participants received a REAL stimulation and in the other two a SHAM stimulation. A block consisted in 60 GO-trials (30 EARLY, 30 LATE) and 60 STOP-trials (30 EARLY, 30 LATE) randomly presented, i.e. 120 trials per block, for a total of 240 trials per stimulation (REAL/SHAM). Order of stimulation was balanced across subjects. The trials considered for the analysis was the ones in which TMS, whether REAL or SHAM, was delivered in the pre-movement or early phase of movement. We measured the accuracy of the subjects in both the types of trials, i.e. the ability to conclude the action required when there was a GO-trial as well as be able to inhibit the action when a stop signal was present. We compared REAL vs. SHAM stimulations and we analyzed separately data from the two cortical regions (PMD and SMA).

## 5.4 RESULTS

None of the subjects reported undesired effects of TMS in both the experiments. The mean of stimulation intensity was 59% of the stimulator output (range 46%-77%, SD 9.5) for Experiment 1 and 78% of the stimulator output (range 60%-90% SD=10.5) for Experiment 2.

Since in trials considered for the analysis TMS was delivered in the pre-movement or early phase of movement, trials in which subjects were particularly fast and TMS arrived after the response phase (i.e. when the movement was already concluded) were excluded from the accuracy analysis. Trials excluded were 7.15% of the total trials of the Experiment 1 and 6.1% of the Experiment 2. Considering the SHAM condition, a high accuracy in GO-trials (70% overall) and a low error rate in the STOP-trials (22% overall) indicate good balance between a demanding task requiring subjects to be focused and presumably putting themselves in a specific state and an acceptable compliance of the participants. Reaction times in the SHAM condition (GO-trials) were on average 425 ms, ranging across 322-717 ms (SD=78.2).

### 5.4.1 Experiment 1: PMD stimulation

The results indicated a strong significant difference between REAL and SHAM stimulation in the STOP-trials only ( $p=0.0007$ ). Indeed, when REAL TMS was delivered over PMD, the accuracy was severely affected (see [Figure 5.5](#)). Stimulation over PMD during the pre-movement or early phase of movement in STOP-trials increased the error rates, leading each subject to be less able to inhibit their actions. All other  $p$ -values were  $> 0.82$ . No effect of EARLY/LATE stimulation was found.

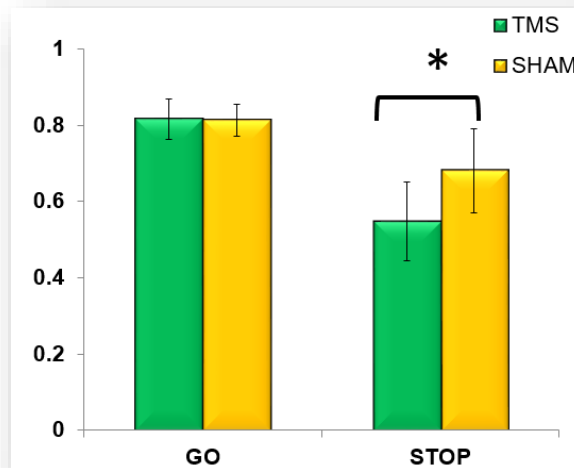
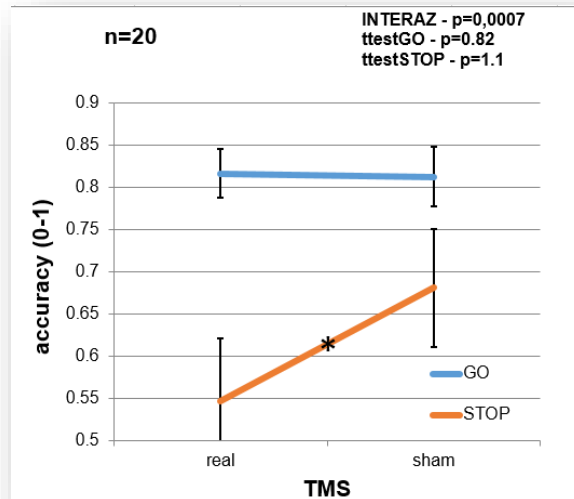


**Figure 5.5** Results of Experiment 1.

#### 5.4.2 Experiment 2: SMA stimulation

Data indicate a significant effect of REAL stimulation over the SMA region ( $p=0.03$ ), resulting in an improvement of the subjects ability to fulfill the task requirements. What is relevant is that the effect is generalized to all conditions and it is not possible to catch a state-dependency of the SMA region stimulation in the pre-movement or early phase of movement of the STOP-trials or the GO-trials.

Compared to the placebo stimulation, both the type of trials with opposite demands were equally affected. At the first glance, the performance seemed to be conditioned in a different manner between the two types of trials, since the stimulation increased the number of responses in the GO-trials and decreased the error rate in the STOP-trials, but the global effect of SMA stimulation is the performance enhancement. All other p-values were  $> 0.06$  (see [Figure 5.6](#)). Neither in this experiment there was no significant effect of EARLY/LATE stimulation found.

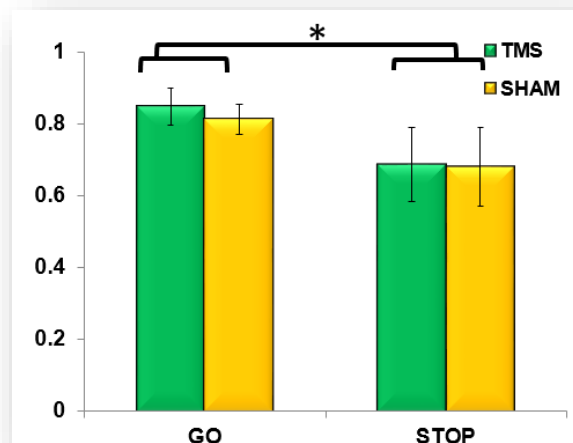


**Figure 5.6** Data from of Experiment 2.

## 5.5 DISCUSSION

The current study aimed at taking advantage of a single-pulse TMS technique to assess whether and how PMD and SMA may play a distinctive role in action inhibition. Single-pulse TMS was applied to the PMD and SMA regions during the pre-movement or early response phase of a stop-signal task. Accuracy in the performance during stimulation was compared to accuracy in the placebo stimulation. There were two main findings.

First, the real stimulation of PMD produced a much stronger and highly replicable increase in error rates than the placebo stimulation. Importantly, this effect concerned the STOP trials only. Indeed, participants had no any impairments in initiating and completing the mouth movements in the NON-STOP trials. Second, the real stimulation of SMA slightly improved participants' performance with respect to the placebo stimulation. However, this effect was not selectively related to the type of trials, being very similar in both STOP and NON STOP trials. Taken together, these findings suggest a differential contribution of PMD and SMA in action inhibition.

As far as the first finding is concerned, it is worth mentioning that our results are in line, partially at least, with previous studies investigating the inhibitory role of PMD in both non-human primates and humans. Indeed, a single cell study recorded from PMD neurons of two monkeys (*Macaca mulatta*) when performing both No-Stop and Stop trials in a countermanding task (Mirabella et al. 2011). In the No-Stop trials, the monkeys should execute a speeded reaching movement at the appearance of a suitable target. In the Stop trials, after a variable delay, a stop signal appeared, instructing the monkeys to inhibit the movement initiation. The results showed that more than one third of recorded PMD neurons involved in motor planning exhibit a countermanding modulation. These neurons changed their pattern of discharge when a reaching movement were executed with respect to when it was inhibited, and this change preceded the end of the stop-signal reaction time.

A distinctive inhibitory role of PMD over movement production seems to be also suggested by GO/NOGO studies. For instance, Kalaska and Crammond (1995) showed that neural activity of PMD neurons changed when a movement

should be suppressed with respect to when it should be executed. Similar results have been also reported by Ledberg et al., (2007), who showed that cortical activity in PMD allowed to predict the monkey's choice after 150 ms.

Although the GO/NOGO and stop-signal paradigms are different, being the latter (but not the former) concerned with an ongoing motor response, nevertheless there are reasons to assume that these different kinds of action restraining may have a cortical overlap (Battaglia-Mayer et al., 2014). This seems to be also consistent with lesion data. Indeed, the injection of GABA-A antagonists within PMD reduces the ability of monkeys to withhold movements (Sawaguchi et al., 1996). Similarly, lesions PMD may result in increased frequency of impulsive and uncontrolled reaching movements (Moll & Kuypers, 1977).

A similar inhibitory role of PMD have been reported also in a human lesion study. Indeed, patients with focal lesions, especially in the left superior portion of BA6 (putative PMD and SMA), have been demonstrated to succumb to an increased number of false alarms, thus revealing a clear deficit in inhibiting responses to a NO/GO stimulus (Picton et al., 2007).

This study allows us to introduce our second finding, that is, the difference between PMD and SMA involvement in action inhibition. Our results does not rule out a contribution of SMA to action inhibition. But they suggest that, differently from PMD, SMA seems to be not selectively related to stopping an ongoing motor response, being equally involved in both No-Stop and Stop trials.

We have already mentioned that in delivering TMS pulses over the mesial portion of BA6 we could not *a priori* restrict the stimulation to proper-SMA or to pre-SMA only. This could explain some apparent inconsistencies between our results and what has been previously reported in the SMA literature.

Indeed, there is a certain amount of brain imaging evidence that pre-SMA activity may be related to altering motor plans (Curtis et al. 2005; Li, Huang, Constable, & Sinha, 2006). Successful stopping turned out to be associated with pre-SMA activation, even though the magnitude of activation in pre-SMA did not correlate with SSRT (Aron et al., 2007). Further evidence indicates that pre-SMA may be also involved in monitoring or resolving the conflict between the opposing task demands in the stop-signal paradigm (Nachev et al., 2007). Interestingly, a meta-analysis (Swick et al., 2011) conducted on 21 brain imaging studies involving either Go/No-Go or stop-signal tasks, pointed to the functional relevance of the pre-SMA for successful performance in response inhibition across these two different tasks. Interestingly, in the case of stop-signal task, pre-SMA activation seems to be related to short SSRT (Chao, Luo, Chang, & Li, 2009).

Finally, Obeso et al (2013) combined repetitive TMS (rTMS) with PET scans during a stop-signal task. The results showed that rTMS over the pre-SMA increased the efficiency of the inhibitory control over powerful ongoing responses. They are also in line with a lesion study, which demonstrated that pre-SMA lesions can lead to a selective deficit in the ability to inhibit a response in the context of competition between actions (Nachev et al., 2008).

Differently from pre-SMA, SMA has been typically considered to be critically involved in action preparation, being also concerned with the suppression of a potential action, but not selectively with the inhibition of an ongoing actual action. As already mentioned in Section 1.2.2.1, SMA has been shown to be active even when people merely view graspable objects, without any intention to act upon them (Grézes & Decety, 2002). Such an activity has been interpreted in terms of an automatic inhibitory process concerning actions, which might be afforded by the

viewed object but are in fact not required to be performed (see Nachev, Kennard, & Husain, 2008). This interpretation is consistent with lesion data indicating that patients with microlesion of SMA, differently from healthy people and control patients with pre-SMA damage, are impaired in automatic suppression of evoked motor plans (Sumner et al., 2007).

Although the above mentioned studies suggest an involvement of pre-SMA, at least, in action inhibition, it is far from clear how selective and distinctive can be such an involvement, especially in relation with PMD inhibitory role. To this regard, it is worth noting that single cell recordings from pre-SMA and proper-SMA neurons in monkeys showed that only a very small percentage of recorded neurons (2.4%) were actually involved in action inhibition (Scangos & Stuphorn, 2010). Even though the presence of a recording bias or other factors that might have influenced the total number of identified neurons could not be excluded, it is also plausible to hypothesize that SMA and pre-SMA are not the main actors in canceling a movement after the appearance of an imperative stop-signal. This interpretation is not in contrast with the finding of Chen et al. (2010) who showed that local field potential (LFP) power spectra obtained from data recorded over SMA display changes in the low-frequency range (10–50 Hz) early enough to suggest that this region is causally involved in movement inhibition. Indeed, changes in LFPs could be caused not by the local activity but by inputs coming from other brain regions (Logothetis, 2003; Mattia et al., 2013).

In conclusion, although further research is needed, our findings seem to indicate a distinctive role for PMD in action control, suggesting that PMD can be selectively involved in promptly interrupting an ongoing action. This does not rule out the possibility that SMA might contribute to this function. However, this

contribution does not seem to be necessarily related to the prompt inhibition of an just started action.

## CHAPTER 6: CONCLUDING REMARKS AND LIMITATIONS OF THE STUDY

Our overall question concerned the putative role of PMD (and SMA) in action initiation and control. In answering this question, we proposed a novel dual-coil TMS approach, investigating for the first time the structural and functional connectivity between PMD and ipsilateral orofacial M1. This investigation paved us the way to start our exploration of the differential role of PMD and SMA in initiating and controlling action.

Six TMS experiments were carried out and presented here. In the first dual-coil TMS study we aimed to assess the existence of short-latency influences of the left PMD on the ipsilateral orofacial M1 by recording MEPs in the active OOr muscles (see Chapter 3). The results showed that condTMS exerted a robust effect on ipsilateral M1 only when applied to one specific portion of the PMD and only at one specific ISI (6 ms). The effect consisted in a systematic suppression of facial MEPs compared to those obtained by testTMS alone.

These results were replicated in our second dual-coil study (see Chapter 4, Experiment 1). Then, the main aim of this study was to explore the functional PMD-M1 connectivity. We therefore tested the short-latency effects of condTMS delivered over the left PMD on the output of testTMS delivered over the ipsilateral orofacial M1, as measured by changes in orofacial MEPs, during a delayed motor task (Experiment 2 and 3). Participants were required to prepare and perform a

specific mouth movement after a variable, but highly predictable, SET-period. The results showed an inhibitory activity in the PMD-M1 module during the SET-period. In order to establish whether the effects of condTMS were time-locked to the start of the delay period or rather time-locked to the predicted GO-signal, we also manipulated the duration of the SET-period (Experiment 3). The results showed condTMS effects were modulated more by the predicted duration of the SET-period (a top-down process regarding the onset of the GO-signal) than by the preceding sensory information on the onset of the SET-signal.

Demonstrating a prominent action-related inhibitory connectivity between PMD and ipsilateral M1 does not imply an inhibiting role of PMD in action control, of course. For this reason, we carried out a single pulse TMS experiment, stimulating PMD during a stop-signal task (see Chapter 5, Experiment 1). We contrasted PMD stimulation with SMA stimulation when participants underwent the same stop-signal task (Experiment 2). The results showed that the stimulation of PMD produced a much stronger and highly replicable increase in error rates than the placebo stimulation – where this effect concerned the STOP trials only. On the contrary, the real stimulation of SMA slightly improved participants' performance with respect to the placebo stimulation. However, this effect was not selectively related to the type of trials, being very similar in both STOP and NO-STOP trials.

## **6.1 Future research**

While our results seem to suggest that PMD, in a different fashion from SMA, can be distinctively involved in action control and inhibition, also due to the limitations of the study, some questions still remain open.

First, in our approach, considered the novelty of the data, we have largely discussed and deeply investigated the presence of a mouth field in PMC.

However, our results cannot rule out the possibility that this premotor region could exert a more general, effector-independent type of influence on the motor output. In a sense this could be everything but a problem, since what we are interested in is a functional task carried out by PMD, as general as possible, and the effectors involved could be secondary. To generalize these data, thus, our stop-signal task (Chapter 5) could be applied also to the hand effector. Subjects could perform a similar task in which they are instructed to initiating and stopping a hand movement analogous to the one performed so far with the mouth. Our bet is that similar effects can be revealed, involving in the inhibition of action exerted by PMD more than a single, specific, effector.

Second, the main priorities for future research should focus on systematically investigating the relationship between PMD short-latency inhibitory effect on M1 and PMD inhibitory role in action control. A way of doing it consists in capitalizing on our double-coil approach, by applying condTMS over PMD during a stop-signal task. A working hypothesis could be that MEP modulations induced by dual-coil TMS stimulation may correlate either with the type of trial (STOP or NO-STOP trials, respectively) or, even more interestingly, with the actual performance (interrupting or not interrupting the ongoing action). Analogous approach should be taken with regard to SMA involvement in action control: even if it is not possible to completely disentangle between the SMA proper and the pre-SMA with the TMS techniques currently available, nonetheless we can move along the SMA area to better assess which specific portion of SMA it is involved in this behavior, and to what extent.

On the other side, we can use the behavioral paradigms to assess whether different portion of PMD are concerned with this behavior at different levels or in

different manners. Since it is possible that we have found a portion of the premotor cortex that is, at the same time, directly connected to the motor cortex as well as displaying the trait of the executive control exerted by more frontal areas, we can move toward the rostral and the caudal part of PMD (and SMA) while the subject is performing a delayed simple motor task or a stop-signal task. Indeed, searching for the boundaries of our action control and inhibition behavior could tell us where the effects we found are no longer present in the premotor cortex and might allow us to draw a topographic map of the anatomical and functional structure of the dorsal precentral region.

Further challenges are related to a possible role of PMD in both action observation and joint action. Single cell recordings from monkey brain showed that PMD neurons might exhibit the same activity patterns when observing as when executing a reaching action on a screen, even during an instructed-delay period before any actual observed motion (Cisek & Kalaska, 2004). Our TMS approach could provide a human counterpart of these findings. In particular, it could be tempting to assess whether the observation of someone else withholding an action to be released at the right time could be mapped by a PMD inhibitory effect M1 as measured by MEPs.

Finally, this approach could be extended from observing another's action to acting together with another individual. Jointly acting often requires to initiating or stopping an action according to what the confederate is actually doing or is about to do. Taking advantage of our TMS approach could be promising also in this case. It could be of interest to investigate whether and to what extent PMD effect on M1 might be modulated not only by one's own action control but also by monitoring the confederate action preparation and performance.



## REFERENCES

- Administration, V. (1996). Motor Areas of the Medial Wall : A Review of Their Location and Functional Activation.
- Alexander, G. E., & Crutcher, M. D. (1990). Preparation for movement: neural representations of intended direction in three motor areas of the monkey. *J Neurophysiol*, *64*(1), 133–150.
- Aron, A. R., Durston, S., Eagle, D. M., Logan, G. D., Stinear, C. M., & Stuphorn, V. (2007). Converging evidence for a fronto-basal-ganglia network for inhibitory control of action and cognition. *The Journal of Neuroscience : The Official Journal of the Society for Neuroscience*, *27*(44), 11860–11864. <https://doi.org/10.1523/JNEUROSCI.3644-07.2007>
- Aron, A. R., Fletcher, P. C., Bullmore, E. T., Sahakian, B. J., & Robbins, T. W. (2003). Stop-signal inhibition disrupted by damage to right inferior frontal gyrus in humans. *Nature Neuroscience*, *6*(2), 115–116. <https://doi.org/10.1038/nn1003>
- Association, W. M. (2009). Declaration of Helsinki. Ethical Principles for Medical Research Involving Human Subjects. Retrieved from <http://philpapers.org/rec/ASSDOH>
- Barbas, H., & Pandya, D. N. (1987). Architecture and frontal cortical connections of the premotor cortex (area 6) in the rhesus monkey. *J Comp Neurol*, *256*(2), 211–228. <https://doi.org/10.1002/cne.902560203>
- Barker, A. T., Jalinous, R., & Freeston, I. L. (1985). Non-Invasive Magnetic Stimulation of Human Motor Cortex. *The Lancet*. [https://doi.org/10.1016/S0140-6736\(85\)92413-4](https://doi.org/10.1016/S0140-6736(85)92413-4)
- Battaglia-Mayer, A., Buiatti, T., Caminiti, R., Ferraina, S., Lacquaniti, F., & Shallice, T. (2014). Correction and suppression of reaching movements in the cerebral cortex: Physiological and neuropsychological aspects. *Neuroscience and Biobehavioral Reviews*. <https://doi.org/10.1016/j.neubiorev.2014.03.002>
- Bäumer, T., Bock, F., Koch, G., Lange, R., Rothwell, J. C., Siebner, H. R., & Münchau, A. (2006). Magnetic stimulation of human premotor or motor cortex produces

interhemispheric facilitation through distinct pathways. *The Journal of Physiology*, 572(Pt 3), 857–68. <https://doi.org/10.1113/jphysiol.2006.104901>

Baumer, T., Schippling, S., Kroeger, J., Zittel, S., Koch, G., Thomalla, G., ... M??nchau, A. (2009). Inhibitory and facilitatory connectivity from ventral premotor to primary motor cortex in healthy humans at rest - A bifocal TMS study. *Clinical Neurophysiology*, 120(9), 1724–1731. <https://doi.org/10.1016/j.clinph.2009.07.035>

Beck, S., Houdayer, E., Richardson, S. P., & Hallett, M. (2009). The role of inhibition from the left dorsal premotor cortex in right-sided focal hand dystonia. *Brain Stimulation*, 2(4), 208–14. <https://doi.org/10.1016/j.brs.2009.03.004>

Bestmann, S., Ruff, C. C., Blankenburg, F., Weiskopf, N., Driver, J., & Rothwell, J. C. (2008). Mapping causal interregional influences with concurrent TMS-fMRI. *Experimental Brain Research*, 1–20. <https://doi.org/10.1007/s00221-008-1601-8>

Burle, B., Vidal, F., Tandonnet, C., & Hasbroucq, T. (2004). Physiological evidence for response inhibition in choice reaction time tasks. *Brain and Cognition*. <https://doi.org/10.1016/j.bandc.2004.06.004>

Cattaneo, L., & Barchiesi, G. (2011). Transcranial Magnetic Mapping of the Short-Latency Modulations of Corticospinal Activity from the Ipsilateral Hemisphere during Rest. *Frontiers in Neural Circuits*, 5(October), 1–13. <https://doi.org/10.3389/fncir.2011.00014>

Cattaneo, L., & Pavesi, G. (2014). The facial motor system. *Neuroscience and Biobehavioral Reviews*, 38(NOVEMBER 2013), 135159. <https://doi.org/10.1016/j.neubiorev.2013.11.002>

Chao, H. H. a, Luo, X., Chang, J. L. K., & Li, C.-S. R. (2009). Activation of the pre-supplementary motor area but not inferior prefrontal cortex in association with short stop signal reaction time--an intra-subject analysis. *BMC Neuroscience*, 10, 75. <https://doi.org/10.1186/1471-2202-10-75>

Chen, W. H., Mima, T., Siebner, H. R., Oga, T., Hara, H., Satow, T., ... Shibasaki, H. (2003). Low-frequency rTMS over lateral premotor cortex induces lasting changes in regional activation and functional coupling of cortical motor areas. *Clinical Neurophysiology*, 114(9), 1628–1637. [https://doi.org/10.1016/S1388-2457\(03\)00063-](https://doi.org/10.1016/S1388-2457(03)00063-)

- Chevrier, A. D., Noseworthy, M. D., & Schachar, R. (2007). Dissociation of response inhibition and performance monitoring in the stop signal task using event-related fMRI. *Human Brain Mapping, 28*(12), 1347–1358. <https://doi.org/10.1002/hbm.20355>
- Chouinard, P. a, Van Der Werf, Y. D., Leonard, G., & Paus, T. (2003). Modulating neural networks with transcranial magnetic stimulation applied over the dorsal premotor and primary motor cortices. *Journal of Neurophysiology, 90*(2), 1071–1083. <https://doi.org/10.1152/jn.01105.2002>
- Cisek, P., & Kalaska, J. F. (2004). Neural correlates of mental rehearsal in dorsal premotor cortex. *Nature, 431*(7011), 993–6. <https://doi.org/10.1038/nature03005>
- Cisek, P., & Kalaska, J. F. (2005). Neural correlates of reaching decisions in dorsal premotor cortex: Specification of multiple direction choices and final selection of action. *Neuron, 45*(5), 801–814. <https://doi.org/10.1016/j.neuron.2005.01.027>
- Civardi, C., Cantello, R., Asselman, P., & Rothwell, J. C. (2001). Transcranial magnetic stimulation can be used to test connections to primary motor areas from frontal and medial cortex in humans. *NeuroImage, 14*(6), 1444–1453. <https://doi.org/10.1006/nimg.2001.0918>
- Cunnington, R., Windischberger, C., Deecke, L., & Moser, E. (2002). The Preparation and Execution of Self-Initiated and Externally-Triggered Movement: A Study of Event-Related fMRI. *NeuroImage, 15*(2), 373–85. <https://doi.org/10.1006/nimg.2001.0976>
- Curtis, C. E., Sun, F. T., Miller, L. M., & D’Esposito, M. (2005). Coherence between fMRI time-series distinguishes two spatial working memory networks. *NeuroImage, 26*(1), 177–183. <https://doi.org/10.1016/j.neuroimage.2005.01.040>
- Daskalakis, Z. J., Christensen, B. K., Fitzgerald, P. B., Roshan, L., & Chen, R. (2002). The mechanisms of interhemispheric inhibition in the human motor cortex. *The Journal of Physiology, 543*(1), 317–326. <https://doi.org/10.1113/jphysiol.2002.017673>
- Davare, M., Lemon, R., & Olivier, E. (2008). Selective modulation of interactions between ventral premotor cortex and primary motor cortex during precision grasping in humans. *The Journal of Physiology, 586*(Pt 11), 2735–2742.

<https://doi.org/10.1113/jphysiol.2008.152603>

- Davare, M., Montague, K., Olivier, E., Rothwell, J. C., & Lemon, R. N. (2009). Ventral premotor to primary motor cortical interactions during object-driven grasp in humans. *Cortex*, *45*(9), 1050–1057. <https://doi.org/10.1016/j.cortex.2009.02.011>
- Davare, M., Rothwell, J. C., & Lemon, R. N. (2010). Causal Connectivity between the Human Anterior Intraparietal Area and Premotor Cortex during Grasp. *Current Biology*, *20*(2), 176–181. <https://doi.org/10.1016/j.cub.2009.11.063>
- Davare, M., Zénon, A., Desmurget, M., & Olivier, E. (2015). Dissociable contribution of the parietal and frontal cortex to coding movement direction and amplitude. *Frontiers in Human Neuroscience*, *9*, 241. <https://doi.org/10.3389/fnhum.2015.00241>
- Deiber, M. P., Honda, M., Ibañez, V., Sadato, N., & Hallett, M. (1999). Mesial motor areas in self-initiated versus externally triggered movements examined with fMRI: effect of movement type and rate. *Journal of Neurophysiology*, *81*(6), 3065–77.
- Deng, Z. De, Lisanby, S. H., & Peterchev, A. V. (2013). Electric field depth-focality tradeoff in transcranial magnetic stimulation: Simulation comparison of 50 coil designs. *Brain Stimulation*, *6*(1), 1–13. <https://doi.org/10.1016/j.brs.2012.02.005>
- Di Lazzaro, V., Oliviero, a, Profice, P., Insola, a, Mazzone, P., Tonali, P., & Rothwell, J. C. (1999). Direct demonstration of interhemispheric inhibition of the human motor cortex produced by transcranial magnetic stimulation. *Exp Brain Res*, *124*(4), 520–524. <https://doi.org/10.1007/s002210050648>
- di Pellegrino, G., & Wise, S. P. (1993). Visuospatial versus visuomotor activity in the premotor and prefrontal cortex of a primate. *The Journal of Neuroscience : The Official Journal of the Society for Neuroscience*, *13*(3), 1227–1243. <https://doi.org/10.3109/08990229309028835>
- Dum, R. P., & Strick, P. L. (1991). The origin of corticospinal projections from the premotor areas in the frontal lobe. *The Journal of Neuroscience : The Official Journal of the Society for Neuroscience*, *11*(March), 667–689. <https://doi.org/S0022510X0200268X> [pii]
- Dum, R. P., & Strick, P. L. (2005). Frontal lobe inputs to the digit representations of the

motor areas on the lateral surface of the hemisphere. *J. Neurosci.*, 25(1529–2401 (Electronic)), 1375–1386. <https://doi.org/10.1523/JNEUROSCI.3902-04.2005>

Ferbert, A., Priori, A., Rothwell, J. C., Day, B. L., Colebatch, J. G., & Marsden, C. D. (1992). Interhemispheric inhibition of the human motor cortex. *J. Physiol (Lond)*, 453(D), 525–546. <https://doi.org/10.1017/CBO9781107415324.004>

Floden, D., & Stuss, D. T. (2006). Inhibitory control is slowed in patients with right superior medial frontal damage. *J Cogn Neurosci*, 18(11), 1843–1849. <https://doi.org/10.1162/jocn.2006.18.11.1843>

Germann, J., Robbins, S., Halsband, U., & Petrides, M. (2005). Precentral sulcal complex of the human brain: Morphology and statistical probability maps. *Journal of Comparative Neurology*, 493(3), 334–356. <https://doi.org/10.1002/cne.20820>

Gerschlagner, W., Siebner, H. R., & Rothwell, J. C. (2001). Decreased corticospinal excitability after subthreshold 1 Hz rTMS over lateral premotor cortex. *Neurology*, 57(3), 449–455. <https://doi.org/10.1212/WNL.57.3.449>

Geyer, S., Ledberg, a, Schleicher, a, Kinomura, S., Schormann, T., Bürgel, U., ... Roland, P. E. (1996). Two different areas within the primary motor cortex of man. *Nature*, 382(6594), 805–807. <https://doi.org/10.1038/382805a0>

Gieben, U., Group, N., Anstalt, A., Munchen, D. U., & Dusseldorf, U. (n.d.). *Reviews and critical articles covering the entire field of normal anatomy ( cytology , histology , cyto- and histochemistry , electron microscopy , macroscopy , experimental morphology and embry- ology and comparative anatomy ) are published in Advances i.*

Godschalk, M., Lemon, R. N., Kuypers, H. G. J. M., & Van Der Steen, J. (1985). The involvement of monkey premotor cortex neurones in preparation of visually cued arm movements. *Behavioural Brain Research*, 18(2), 143–157. [https://doi.org/10.1016/0166-4328\(85\)90070-1](https://doi.org/10.1016/0166-4328(85)90070-1)

Grèzes, J., & Decety, J. (2002). Does visual perception of object afford action? Evidence from a neuroimaging study. *Neuropsychologia*, 40(2), 212–222. [https://doi.org/10.1016/S0028-3932\(01\)00089-6](https://doi.org/10.1016/S0028-3932(01)00089-6)

Groppa, S., Schlaak, B. H., Münchau, A., Werner-Petroll, N., Dünneberger, J., Bäumer, T.,

- ... Siebner, H. R. (2012). The human dorsal premotor cortex facilitates the excitability of ipsilateral primary motor cortex via a short latency cortico-cortical route. *Human Brain Mapping, 33*(2), 419–430. <https://doi.org/10.1002/hbm.21221>
- Hanajima, R., Ugawa, Y., Machii, K., Mochizuki, H., Terao, Y., Enomoto, H., ... Kanazawa, I. (2001). Interhemispheric facilitation of the hand motor area in humans. *Journal of Physiology, 531*(3), 849–859. <https://doi.org/10.1111/j.1469-7793.2001.0849h.x>
- Hatanaka, N., Nambu, A., Yamashita, A., Takada, M., & Tokuno, H. (2001). Somatotopic arrangement and corticocortical inputs of the hindlimb region of the primary motor cortex in the macaque monkey. *Neuroscience Research, 40*(1), 9–22. [https://doi.org/10.1016/S0168-0102\(01\)00210-3](https://doi.org/10.1016/S0168-0102(01)00210-3)
- He, S. Q., Dum, R. P., & Strick, P. L. (1995). Topographic organization of corticospinal projections from the frontal lobe: motor areas on the medial surface of the hemisphere. *Journal of Neuroscience, 15*(5 Pt 1), 3284–3306.
- Hoshi, E., & Tanji, J. (2002). Contrasting neuronal activity in the dorsal and ventral premotor areas during preparation to reach. *Journal of Neurophysiology, 87*(2), 1123–8. <https://doi.org/10.1152/jn.00496.2001>
- Hoshi, E., & Tanji, J. (2006). Differential involvement of neurons in the dorsal and ventral premotor cortex during processing of visual signals for action planning. *Journal of Neurophysiology, 95*(6), 3596–3616. <https://doi.org/10.1152/jn.01126.2005>
- Hoshi, E., Tanji, J., Gallivan, J. P., Mclean, D. A., Flanagan, J. R., & Culham, J. C. (2014). Contrasting Neuronal Activity in the Dorsal and Ventral Premotor Areas During Preparation to Reach Contrasting Neuronal Activity in the Dorsal and Ventral Premotor Areas During Preparation to Reach, 1123–1128.
- Jenkins, I. H., Jahanshahi, M., Jueptner, M., Passingham, R. E., & Brooks, D. J. (2000). Self-initiated versus externally triggered movements II. The effect of movement predictability on regional cerebral blood flow. *Brain, 123*, 1216–1228. <https://doi.org/10.1093/brain/123.6.1216>
- Johansen-Berg, H., Behrens, T. E. J., Robson, M. D., Drobnjak, I., Rushworth, M. F. S., Brady, J. M., ... Matthews, P. M. (2004). Changes in connectivity profiles define functionally distinct regions in human medial frontal cortex. *Proceedings of the*

*National Academy of Sciences of the United States of America* , 101(36), 13335–13340. <https://doi.org/10.1073/pnas.0403743101>

Johansen-Berg, H., Rushworth, M. F. S., Bogdanovic, M. D., Kischka, U., Wimalaratna, S., & Matthews, P. M. (2002). The role of ipsilateral premotor cortex in hand movement after stroke. *Proceedings of the National Academy of Sciences of the United States of America*, 99(22), 14518–14523. <https://doi.org/10.1073/pnas.222536799>

Kalaska, J. F., & Crammond, D. J. (1995). Deciding not to GO: Neuronal correlates of response selection in a GO/NOGO task in primate premotor and parietal cortex. *Cerebral Cortex*, 5(5), 410–428. <https://doi.org/10.1093/cercor/5.5.410>

Kiefer, M., Marzinzik, F., Weisbrod, M., Scherg, M., & Spitzer, M. (1998). The time course of brain activations during response inhibition: evidence from event-related potentials in a go/no go task. *Neuroreport*, 9(4), 765–770. <https://doi.org/10.1097/00001756-199803090-00037>

Koch, G., Franca, M., Del Olmo, M. F., Cheeran, B., Milton, R., Alvarez Saucó, M., & Rothwell, J. C. (2006). Time course of functional connectivity between dorsal premotor and contralateral motor cortex during movement selection. *The Journal of Neuroscience : The Official Journal of the Society for Neuroscience*, 26(28), 7452–9. <https://doi.org/10.1523/JNEUROSCI.1158-06.2006>

Kurata, K. (1989). Distribution of neurons with set- and movement-related activity before hand and foot movements in the premotor cortex of rhesus monkeys. *Experimental Brain Research*, 77(2), 245–256. <https://doi.org/10.1007/BF00274982>

Kurata, K. (1994). Site of origin of projections from the thalamus to dorsal versus ventral aspects of the premotor cortex of monkeys. *Neuroscience Research*, 21(1), 71–76. [https://doi.org/10.1016/0168-0102\(94\)90069-8](https://doi.org/10.1016/0168-0102(94)90069-8)

Kurata, K., & Wise, S. P. (1988). Premotor and supplementary motor cortex in. *Experimental Brain Research*, 72, 237–248.

Kurata, K., & Wise, S. P. (1988). Premotor cortex of rhesus monkeys: set-related activity during two conditional motor tasks. *Experimental Brain Research*, 69(2), 327–343. <https://doi.org/10.1007/BF00247578>

- KUYPERS, H. G. J. M. (1958). CORTICOBULBAR CONNEXIONS TO THE PONS AND LOWER BRAIN-STEM IN MAN. *Brain*, 81(3), 364–388.  
<https://doi.org/10.1093/brain/81.3.364>
- Ledberg, A., Bressler, S. L., Ding, M., Coppola, R., & Nakamura, R. (2007). Large-scale visuomotor integration in the cerebral cortex. *Cerebral Cortex*, 17(1), 44–62.  
<https://doi.org/10.1093/cercor/bhj123>
- Li, C. R., Huang, C., Constable, R. T., & Sinha, R. (2006). Imaging Response Inhibition in a Stop-Signal Task: Neural Correlates Independent of Signal Monitoring and Post-Response Processing. *The Journal of Neuroscience*, 26(1), 186–192.  
<https://doi.org/10.1523/JNEUROSCI.3741-05.2006>
- Logothetis, N. K. (2003). The underpinnings of the BOLD functional magnetic resonance imaging signal. *The Journal of Neuroscience*, 23(10), 3963–3971.  
<https://doi.org/23/10/3963> [pii]
- Luppino, G., Calzavara, R., Rozzi, S., & Matelli, M. (2001). Projections from the superior temporal sulcus to the agranular frontal cortex in the macaque. *European Journal of Neuroscience*, 14(6), 1035–1040. Retrieved from <http://doi.wiley.com/10.1046/j.0953-816x.2001.01734.x>
- Luppino, G., Matelli, M., Camarda, R. M., Gallese, V., & Rizzolatti, G. (1991). Multiple representations of body movements in mesial area 6 and the adjacent cingulate cortex: an intracortical microstimulation study in the macaque monkey. *The Journal of Comparative Neurology*, 311(4), 463–482. <https://doi.org/10.1002/cne.903110403>
- Luppino, G., Matelli, M., Camarda, R., & Rizzolatti, G. (1993). Corticocortical connections of area F3 (SMA-proper) and area F6 (pre-SMA) in the Macaque monkey. *Journal of Comparative Neurology*, 338(1), 114–140. <https://doi.org/10.1002/cne.903380109>
- Luppino, G., & Rizzolatti, G. (2000). The Organization of the Frontal Motor Cortex. *News in Physiological Sciences : An International Journal of Physiology Produced Jointly by the International Union of Physiological Sciences and the American Physiological Society*, 15(October), 219–224. <https://doi.org/10.1093/cercor/bhg093>
- Luppino, G., Rozzi, S., Calzavara, R., & Matelli, M. (2003). Prefrontal and agranular cingulate projections to the dorsal premotor areas F2 and F7 in the macaque monkey.

*European Journal of Neuroscience*, 17(3), 559–578. <https://doi.org/10.1046/j.1460-9568.2003.02476.x>

Marconi, B., Genovesio, A., Giannetti, S., Molinari, M., & Caminiti, R. (2003). Callosal connections of dorso-lateral premotor cortex. *European Journal of Neuroscience*, 18(4), 775–788. <https://doi.org/10.1046/j.1460-9568.2003.02807.x>

Matelli, M., Luppino, G., & Rizzolatti, G. (1985). Patterns of cytochrome oxidase activity in the frontal agranular cortex of the macaque monkey. *Behavioural Brain Research*, 18(2), 125–136. [https://doi.org/10.1016/0166-4328\(85\)90068-3](https://doi.org/10.1016/0166-4328(85)90068-3)

Matelli, M., Luppino, G., & Rizzolatti, G. (1991). Architecture of superior and mesial area 6 and the adjacent cingulate cortex in the macaque monkey. *The Journal of Comparative Neurology*, 311(4), 445–462. <https://doi.org/10.1002/cne.903110402>

Matsuzaka, Y., Aizawa, H., & Tanji, J. (1992). A motor area rostral to the supplementary motor area (presupplementary motor area) in the monkey: neuronal activity during a learned motor task. *Journal of Neurophysiology*, 68(3), 653–662.

Mattia, M., Pani, P., Mirabella, G., Costa, S., Del Giudice, P., & Ferraina, S. (2013). Heterogeneous attractor cell assemblies for motor planning in premotor cortex. *Journal of Neuroscience*, 33(27), 11155–11168. <https://doi.org/10.1523/JNEUROSCI.4664-12.2013>

Maule, F., Barchiesi, G., Brochier, T., & Cattaneo, L. (2015). Haptic working memory for grasping: The role of the parietal operculum. *Cerebral Cortex*, 25(2), 528–537. <https://doi.org/10.1093/cercor/bht252>

Mayka, M. A., Corcos, D. M., Leurgans, S. E., & Vaillancourt, D. E. (2006). Three-dimensional locations and boundaries of motor and premotor cortices as defined by functional brain imaging: A meta-analysis. *NeuroImage*, 31(4), 1453–1474. <https://doi.org/10.1016/j.neuroimage.2006.02.004>

Miniussi, C., Cappa, S. F., Cohen, L. G., Floel, A., Fregni, F., Nitsche, M. A., ... Walsh, V. (2008). Efficacy of repetitive transcranial magnetic stimulation/transcranial direct current stimulation in cognitive neurorehabilitation. *Brain Stimulation*. <https://doi.org/10.1016/j.brs.2008.07.002>

- Miniussi, C., Ruzzoli, M., & Walsh, V. (2010). The mechanism of transcranial magnetic stimulation in cognition. *Cortex*, *46*(1), 128–130.  
<https://doi.org/10.1016/j.cortex.2009.03.004>
- Mirabella, G., Pani, P., & Ferraina, S. (2011). Neural correlates of cognitive control of reaching movements in the dorsal premotor cortex of rhesus monkeys. *Journal of Neurophysiology*, *106*(3), 1454–1466. <https://doi.org/10.1152/jn.00995.2010>
- Mochizuki, H., Huang, Y.-Z., & Rothwell, J. C. (2004). Interhemispheric interaction between human dorsal premotor and contralateral primary motor cortex. *The Journal of Physiology*, *561*(Pt 1), 331–8. <https://doi.org/10.1113/jphysiol.2004.072843>
- Moll, L., & Kuypers, H. G. (1977). Premotor cortical ablations in monkeys: contralateral changes in visually guided reaching behavior. *Science (New York, N.Y.)*, *198*(4314), 317–319. <https://doi.org/10.1126/science.410103>
- Morecraft, R. J., Louie, J. L., Herrick, J. L., & Stilwell-Morecraft, K. S. (2001). Cortical innervation of the facial nucleus in the non-human primate: A new interpretation of the effects of stroke and related subtotal brain trauma on the muscles of facial expression. *Brain*, *124*(September), 176–208. <https://doi.org/10.1093/brain/124.1.176>
- Muakkassa, K. F., & Strick, P. L. (1979). Frontal lobe inputs to primate motor cortex: evidence for four somatotopically organized “premotor” areas. *Brain Research*, *177*(1), 176–182. [https://doi.org/10.1016/0006-8993\(79\)90928-4](https://doi.org/10.1016/0006-8993(79)90928-4)
- Münchau, A., Bloem, B. R., Irlbacher, K., Trimble, M. R., & Rothwell, J. C. (2002). Functional connectivity of human premotor and motor cortex explored with repetitive transcranial magnetic stimulation. *The Journal of Neuroscience*, *22*(2), 554–561.  
<https://doi.org/22/2/554> [pii]
- Nachev, P., Kennard, C., & Husain, M. (2008). Functional role of the supplementary and pre-supplementary motor areas. *Nature Reviews. Neuroscience*, *9*(11), 856–869.  
<https://doi.org/10.1038/nrn2478>
- Nachev, P., Rees, G., Parton, A., Kennard, C., & Husain, M. (2005). Volition and conflict in human medial frontal cortex. *Current Biology: CB*, *15*(2), 122–8.  
<https://doi.org/10.1016/j.cub.2005.01.006>

- Nachev, P., Wydell, H., O'Neill, K., Husain, M., & Kennard, C. (2007). The role of the pre-supplementary motor area in the control of action. *NeuroImage*, *36*(SUPPL. 2).  
<https://doi.org/10.1016/j.neuroimage.2007.03.034>
- Nakamura, K., Sakai, K., & Hikosaka, O. (1998). Neuronal activity in medial frontal cortex during learning of sequential procedures. *Journal of Neurophysiology*, *80*(5), 2671–87.
- O'Shea, J., Sebastian, C., Boorman, E. D., Johansen-Berg, H., & Rushworth, M. F. S. (2007). Functional specificity of human premotor-motor cortical interactions during action selection. *The European Journal of Neuroscience*, *26*(7), 2085–95.  
<https://doi.org/10.1111/j.1460-9568.2007.05795.x>
- Obeso, I., Cho, S. S., Antonelli, F., Houle, S., Jahanshahi, M., Ko, J. H., & Strafella, A. P. (2013). Stimulation of the pre-SMA influences cerebral blood flow in frontal areas involved with inhibitory control of action. *Brain Stimulation*, *6*(5), 769–776.  
<https://doi.org/10.1016/j.brs.2013.02.002>
- Ohbayashi, X. M., Picard, N., & Strick, P. L. (2016). Inactivation of the Dorsal Premotor Area Disrupts Internally Generated , But Not Visually Guided , Sequential Movements. *The Journal of Neuroscience*, *36*(6), 1971–1976.  
<https://doi.org/10.1523/JNEUROSCI.2356-15.2016>
- Parmigiani, S., Barchiesi, G., & Cattaneo, L. (2015). The dorsal premotor cortex exerts a powerful and specific inhibitory effect on the ipsilateral corticofacial system: a dual-coil transcranial magnetic stimulation study. *Experimental Brain Research*.  
<https://doi.org/10.1007/s00221-015-4393-7>
- Picton, T. W., Stuss, D. T., Alexander, M. P., Shallice, T., Binns, M. A., & Gillingham, S. (2006). Effects of Focal Frontal Lesions on Response Inhibition. *Cerebral Cortex*, *17*(4), 826–838. <https://doi.org/10.1093/cercor/bhk031>
- Pirio Richardson, S., Beck, S., Bliem, B., & Hallett, M. (2014). Abnormal dorsal premotor-motor inhibition in writer's cramp. *Movement Disorders*, *29*(6), 797–803.  
<https://doi.org/10.1002/mds.25878>
- Rizzolatti, G., Gentilucci, M., Camarda, R. M., Gallese, V., Luppino, G., Matelli, M., & Fogassi, L. (1990). Neurons related to reaching-grasping arm movements in the

rostral part of area 6 (area 6a $\beta$ ). *Experimental Brain Research*, 82(2), 337–350.  
<https://doi.org/10.1007/BF00231253>

Rizzolatti, G., Luppino, G., & Matelli, M. (1998). The organization of the cortical motor system: new concepts. *Electroencephalography and Clinical ...* Retrieved from <http://www.sciencedirect.com/science/article/pii/S0013469498000224>

Rossi, S., & Hallett, M. (2009). Safety, ethical considerations, and application guidelines for the use of transcranial magnetic stimulation in clinical practice and research. *Clinical Neurophysiology*, 120(12), 2008–2039.  
<https://doi.org/10.1016/j.clinph.2009.08.016>

Rothwell, J. C. (2011). Human Movement Science Using transcranial magnetic stimulation methods to probe connectivity between motor areas of the brain. *Human Movement Science*, 30(5), 906–915. <https://doi.org/10.1016/j.humov.2010.07.007>

Rubia, K., Smith, A. B., Brammer, M. J., & Taylor, E. (2003). Right inferior prefrontal cortex mediates response inhibition while mesial prefrontal cortex is responsible for error detection. *NeuroImage*, 20(1), 351–358. [https://doi.org/10.1016/S1053-8119\(03\)00275-1](https://doi.org/10.1016/S1053-8119(03)00275-1)

Sato, M., Buccino, G., Gentilucci, M., & Cattaneo, L. (2010). On the tip of the tongue: Modulation of the primary motor cortex during audiovisual speech perception. *Speech Communication*, 52(6), 533–541. <https://doi.org/10.1016/j.specom.2009.12.004>

Sawaguchi, T., Yamane, I., & Kubota, K. (1996). Application of the GABA antagonist bicuculline to the premotor cortex reduces the ability to withhold reaching movements by well-trained monkeys in visually guided reaching task. *Journal of Neurophysiology*, 75(5), 2150–2156.

Scangos, K. W., & Stuphorn, V. (2010). Medial Frontal Cortex Motivates But Does Not Control Movement Initiation in the Countermandering Task. *The Journal of Neuroscience*, 30(5), 1968–1982. <https://doi.org/10.1523/JNEUROSCI.4509-09.2010>

Schluter, N. D., Rushworth, M. F. S., Passingham, R. E., & Mills, K. R. (1998). Temporary interference in human lateral premotor cortex suggests dominance for the selection of movements. A study using transcranial magnetic stimulation. *Brain*, 121(5), 785–799. <https://doi.org/10.1093/brain/121.5.785>

- Shima, K., & Tanji, J. (1998). Role for cingulate motor area cells in voluntary movement selection based on reward. *Science (New York, N.Y.)*, *282*(5392), 1335–8. <https://doi.org/10.1126/science.282.5392.1335>
- Sumner, P., Nachev, P., Morris, P., Peters, A. M., Jackson, S. R., Kennard, C., & Husain, M. (2007). Human Medial Frontal Cortex Mediates Unconscious Inhibition of Voluntary Action. *Neuron*, *54*(5), 697–711. <https://doi.org/10.1016/j.neuron.2007.05.016>
- Tanji, J., Shima, K., & Matsuzaka, Y. (2002). Reward-based planning of motor selection in the rostral cingulate motor area. *Advances In Experimental Medicine and Biology*, *508*, 417–423.
- Tokuno, H., & Nambu, a. (2000). Organization of nonprimary motor cortical inputs on pyramidal and nonpyramidal tract neurons of primary motor cortex: An electrophysiological study in the macaque monkey. *Cerebral Cortex (New York, N.Y. : 1991)*, *10*(1), 58–68.
- Tokuno, H., & Tanji, J. (1993). Input organization of distal and proximal forelimb areas in the monkey primary motor cortex: a retrograde double labeling study. *The Journal of Comparative Neurology*, *333*, 199–209. <https://doi.org/10.1002/cne.903330206>
- Tomassini, V., Jbabdi, S., Klein, J. C., Behrens, T. E. J., Pozzilli, C., Matthews, P. M., ... Johansen-Berg, H. (2007). Diffusion-weighted imaging tractography-based parcellation of the human lateral premotor cortex identifies dorsal and ventral subregions with anatomical and functional specializations. *The Journal of Neuroscience : The Official Journal of the Society for Neuroscience*, *27*(38), 10259–10269. <https://doi.org/10.1523/JNEUROSCI.2144-07.2007>
- Tukey, J. W. (1977). Exploratory Data Analysis. *Analysis*, *2*(1999), 688. <https://doi.org/10.1007/978-1-4419-7976-6>
- Verbruggen, F., & Logan, G. (2008). Response inhibition in the stop-signal paradigm. *Trends in Cognitive Sciences*, *12*(11), 418–424. <https://doi.org/10.1016/j.tics.2008.07.005.Response>
- Von Bonin, G., & Bailey, P. (1947). *The neocortex of Macaca mulatta*. *Illinois Monogr. med. Sci.* (Vol. 5). <https://doi.org/10.1001/jama.1948.02890460089032>

- Vorobiev, V. (1998). Parcellation of human mesial area 6: Cytoarchitectonic evidence for three separate areas. *European Journal of Neuroscience*, *10*(6), 2199–2203. <https://doi.org/10.1046/j.1460-9568.1998.00236.x>
- Watkins, K. E., Strafella, A. P., & Paus, T. (2003). Seeing and hearing speech excites the motor system involved in speech production. *Neuropsychologia*, *41*(8), 989–994. [https://doi.org/10.1016/S0028-3932\(02\)00316-0](https://doi.org/10.1016/S0028-3932(02)00316-0)
- Watkins, K., & Paus, T. (2004). Modulation of motor excitability during speech perception: the role of Broca's area. *Journal of Cognitive Neuroscience*, *16*(6), 978–987. <https://doi.org/10.1162/0898929041502616>
- Weinrich, M., & Wise, S. P. (1982). The premotor cortex of the monkey. *J Neurosci*, *2*(9), 1329–1345.
- Weinrich, M., Wise, S. P., & Mauritz, K. H. (1984). A neurophysiological study of the premotor cortex in the rhesus monkey. *Brain*, *107* ( Pt 2), 385–414.
- Wise, S. P. (1985). The primate premotor cortex: past, present, and preparatory. *Annual Review of Neuroscience*, *8*, 1–19. <https://doi.org/10.1146/annurev.ne.08.030185.000245>
- Wise, S. P., Boussaoud, D., Johnson, P. B., & Caminiti, R. (1997). PREMOTOR AND PARIETAL CORTEX: Corticocortical Connectivity and Combinatorial Computations 1. *Annu. Rev. Neurosci*, *20*, 25–42. <https://doi.org/10.1146/annurev.neuro.20.1.25>
- Zilles, K., & Amunts, K. (2010). Centenary of Brodmann's map--conception and fate. *Nature Reviews Neuroscience*, *11*(2), 139–145. <https://doi.org/10.1038/nrn2776>